KERNFORSCHUNGSANLAGE JÜLICH GmbH
Institut für Kernphysik

Untersuchung der Niveauschemata von ^{75}Se, ^{76}Se and ^{77}Se durch Einfang thermischer Neutronen

von

Y. Tokunaga

Jül-Spez-158
Juni 1982
ISSN 0343-7639

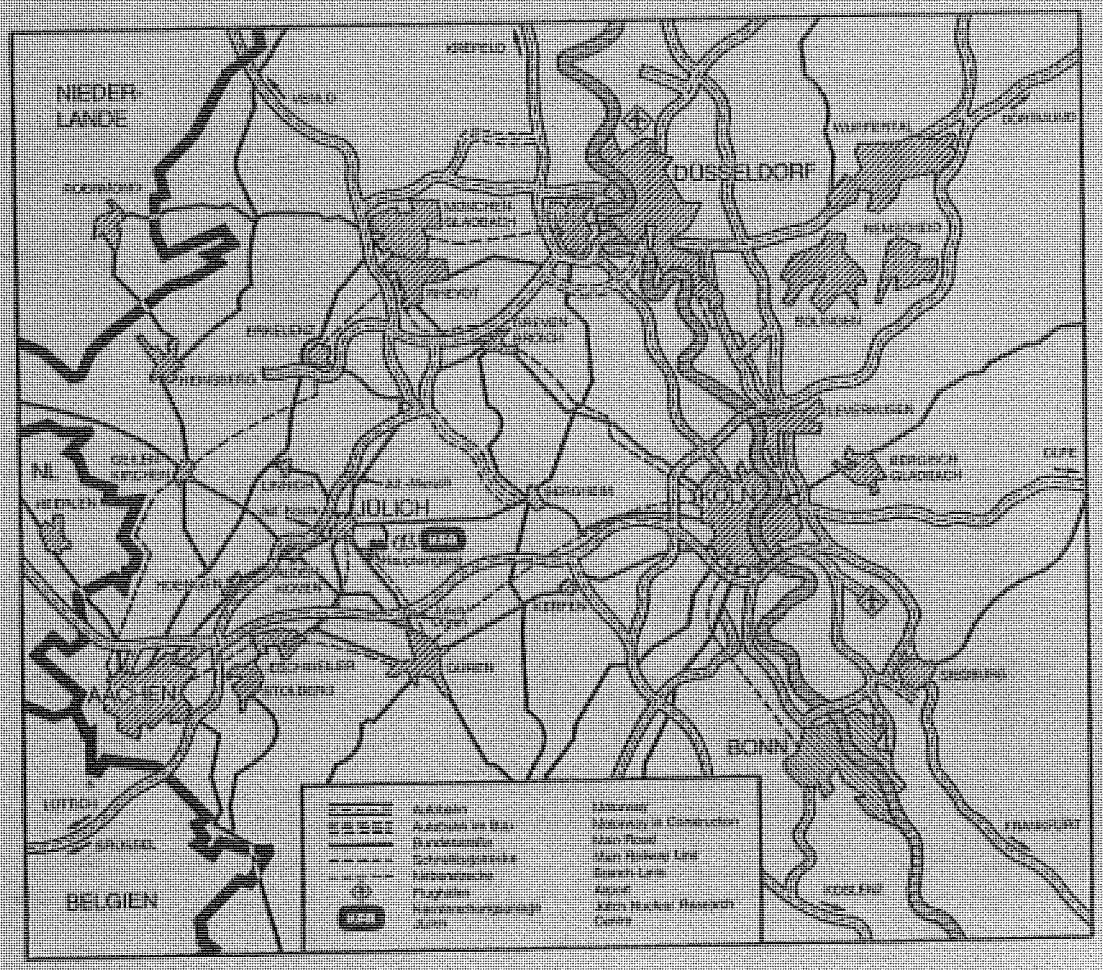

Als Manuskript gedruckt

Berichte der Kernforschungsanlage Jülich - Nr. 158

Institut für Kernphysik Jül - Spez - 158

Zu beziehen durch: ZENTRALBIBLIOTHEK der Kernforschungsanlage Jülich GmbH
Postfach 1913 · D-5170 Jülich (Bundesrepublik Deutschland)
Telefon: 02461/610 · Telex: 833556 kfa d

Untersuchung der Niveauschemata von ^{75}Se, ^{76}Se and ^{77}Se durch Einfang thermischer Neutronen

von

Y. Tokunaga

D 38 (Diss. Uni. Köln)

Zusammenfassung

Nach dem Einfang thermischer Neutronen wurde unter Verwendung metallischer ^{74}Se-und ^{76}Se-Targets in Jülich das hochenergetische (n,γ)-Spektrum mit einem Paarspektrometer gemessen. In Grenoble wurde die γ-Strahlung von Targets aus ^{74}SePb und ^{76}SePb in der Nähe des Reaktorkerns mit einem Paarspektrometer untersucht zur Ermittlung primärer Übergänge. Niederenergetische γ-Linien wurden gleichzeitig mit sehr hoher Auflösung mit den Kristallspektrometern registriert. Mit dem Konversionselektronenspektrometer BILL wurden die intensivsten (n,e$^-$)-Linien bestimmt.

Mit Hilfe der gewonnenen Daten wurden mit hoher Energiegenauigkeit die Niveauschemata von $^{75-78}$Se und von ^{75}As konstruiert. Für einige Zustände wurden J^π-Zuordnungen getroffen, für andere wurden Mehrdeutigkeiten beseitigt.

Die ^{75}Se(n,γ)-Reaktion wurde über den suksessiven Neutroneneinfang bei Bestrahlung des ^{74}Se Targets im Hochflußreaktor erstmals beobachtet. Der Wirkungsquerschnitt der ^{75}Se(n,γ)-Reaktion ergibt sich daraus zu $\sim$ 300±100 b.

Die Verwendung der SePb-Targets erlaubt auch eine Untersuchung der natürlichen der Pb K-Röntgenlinien. Diese Breiten weichen etwas von den theoretisch erwarteten ab.

Ein Vergleich der (n,γ)-Stärken mit den entsprechenden spektroskopischen Faktoren der (d,p)-Reaktionen weist auf einen erheblichen Unterschied der Einfangmechanismen in ^{74}Se und ^{76}Se hin.

Eine Betrachtung der $^{75-77}$Se-Niveauschemata und der Termschemata der Nachbarkerne und ihr Vergleich mit den vorliegenden Kernstrukturmodellen zeigt, daß die derzeitigen Theorien noch nicht in der Lage sind, die Eigenschaften der Zustände mit niedrigen Spins und geringer Anregungsenergie in den neutronenarmen Se-Kernen befriedigend zu beschreiben.

I dedicate this thesis
to my mother,
who passed away
at the age of thirty-eight.
She hoped me to be a physisist.

CONTENTS

CONTENTS

CONTENTS

Abstract

Slow-neutron capture γ-ray spectroscopy was carried out with metallic targets of ^{74}Se and ^{76}Se at Jülich, where the high-energy (n,γ) spectrum was measured with a pair spectrometer, and at Grenoble, where ^{74}SePb and ^{76}SePb alloy targets were exposed in high neutron flux regions for pair spectroscopy of the primary (n,γ) lines, for low-energy (n,γ) spectroscopy with the high-resolution curved crystal spectrometers, and for (n,e^-)-measurements with the conversion-electron spectrometer BILL.

Gamma-decay schemes were constructed and very precise energies were obtained for $^{75-78}$Se and for ^{75}As. For several states new J^π assignments could be made and for others ambiguities could be resolved.

The ^{75}Se(n,γ) reaction was observed for the first time due to successive neutron capture in ^{74}Se in the high flux reactor at Grenoble. The cross section of this reaction was found to be $\sim$ 300±100 b.

The SePb targets have also allowed a study of the K X-ray widths of Pb. These widths show small deviations from theoretical values.

Comparison of the primary (n,γ) transition strengths and the corresponding (d,p)-spectroscopic factors have revealed a significant difference in the neutron capture mechanisms for ^{74}Se(n,γ) and ^{76}Se(n,γ).

The comparisons of the $^{75-77}$Se level schemes with those of neighbouring nuclei and with the predictions of various nuclear models show that present theories are not yet able to describe the structures of the low-spin states in the neutron deficient Se isotopes satisfactorily.

1. Introduction

The selenium isotopes (Z=34) show many different nuclear excitation modes. The heavy even mass isotopes (^{76,78,80,82}Se) have typical vibrational spectra, i.e. a 2^+_1 level and the 0^+_2, 2^+_2, 4^+_1 2-phonon triplet. Further the low-lying negative parity states in odd mass nuclei seem to follow well the picture, where the $(p_{1/2})^{-1}$-state is coupled to a vibrational core /Sh61,Ki63/. On the other hand, considerable anharmonicities are seen in the light even mass isotopes (^{72,74}Se), where a very low-lying 0^+_2-level occurs. In addition to these phenomena the strange behaviour of positive parity states arising from the $(\nu g_{9/2})^n$ configuration (see Fig. 1.1) in the odd-mass isotopes (very low-lying $5/2^+$, $7/2^+$ states; anomalous coupling states, ACS) is not well understood theoretically. Similar phenomena are also found in Ge-isotopes. Thus studies in this region are of interest and experiments should provide the data to help the theoretical understanding.

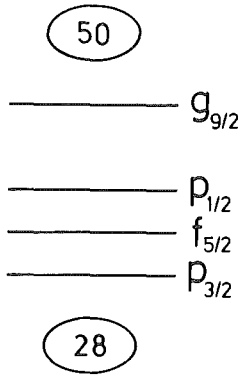

Fig. 1.1
Shell-model orbitals which are relevant for neutrons as well as for protons in Se-isotopes.

The three nuclei ^{75}Se, ^{76}Se, and ^{77}Se, which are mainly studied in the present work, are just lying in this interesting region. Many different experimental approaches have been made for these nuclei: particle transfer reactions, β-decay studies, in-beam γ-spectroscopies, (n,γ) spectroscopies (except ^{76}Se), etc., which will be individually referred to in the following chapters.

Studies of high spin states by in-beam γ-spectroscopy have revealed rotational-like structures even in Se-isotopes (as for even mass Se-isotopes see /Ah81, He74, Pi78, We80/, and as for odd mass nuclei see /Be76, Ze76b, Ze75, Sa76a, Ze76a/).

However, the low-lying low spin states in this region often show very complex structure (see for example /He74, Ku75, Li75, Na78/). Therefore, the structure of these states should not be discussed only on the basis of the in-beam studies

alone, but also results should be used from the (n,γ), (p,nγ), and particle transfer reactions, and β-decay, which are suitable for studies of low-spin states.

The slow neutron capture reaction is very well suited for the study of low-spin states and has the advantage that most of the low-lying low spin states can be excited in many cases due to complexity of γ-decay process after neutron capture. In addition, spin- and parity assignment in this reaction is largely facilitated by the fact that the spin and parity of the neutron capture state are quite well defined. For example in the case of an even-even target only $J^{\pi} = 1/2^{+}$ is possible for an s-wave capture state. This is because in the low energy region of incident neutrons, only the s-wave is relevant in the capture process (see Fig. 1.2).

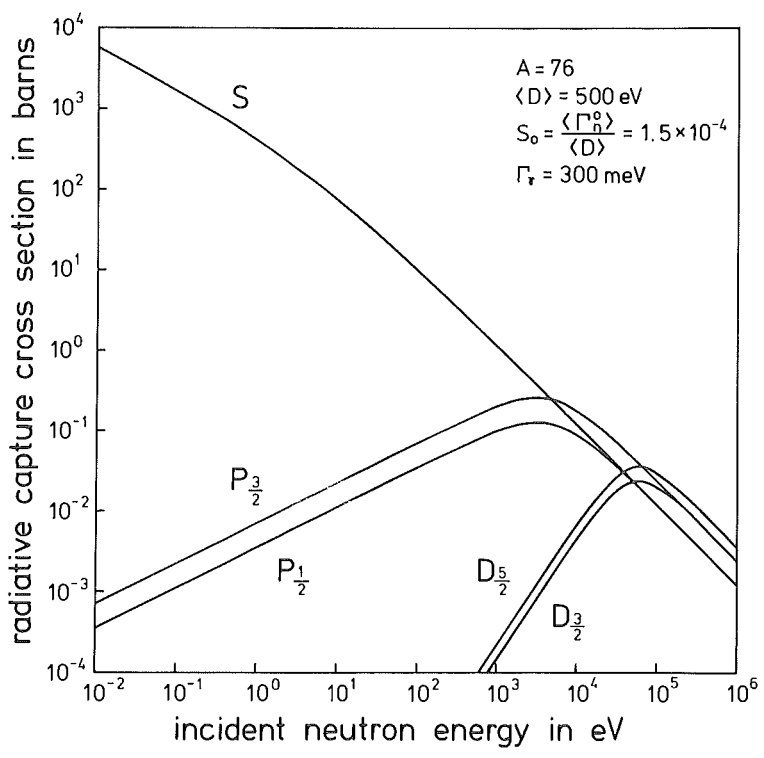

Fig. 1.2
A hypothetical neutron capture cross section calculated in a manner similar to that of Cameron et al./Ca63/ using the parameters given in the figure.

The $^{74}Se(n,\gamma)$, $^{76}Se(n,\gamma)$ reactions have been previously investigated (thermal neutron capture) /Ru70, Ak73a, Kn71, Ra71, Br79, En81/. However, identification of high energy γ-rays in the $^{74}Se(n,\gamma)$ reaction was rather limited. Further the low energy part of those γ-spectra of both reactions is so complex that it requires measurements with improved resolution.

The $^{75}Se(n,\gamma)$ reaction, which enables the study of ^{76}Se, was for the first time observed in the present work due to the high neutron flux at the HFR/Grenoble. This reaction will be briefly discussed in chapter 2.6.

As will be shown in the next chapter, in the present work five instruments of three different types of detectors were exploited for the investigation of the (n,γ) reactions, and they are the following:

- curved crystal spectrometers GAMS 1 and GAMS 2/3 for precision measurement of low energy γ-lines.
- β-spectrometer BILL for conversion electron measurements.
- two pair spectrometers in Jülich and Grenoble.

These instruments cover different energy regions (see Fig. 1.3), providing an almost complete set of not too weak γ-rays of the (n,γ) reaction.

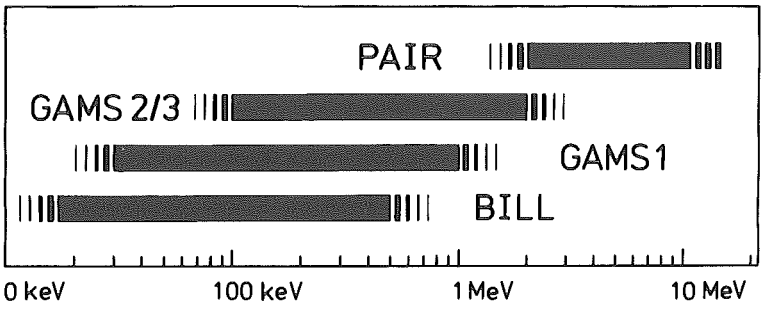

Fig. 1.3
Energy region which is effectively investigated by various instruments. The performance of BILL is much higher than shown in this figure, but is limited due to low conversion coefficients in Se-isotopes (Z=34).

We give in the present work information about three nuclei ^{75}Se, ^{76}Se, and ^{77}Se using the data extracted from the present experiments. We also discuss some systematics of the structures of Se-isotopes, together with other neighbouring nuclei.

In addition, some information has been obtained on

- precise energies of γ-rays from ^{78}Se and ^{75}As
- Pb K-X ray natural widths
- neutron separation energies of four Se-isotopes (A=75,76,77,78).

These results are shown and discussed in chapter 4.

2. Experiments

In the present work three different types of measurements were carried out:

- a measurement of low energy γ-rays ($\lesssim$ 2 MeV) with the use of the curved crystal spectrometers GAMS 1 and GAMS 2/3 /Ko80b/
- a measurement of conversion electrons with the β-spectrometer BILL /Ma78/
- a measurement of high energy γ-rays (from 2 MeV up to the neutron binding energy) with the use of pair spectrometers.

The measurement with a pair spectrometer was performed both at the High-Flux Reactor (HFR) of the Institute Laue-Langevin (ILL) in Grenoble and at the research reactor FRJ-2 (DIDO) of the Kernforschungsanlage (KFA) in Jülich. The other experiments were all performed at the HFR/Grenoble. In Jülich, the external target geometry with low neutron flux ($\sim 10^8$ n/s·cm^2) was exploited, whereas in Grenoble the internal target geometry was used with very high neutron flux (5×10^{14} n/s·cm^2) at the target position of GAMS 1 and GAMS 2/3.

If the experimental conditions are optimized (source strength, solid angle of the detector, etc.), both pair spectrometers placed in Jülich and in Grenoble show comparable performance. However, the essential difference between the experimental conditions for both pair spectrometers was that in Grenoble one can often observe the double neutron capture reaction due to the high neutron flux. This process is unobservable in Jülich. Since it was expected from the (n,γ) cross sections of Se-isotopes that the double neutron capture reaction on ^{74}Se and ^{76}Se would occur, it was clear that the comparison of two spectra taken in Jülich and in Grenoble would clarify the existence of any γ-rays from this double neutron capture reaction. The observation of these double capture γ-rays was facilitated by the odd-even mass difference, i.e. the neutron binding energies of the odd-A nucleus and the e-e nucleus, which are formed through the single neutron and the double neutron capture in the present case, differ by $\sim$ 3 MeV. Such details will be further discussed in chapter 2.6.

On the other hand, it is possible to distinguish the low energy double neutron capture γ-rays already in a single measurement in Grenoble due to the excellent resolution of the curved crystal spectrometers GAMS 1 and GAMS 2/3. For details see § 2.6.

In this chapter the GAMS 1, GAMS 2/3, BILL, and the two pair spectrometers (Jülich, Grenoble) are briefly described.

2.1 The curved crystal spectrometers GAMS 1 and GAMS 2/3

There are three types of crystal spectrometers, i.e. flat, DuMond, and Cauchois crystal spectrometers (Fig. 2.1)

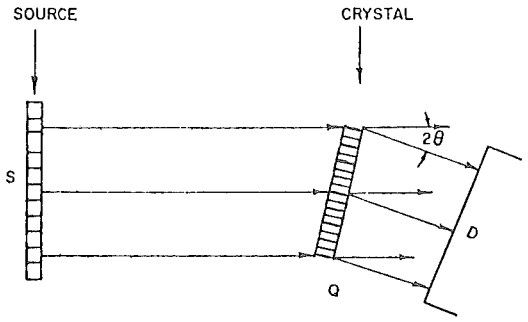

(a) flat crystal spectrometer

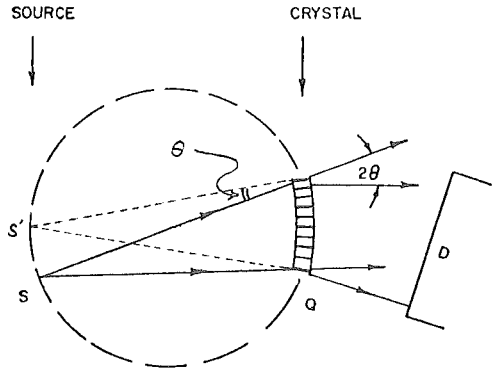

(b) DuMond curved crystal spectrometer

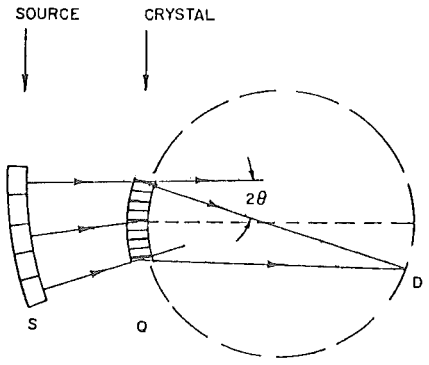

(c) Cauchois curved crystal spectrometer

Fig. 2.1

Three types of crystal diffraction spectrometers

S: γ-source
Q: diffraction crystal
Θ: diffraction angle
D: photon detector
S': γ-source at $\theta=0^{\circ}$

All of these geometries make use of Bragg reflection, where the wave length is determined by the grating constant of the crystals and the "Bragg angle":

$$n\lambda = 2d \sin\Theta \quad (n = 1,2,3,4,5,\ldots \text{ diffraction order}) \qquad \text{(eq. 2.1)}$$

λ: wave length of incident photon

d: spacing of lattice planes

Θ: Bragg diffraction angle

or, with $E_\gamma = \frac{hc}{\lambda}$:

$$\frac{2d \sin\Theta}{hc} = \frac{n}{E_\gamma} \qquad \ldots\ldots \quad \text{eq. 2.1a}$$

h: Planck constant
c: velocity of light
E_γ: incident photon energy,

from which follows for the diffraction line width:

$$\Delta E_\gamma = \frac{2d}{nhc} E_\gamma^2 \cos\Theta \, \Delta\Theta \qquad \ldots\ldots \quad \text{eq. 2.1b}$$

$\cos\Theta$ is a very slow-varying function and the angular width of the line $\Delta\Theta$ is almost constant and depends on the target shape, the source-crystal geometry and the crystal structure /Su00, Kn79, Ko80b/. The width ΔE_γ can thus be expressed approximately by

$$\Delta E_\gamma \simeq \frac{\text{const.}}{n} \cdot E_\gamma^2 \qquad \ldots\ldots \quad \text{eq. 2.1c}$$

In the case of the single flat crystal spectrometers a relatively small γ-source and small slits and/or thin slices of the crystal have to be used in order to obtain good energy resolution, while in the case of a double flat crystal spectrometer a large source is adopted for an increase in luminosity /Kn79/. The geometries of DuMond and Cauchois spectrometers are just reversed beam geometries with the difference that in the DuMond geometry a thin γ-source is used together with an extended detector, whereas the Cauchois spectrometer needs a broad γ-source (large quantities of target material) and a slit in front of the detector or a photoplate.

The curved crystal spectrometers GAMS 1 and GAMS 2/3 /Bö76, Ko80b/ use the DuMond geometry /Du47/. The thin sources needed are especially well suited for an internal target geometry and for studies that require enriched material. With this internal target geometry one can exploit the high neutron flux near the reactor core, thus providing a very strong γ-source. This strong γ-source also compensates for the relatively low luminosity of crystal spectrometers. A general and detailed description of crystal diffraction spectrometers is given elsewhere /Su , Ka79/.

The GAMS 1 and GAMS 2/3 spectrometers use crystals of different thickness (4 mm and 13 mm respectively). The total detection efficiency of a DuMond type spectrometer results from the following factors:

- γ-ray self-absorption in the target
- attenuation of the γ-ray beam on its way from the target to the detector
- reflectivity of the crystal
- transmission loss due to the Soller collimators
- detection efficiency of the NaI detectors.

The beam tube (H6-H7, see Fig. 2.2) is filled with He-gas. However, the attenuation by this He-gas is negligible.

When taking into account reflectivity and absorption the total efficiencies of GAMS 1 and GAMS 2/3 have broad maxima at $\sim$ 200 keV and $\sim$ 400 keV, respectively. The two crystal spectrometers are complementary in view of efficiency in different energy regions.

The focal lengths of GAMS 1 and GAMS 2/3 are 5.8 m and 24 m, respectively. In the energy range where the crystal reflectivity is not saturated and proportional to the crystal thickness, one can establish the following relation for the sensitivity:

$$I \propto t \cdot S/\ell^2 \qquad \text{..... eq. 2.2}$$

I: observed γ-intensity
S: area of crystal
ℓ: distance between the target and the crystal
t: crystal thickness

With the values of t and S given in Table 2.1, one can see that I is nearly equal for GAMS 1 and GAMS 2/3 in the energy range where the crystal reflectivity is not saturated.

In the DuMond geometry, a target movement has to be taken into account. Close to the reactor core at the source position an ambient temperature of $\sim$ 300 ^{o}C is observed due to β- and γ-heating and hence the sources move with an amplitude of $\sim$ 0.1 mm, which generally corresponds to the resolution obtained with the crystals used. This difficulty has been overcome by introducing the "control crystal" in the case of GAMS 1 and the "parallel operation" of GAMS 2 and GAMS 3 /Ko80b/.

Fig. 2.2 shows the whole experimental arrangement of the GAMS 1 and GAMS 2/3 systems at the high flux reactor of the ILL.

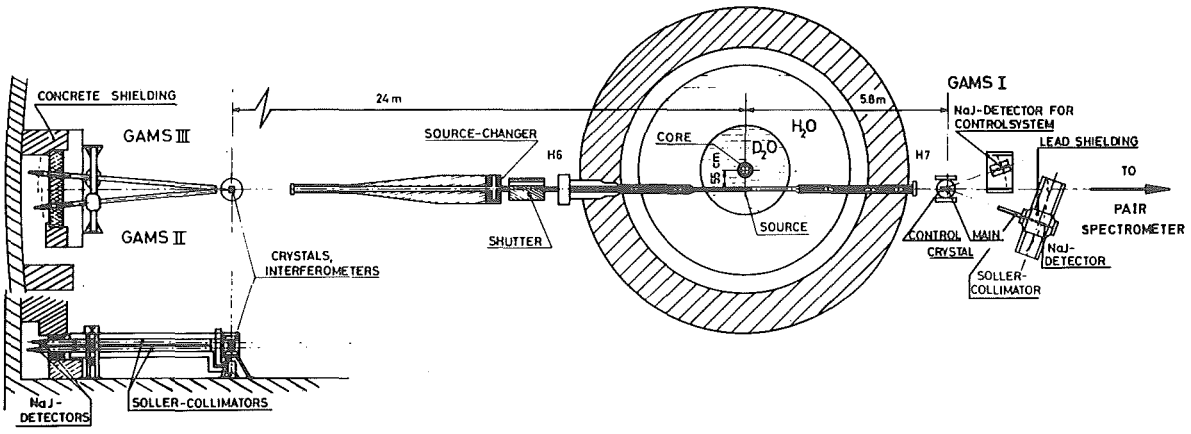

Fig. 2.2 Bent Crystal Gamma-Ray Spectrometers at the Through-Tube H6-H7

The measuring systems of GAMS 1 and GAMS 2/3 are briefly discussed in ref. /Ko80b/.

GAMS 1 uses a control crystal system which corrects for the target movement (Fig. 2.3 and 2.2). An independent γ-ray detection system using a second crystal observes one specific strong γ- (or X-ray) line. In the present a Pb X-ray was used for this purpose. The source movement (Fig. 2.3) is recorded for each measuring point and used later for correction of the γ-ray peak positions (using the peak-fit program (chapter 2.5)). After the correction of the target movement, the reproducilibity of the peak position of the same line is $\sim$ 0.033".

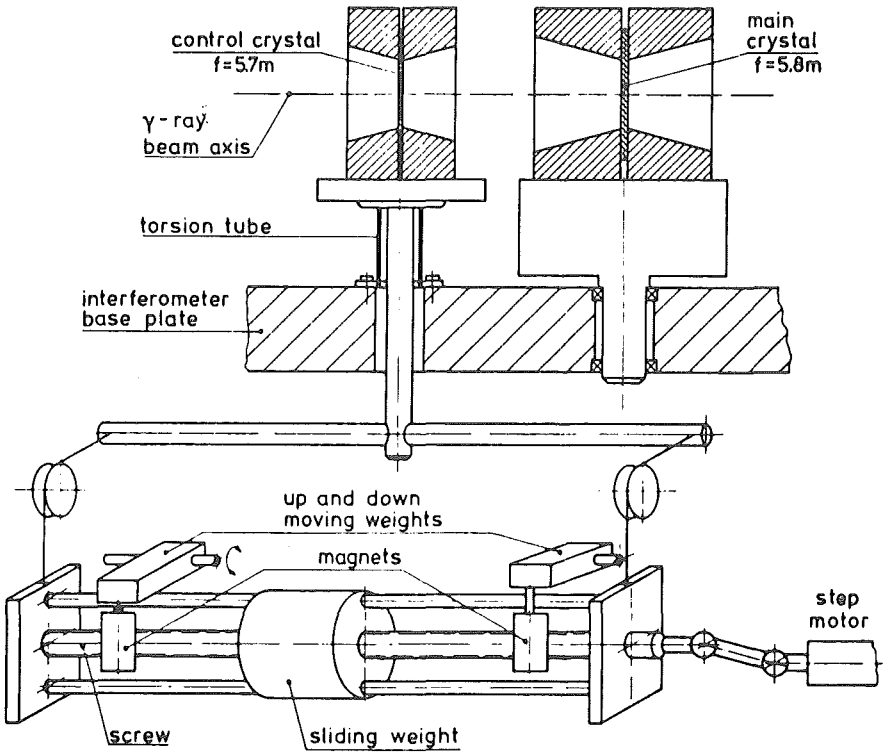

Fig. 2.3 Control Crystal System of GAMS 1 (Figure taken from /Ko80b/).

The high energy precision of GAMS 1 and GAMS 2/3 is achieved by measuring the diffraction angles with an interferometer system. The arrangement for GAMS 1 is shown in Fig. 2.4.

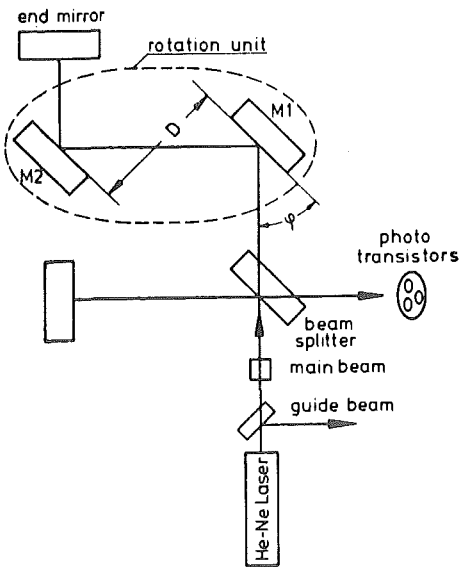

Fig. 2.4

GAMS 1 interferometer system (Figure taken from /Ko80b/).

The length of one light path is changed as a function of

$$L-L_o = 4D\,(\sin(\theta+\varphi) - \sin\varphi) \qquad \text{eq. 2.3}$$

$L-L_o$ is related to the number of interference maxima and minima observed ($N-N_o$; N_o corresponds to $\theta=0$). Using the relation $L-L_o = \lambda_\ell(N-N_o)$ where λ_ℓ is the wave length of He-Ne laser (λ_ℓ = 632.8 nm) the following expression is obtained

$$N = N_o + \frac{4D}{\lambda_\ell}\,(\sin(\theta+\varphi) - \sin\varphi) \qquad \text{eq. 2.4}$$

With eq. 2.1a we find

$$\frac{1}{E_\gamma} = \frac{2d}{nhc}\,\sin\{\arcsin(\sin\varphi + \frac{\lambda_\ell}{4D}\,(N-N_o)) - \varphi\} \qquad \text{eq. 2.4a}$$

In eq. 2.4a the terms $\frac{2d}{hc}$, φ and $\frac{\lambda_\ell}{4D}$ are the characteristical constants of the spectrometer. Actually, $\frac{\lambda_\ell}{4D}$ and N_o are determined by a least-squares fit using ca. 15 prominent γ-lines measured in different orders of diffraction (n = 1,2, 3,4,5,...8). A small change of φ is not sensitive to this least-squares fit; therefore it is always fixed. The term $\frac{2d}{hc}$ is the proportional constant to calculate the γ-ray energy. In the present work this term was determined using the well-known Pb X-ray energy /La77/.

In the case of GAMS 2/3 an interferometer with better precision was needed due to the higher angular resolution ($\Delta\theta \sim 1''$ was achieved in the present experiment of the $^{74}Se(n,\gamma)$ reaction). Fig. 2.5 shows the arrangement of the interferometer for GAMS 2/3. In this arrangement the difference of the light path L_1-L_o caused by the rotation of the diffraction crystal θ is given as follows:

$$L-L_o = 4D\sin\theta \quad \text{and} \quad N-N_o = \frac{4D}{\lambda_\ell}\sin\theta \qquad \text{eq. 2.5}$$

With eq. 2.1a one obtaines

$$\frac{1}{E_\gamma} = \frac{2d}{nhc}\,\frac{\lambda_\ell}{4D}\,(N-N_o) \qquad \text{eq. 2.5a}$$

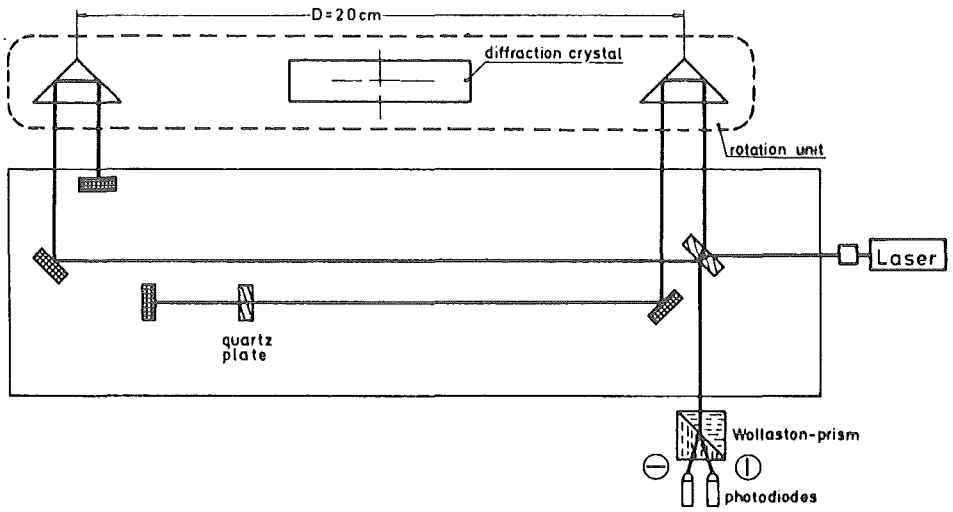

Fig. 2.5 Interferometer System for GAMS 2/3

If the alignment of the two prisms in Fig. 2.5 is not perfect, non-linear terms of $(N-N_0)$ should be added to eq. 2.5a. Practically, for the data evaluation a third order polynomial in $(N-N_0)$ was used

$$\frac{1}{E\gamma} = \frac{2d}{nhc}\frac{\lambda_\ell}{4D}\sum_{m=1}^{3} a_m(N-N_0)^m \qquad \text{..... eq. 2.5b}$$

The coefficients a_m and N_0 are again fitted with a least-squares fit program in a similar manner as for GAMS 1. The proportional constant $\frac{2d}{hc}\frac{\lambda_\ell}{4D}$ is again experimentally determined using a well-known γ-ray (for example, γ-lines already determined by GAMS 1 or any standard γ-rays).

As will be shown later in chapter 3.1, in the process of data analysis, the effect caused by the target movement is cancelled out by the parallel operation of GAMS 2 and GAMS 3. The target movement causes the same amount of shift of interferometer steps ΔN. The numbers of interferometer steps of GAMS 2 and GAMS 3 are changed to be

GAMS 2: $N_{G2} = N+\Delta N$ or $N_{G2} = N-\Delta N$

GAMS 3: $N_{G3} = N-\Delta N$ or $N_{G3} = N+\Delta N$

The numbers N_{G2} and N_{G3} are therefore added

$$N_{G2} + N_{G3} = 2N \ .$$

Actually the diffraction angle is measured by 2N and the evaluation of eq. 2.5b is done by using 2N in place of N.

The spectrometers GAMS 1 and GAMS 2/3 are independently controlled by CAMAC systems based on PDP11 computers (Fig. 2.6). The data are taken point by point at different diffraction angles as mentioned before.

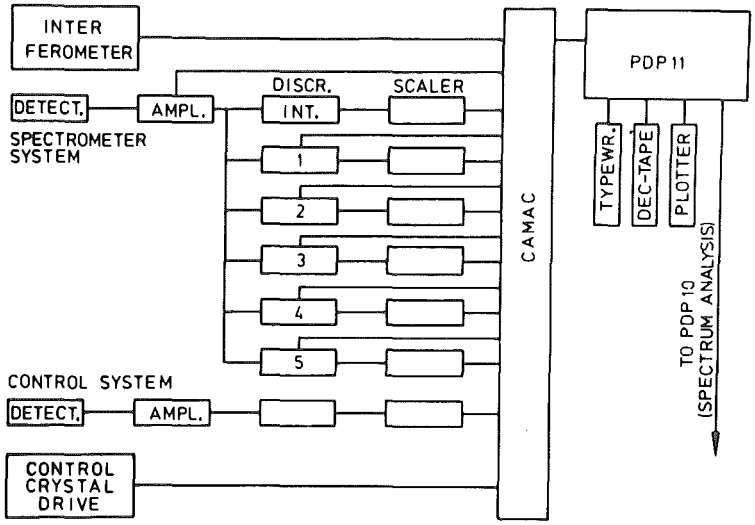

Fig. 2.6
Pulse counting system and CAMAC of GAMS 1 and GAMS 2/3 (Figure taken from /Ko80b/).

In the present work the measuring time for one point was $\sim$ 40 sec in the case of GAMS 1 and $\sim$ 2 min in the case of GAMS 2/3. The measuring time is controlled by the accumulated counts in a ^3He neutron detector, which counts the neutrons scattered from the target and is situated behind the source changer on the G 2/3 side (see Fig. 2.2).

After crystal diffraction the γ-rays are detected by the NaI-scintillation counters. The electronic pulses, after passing the linear amplifier, are fed to six single channel analyser-discriminators (SCA-discriminator). The SCA-discriminators numbered as 1, 2, 3, 4, and 5 in Fig. 2.6 analyse the γ-ray pulses of 1st, 2nd, 3rd, 4th, and 5th order of diffraction from the crystal respectively. The 6th SCA-discriminator accepts the pulses of the total spectrum. The peaks of different orders of diffractions in the pulse height distributions change their positions during the experiment due to the change of crystal diffraction angle. The windows of each numbered SCA-discriminator follow automatically this peak position shift.

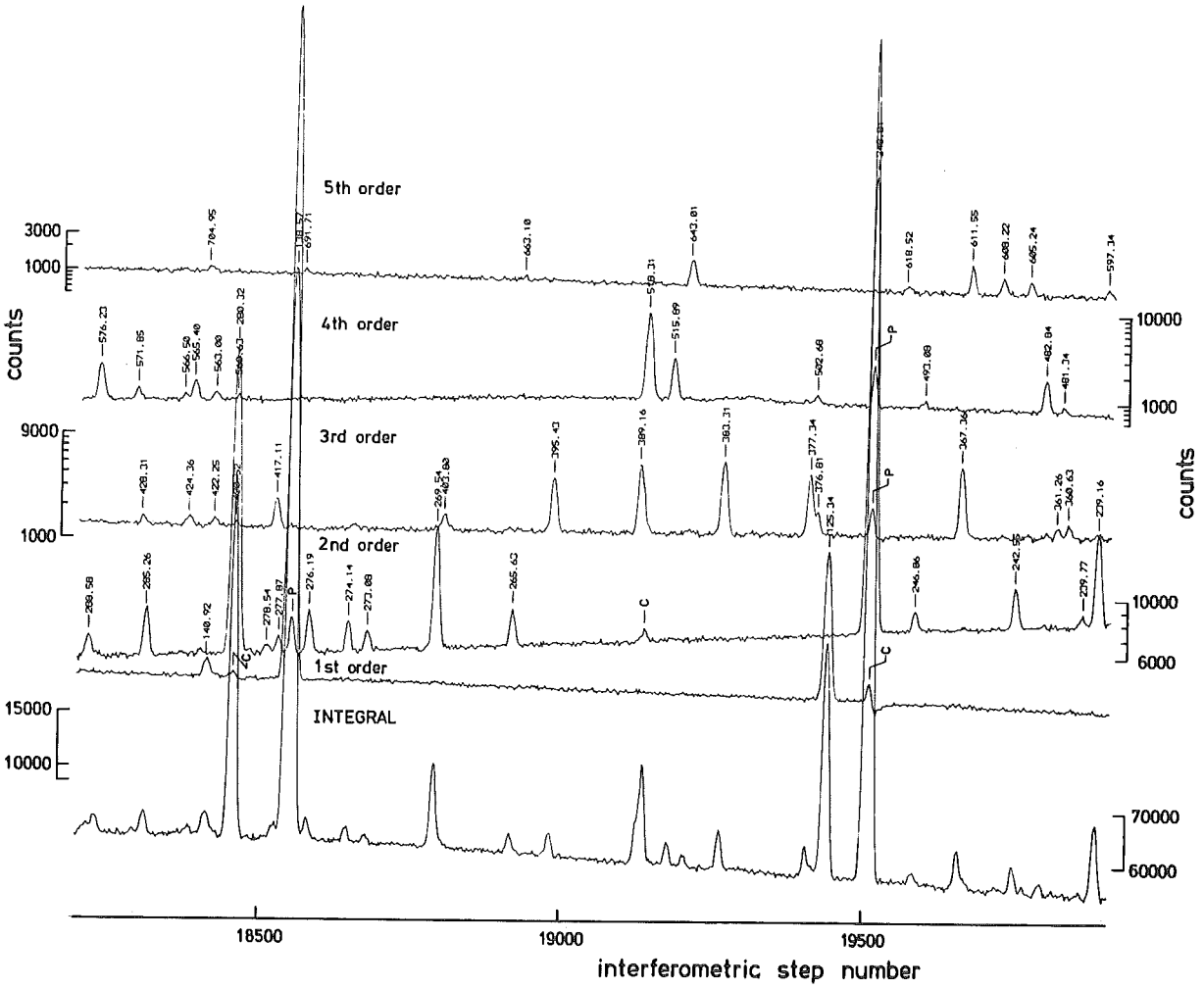

Fig. 2.7 Part of a spectrum in the $^{76}Se(n,\gamma)$ reaction taken with GAMS 1 spectrometer

Figs. 2.7 and 2.8 show a part of a spectrum taken by GAMS 1 and GAMS 2 in the measurement of the $^{76}Se(n,\gamma)$ reaction, respectively. The resolution is $\sim$ 16 eV at 100 keV γ-energy in the 3rd order diffraction in Fig. 2.7 and $\sim$ 100eV(FWHM) at 500 keV γ-energy in the 3rd order diffraction in Fig. 2.8 The resolution of GAMS 1 and GAMS 2 found in the measurement of the $^{74}Se(n,\gamma)$ reaction is schematically depicted in Fig. 2.9, which is clearly showing the superiority of the crystal spectrometer over the semiconductor detectors in the energy range of $E\gamma \lesssim 2$ MeV.

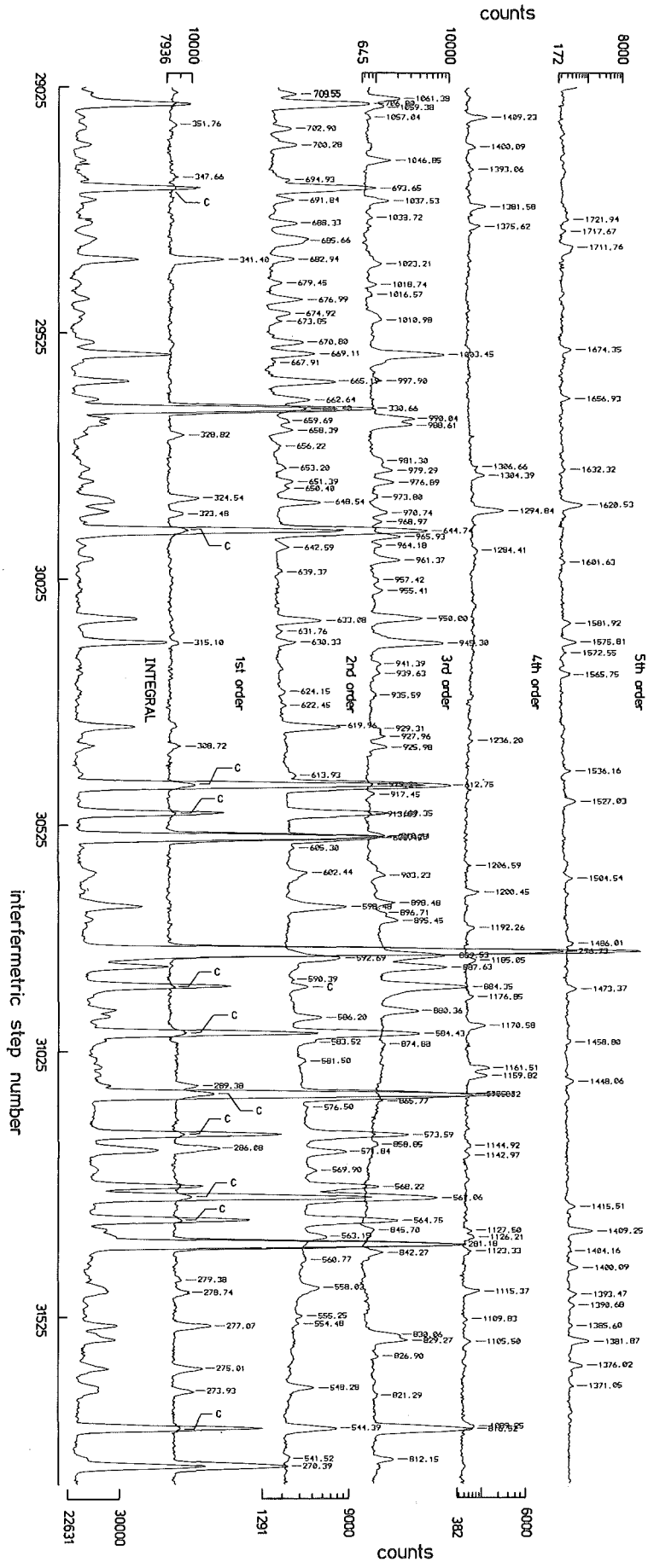

Fig. 2.8 Part of a spectrum in the $^{76}Se(n,\gamma)$ reaction taken with GAMS 2 spectrometer.

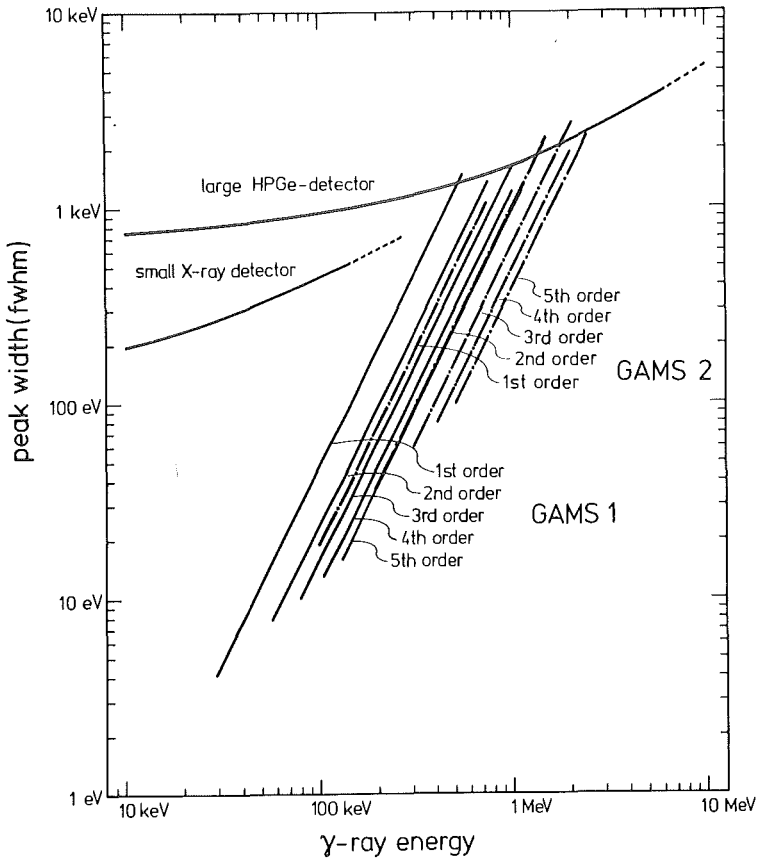

Fig. 2.9

Resolution of GAMS 1 and GAMS 2 found in the $^{74}Se(n,\gamma)$ reaction.

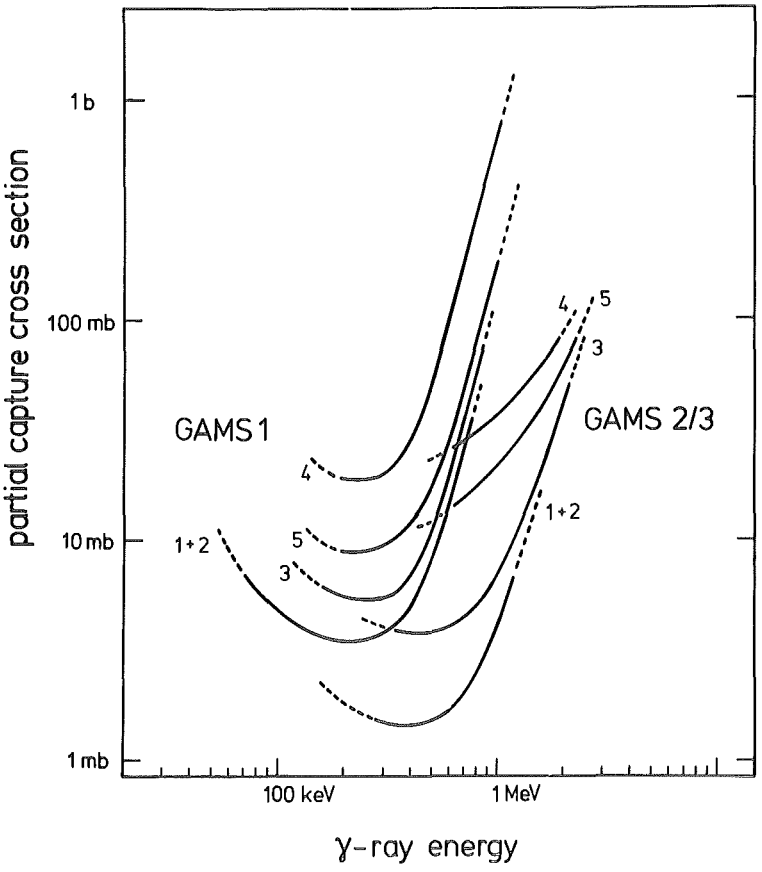

Fig. 2.10

Detection limits for γ-rays in the measurement of the $^{76}Se(n,\gamma)$ reaction.

Fig. 2.10 gives the detection limit for γ-rays by GAMS 1 and GAMS 2/3. One can see in this figure that a dynamic range of GAMS system is more than 10^4.

In the present study the strongest γ-ray was observed up to 8th order diffraction. However data are shown only up to 5th order.

A quick comparison of the outlines of the curved crystal spectrometer GAMS 1 and GAMS 2/3 is given in Table 2.1 /Ko80b/.

Table 2.1 Data characteristic for the curved crystal spectrometers

	GAMS 1	GAMS 2/3
Typical energy range (keV)	30-400	200-1500
Radius of curvature (m)	5.8	24
Angular range (deg.)	-0.5 to 12[a)]	-0.1 to 4.5
Diffraction crystal and lattice plane	quartz, 110	quartz, 110
Reflection orders (recorded in parallel)	n = 1-5	n = 1-5
Product energy x Bragg angle (keV)	$\sim$2.52 x n	$\sim$2.52 x n
Geometrical low-energy limit (keV)	12 x n	32 x n
Crystal thickness (mm)	4	13
Crystal window	38 mm Ø	60 mm x 60 mm
Angular step interval (")	$\sim$0.46	0.16

a) The spectrometer GAMS 1 can be moved on rails towards the reactor in order to fulfill the focusing condition at large angles of reflection.

2.2 The β-spectrometer BILL

The β-spectrometer BILL is a double focusing electron-spectrometer based on iron core magnets (Fig. 2.11)/Ma78/. It is mainly used for conversion electron spectroscopy. The best electron momentum resolution achieved was $\frac{\Delta P}{P} = 8 \times 10^{-5}$ at 300 keV. This resolution and the high energy precision of BILL are superior to GAMS 1, GAMS 2/3 and any semiconductor detectors in the energy range above 700 keV /Ma78/. However, due to the high background and the low conversion coefficient of selenium (Z=34) electron lines were observed only up to 500 - 600 keV (Fig. 1.3).

The target is irradiated at the source position where the thermal neutron flux is 3×10^{14} n/cm^2·s. Conversion electrons emitted from the target fly through the vacuum tube ($\sim 10^{-5}$ torr), pass two energy-analyzing magnets (Fig. 2.11), and are counted by the multi-wire proportional counter (5-wire detector was used in the present work).

The automated point-by-point measurement according to the electron energy is accomplished by the CAMAC system based on the PDP11 computer. The measuring time of each point ($\sim$ 30 sec/point in the present work) is controlled by the integral counts of neutrons, which are scattered from the target and detected by the BF_3 counter. The change of the fields of two magnets corresponding to the electron energy is accomplished by specially designed stabilizers /Ma78/ under the control of CAMAC system. A detailed description of BILL and of the data analysis is given in the works of Jeuch /Je76/ and Braumandl /Br79b/. Data taken by PDP11 computer are transferred to the PDP10 central computer using a DEC tape, for off-line data analysis.

A portion of the spectrum taken in the present work is shown in Fig. 2.12. Intensity calibration of the electron lines is performed together with the calculation of conversion coefficients (see chapter 3.2) using the measured detection efficiency which is given in eq. 2.6 :

$$\text{Efficiency} = \text{Min}(1.0,\ 0.278\times(E_e-10.5)^{0.27}) \qquad \text{.....} \quad \text{eq. 2.6}$$

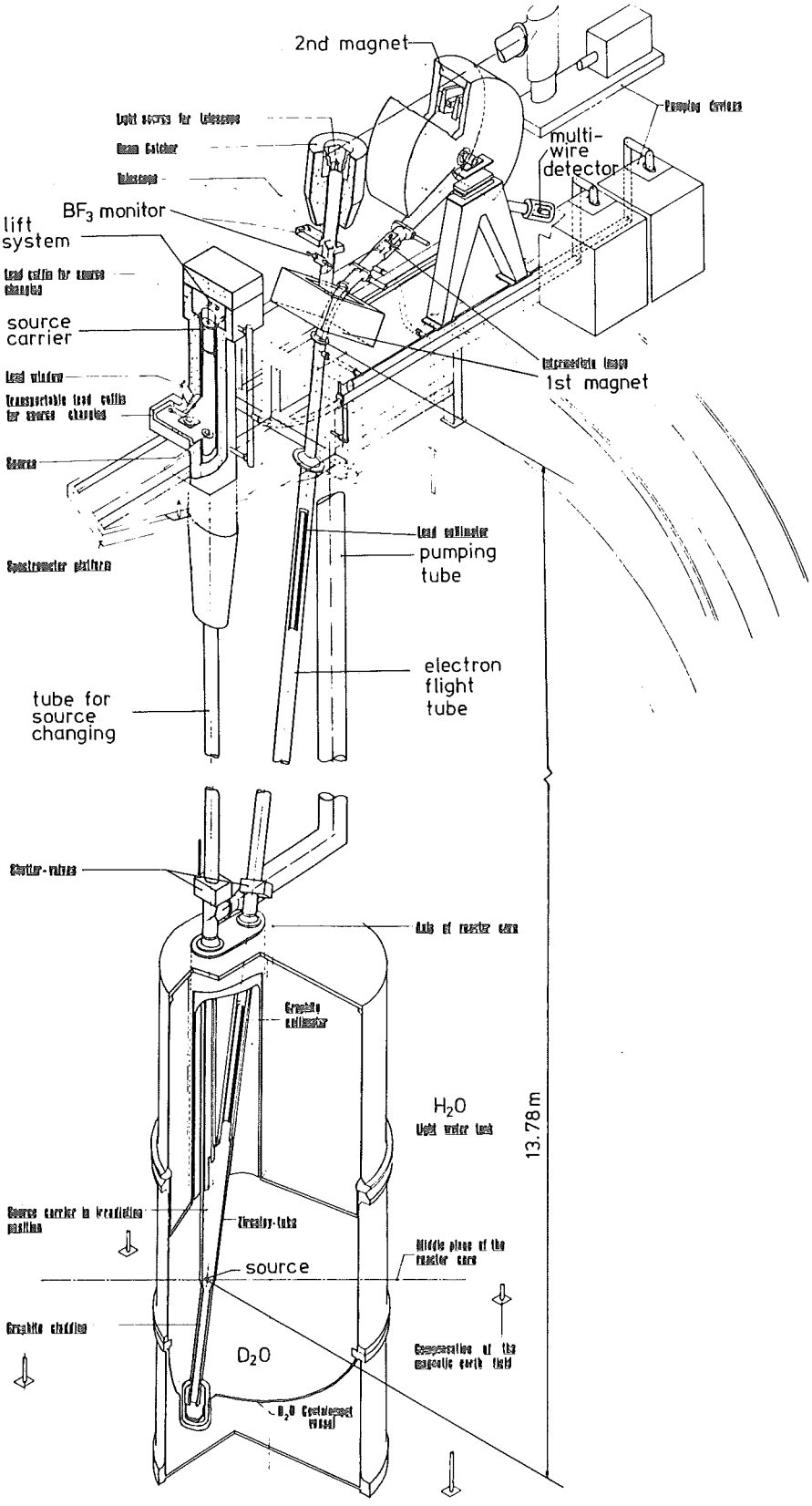

Fig. 2.11 A schematic diagram of the β-spectrometer BILL at the HFR/Grenoble (Fig. taken from /Ma78/)

Energy calibration is performed by the least-squares method using a polynomial function $f(x) = \sum_{i=0}^{n} a_i x^i$, where x is the peak position which is measured as the $B\rho$-value in the case of BILL. The standard variance covariance matrix method was used for minimizing the χ-square to determine the coefficients a_i /Br79a/. Calibrated γ-ray energies from GAMS 1 and GAMS 2/3 were used as reference energies in the present work.

The sensitivity is strongly dependent on the target and the measuring time. In the present work a thin target fabricated by evaporation of target material onto an Al-foil was used (chapter 2.4).

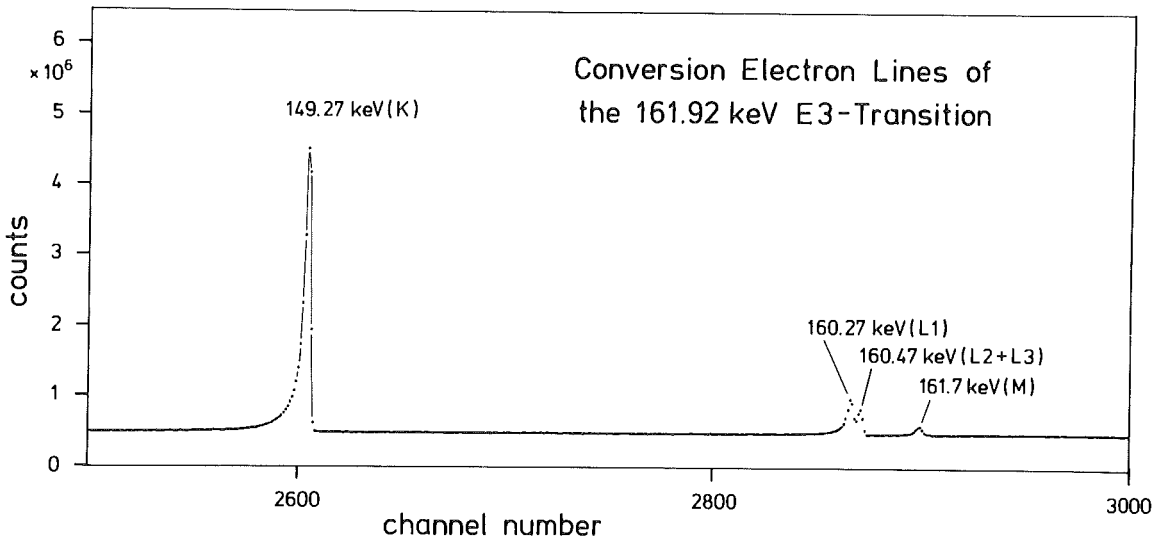

Fig. 2.12 Part of a spectrum taken with the β-spectrometer BILL

2.3 The pair spectrometers in Jülich and in Grenoble

Pair spectrometers are assembled systems of three detection crystals to reduce the background radiation and to extend the dynamic range of the detection system (see Fig. 2.16 and 2.17)

γ-rays with energy of more than 1.022 MeV ($2m_ec^2$, m_e=electron mass) can be detected by pair formation ($e^+ + e^-$). If the γ-rays enter the central (main) crystal (Ge(Li) or pure Ge etc.), a positron created by pair formation makes a positronium after slowing down. Most of the positronium (99.7%) decay into 2 photons of about same energy ($\sim$ 0.511MeV). A detailed description of the positronium is given in /He57/. These 2 photons are emitted in opposite directions, and one of them or both of them can be detected by NaI(Tl)- scintillators, i.e. part of the energy escapes from the central crystal. The rest ($E\gamma-2m_ec^2$) of the energy $E\gamma$ of the incident photon is absorbed by the main crystal.

By the singles measurement of high energy γ-rays using any detectors one usually observes three γ-lines which correspond to the "full energy" peak (100% of the incident energy is absorbed), the "single escape" peak (one annihilation photon (0.511MeV) has escaped) and the "double escape" peak (both of annihilation photons have escaped). The operation as a pair spectrometer eliminates the full energy peak and the single escape peak using a coincidence technique (see Fig. 2.16 and 2.17).

The energy resolution ΔE of a pair spectrometer is that of the main crystal, and is roughly given by the following equation,

$$\Delta E = \sqrt{(\Delta E_N)^2 + C\cdot(E-1.022MeV)} \qquad \ldots\ldots \text{ eq. 2.7}$$

where ΔE_N is the contribution from the electronic circuit, and E is the energy of incident photon. The calculation with experimental data using eq. 2.7 is done in the peak-fit routine (§ 3.3).

The energy calibration of the detection system was done by using the known γ-lines from the reactions, $^{14}N(n,\gamma)$, $^{1}H(n,\gamma)$ and $^{12}C(n,\gamma)$ as will be described in § 3.3.

The intensity calibration was done by using the intensities of γ-rays from the $^{14}N(n,\gamma)$ reaction /Th68/. The efficiency curve of a pair spectrometer can also

be calculated theoretically /En80/, and good agreement between the theoretical and experimental values is obtained for incident γ-energies of $\gtrsim$ 2 MeV. However in the present work the whole energy region which provides an extensive set of data (1.6MeV - neutron binding energy) was calibrated experimentally as mentioned above (§ 3.3).

In summary, the good points of the pair spectrometer are as follows ;

- Background is reduced (large peak-to-Compton ratio)
- The complexity of a singles spectrum in the (n,γ) reaction is largely lightened (elimination of full energy and single escape peaks).
- The width of a double escape peak is narrower than full energy and single escape γ-lines (See eq. 2.7. The single escape γ-line is more broadened due to the inexactly same energy of two annihilation photons), thus providing better resolution.

2.3.1 The pair spectrometer in Jülich

The Jülich pair spectrometer is installed at the research reactor FRJ-2 (DIDO). A 50cm^3 true coaxial Ge(Li)-detector, which was carefully selected to show very good resolution especially for high energy γ-rays (tested by the 7.5MeV doublet of the $^{56}Fe(n,\gamma)$ reaction), is used as the central crystal. Very good resolution (4.2keV(FWHM) at 6MeV) was observed with this system (see Fig. 2.13).

Fig. 2.14 shows the neutron beam geometry. Thermalized neutrons are scattered from a graphite block close to the core up into the target position. The neutron beam passes through several collimators and a Bi-single crystal which filters out neutrons of higher energies than thermal and which strongly absorbs scattered γ-rays. The average wave length of the extracted neutron beam is λ = 2.9 Å (as for the neutron energy spectrum see ref./Ba71/). The FRJ-2(DIDO) reactor is normally operated at 23 MW thermal power. The neutron beam flux at the target position was $\sim 10^8$ n/cm^2·s. The end of the neutron beam tube was filled with constantly flowing He-gas in order to avoid back ground γ-rays from the $^{14}N(n,\gamma)$ reaction.

The target was placed in the middle of a small beam tube which had two coaxial walls, an internal 1 mm graphite wall and an external Aluminum wall(0.3mm thick close to the target position, otherwise thicker). Neutrons scattered by the target are absorbed by ^{6}LiD-powder which is placed into the space between the two walls. Further, the pair spectrometer is covered with 1 cm thick B_4C-plastic to block stray-neutrons. The pair spectrometer unit is well shielded

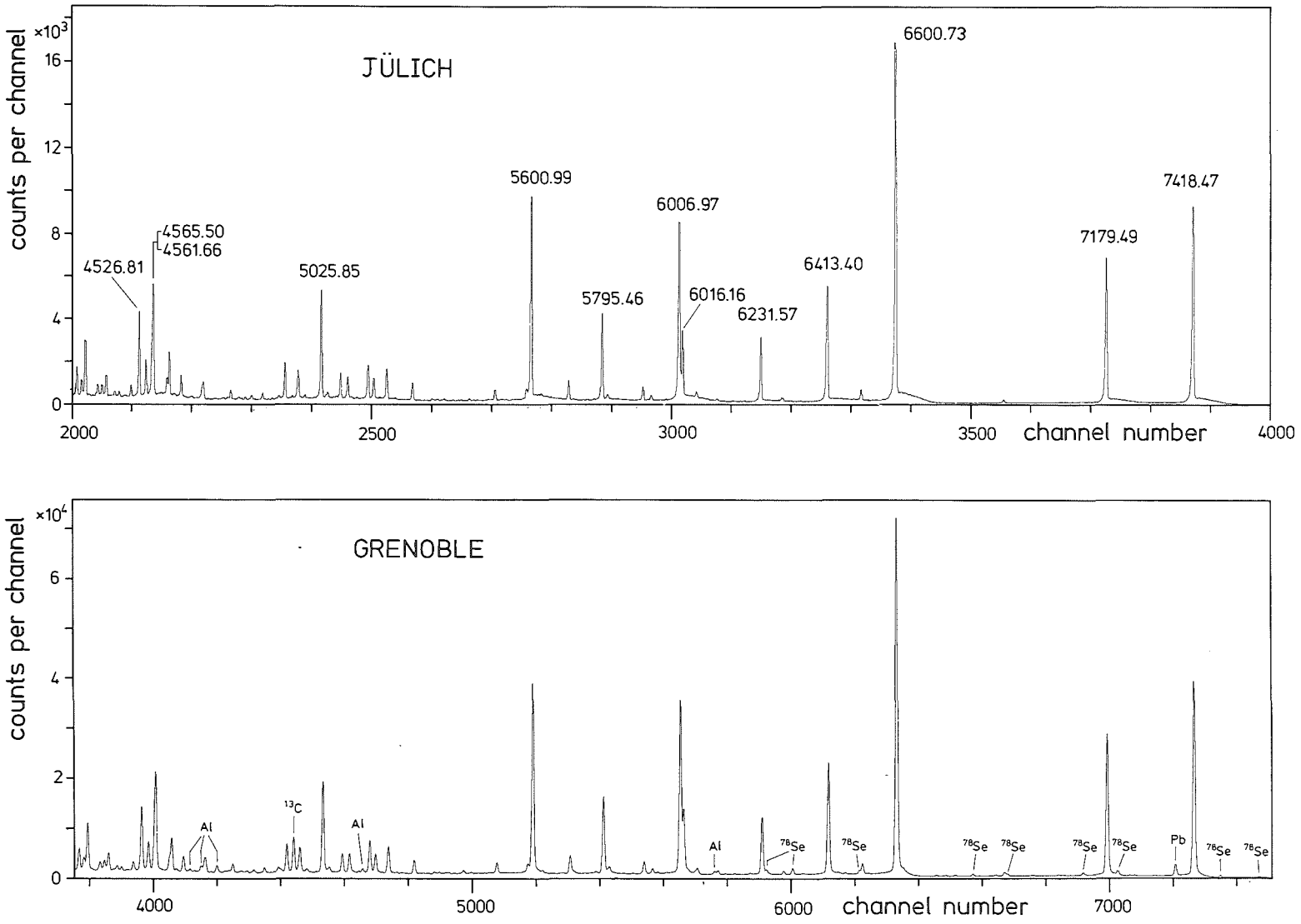

Fig. 2.13 Parts of spectra in the $^{76}Se(n,\gamma)$ reaction taken with the pair spectrometers in Jülich and in Grenoble. The γ-lines marked as ^{78}Se in the lower figure are from the double neutron capture reaction.

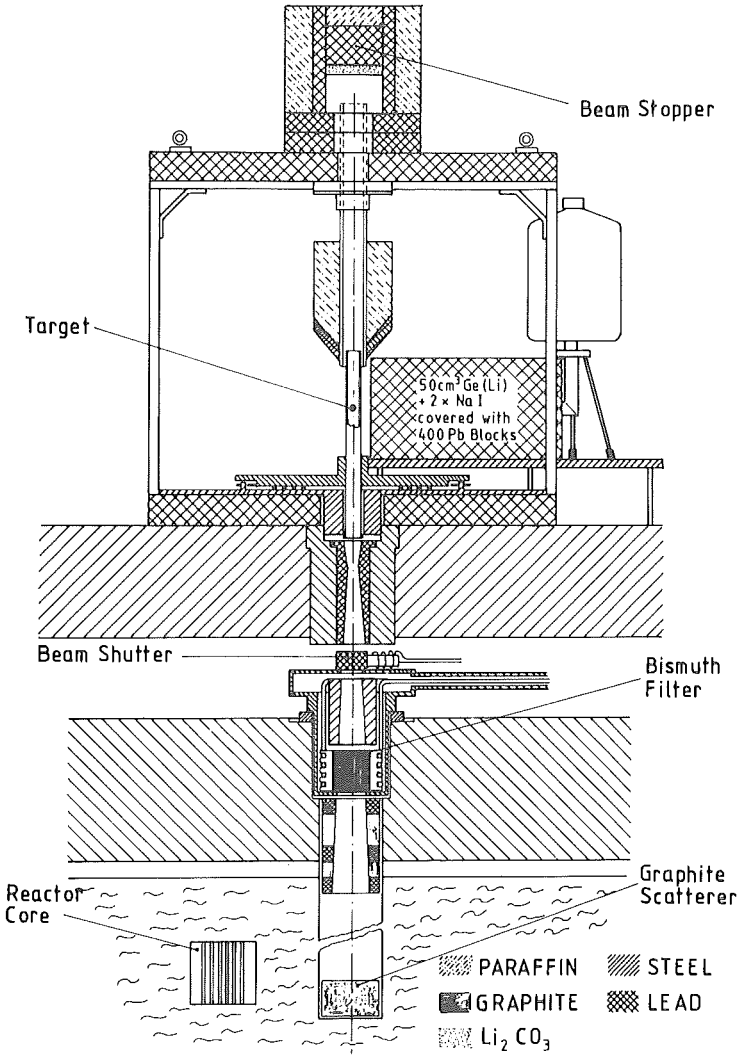

Fig. 2.14

Schematic diagram of the vertical neutron beam tube and the pair spectrometer at the research reactor FRJ-2(DIDO)

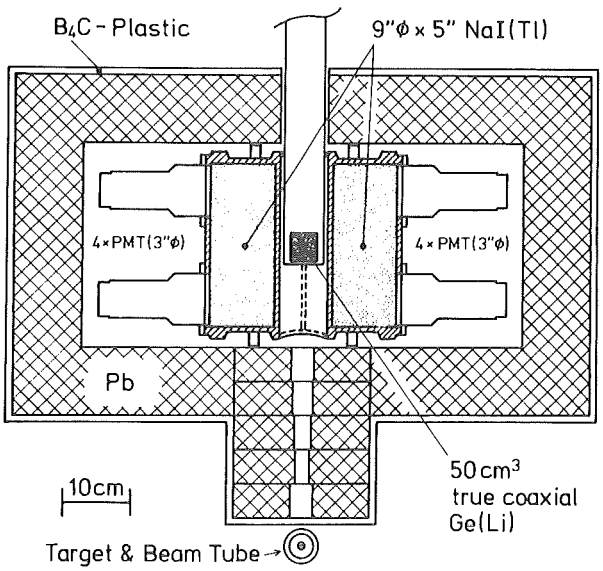

Fig. 2.15

A horizontal cross section of the pair spectrometer in Jülich

from the background γ-rays by surrounding with 400 Pb-blocks of 5×10×20 cm. Both NaI(Tl)-crystals have the same size of 9"ϕ×5". Four 3" photomultiplier tubes are attached to each NaI(Tl)-crystal, and operated in parallel.

The logical coincidence circuit adopted for the Jülich pair spectrometer(Fig. 2.16) is a little different from that of the Grenoble pair spectrometer(Fig. 2.17). While the Grenoble pair spectrometer does coincidence once (1×triple coincidence), the Jülich pair spectrometer performs coincidence twice (2×triple coincidence).

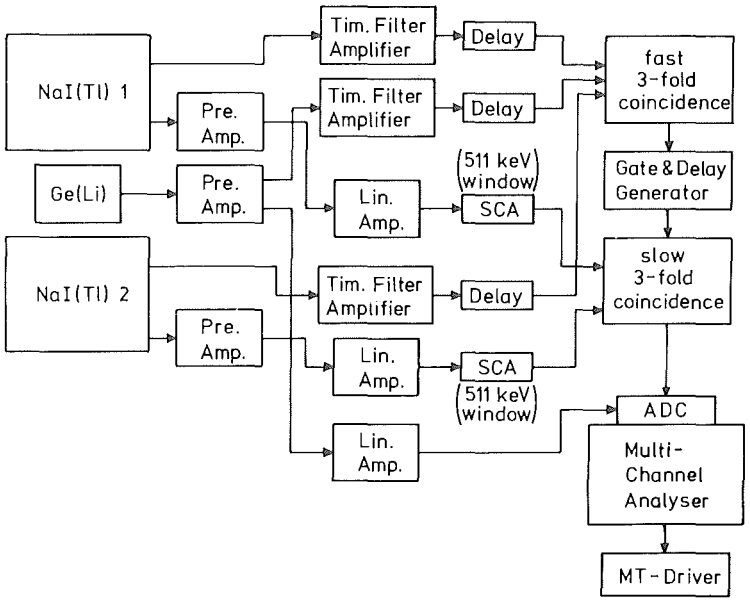

Fig. 2.16

Schematic diagram of the electronic circuit adopted for the Jülich pair spectrometer

As a pulse counting system the Jülich pair spectrometer is more reliable to reject pulses of randam coincidences. However in Grenoble the background γ-rays from the surrounding materials of the detector are practically zero, and only the γ-rays from the beam tube are observed. Thus the total performances of the two pair spectrometers are not so different.

2.3.2 The pair spectrometer in Grenoble

The Grenoble pair spectrometer uses a planar Ge(Li)-central crystal placed between two 6"ϕ × 4" NaI(Tl)-crystals (Fig. 2.17).

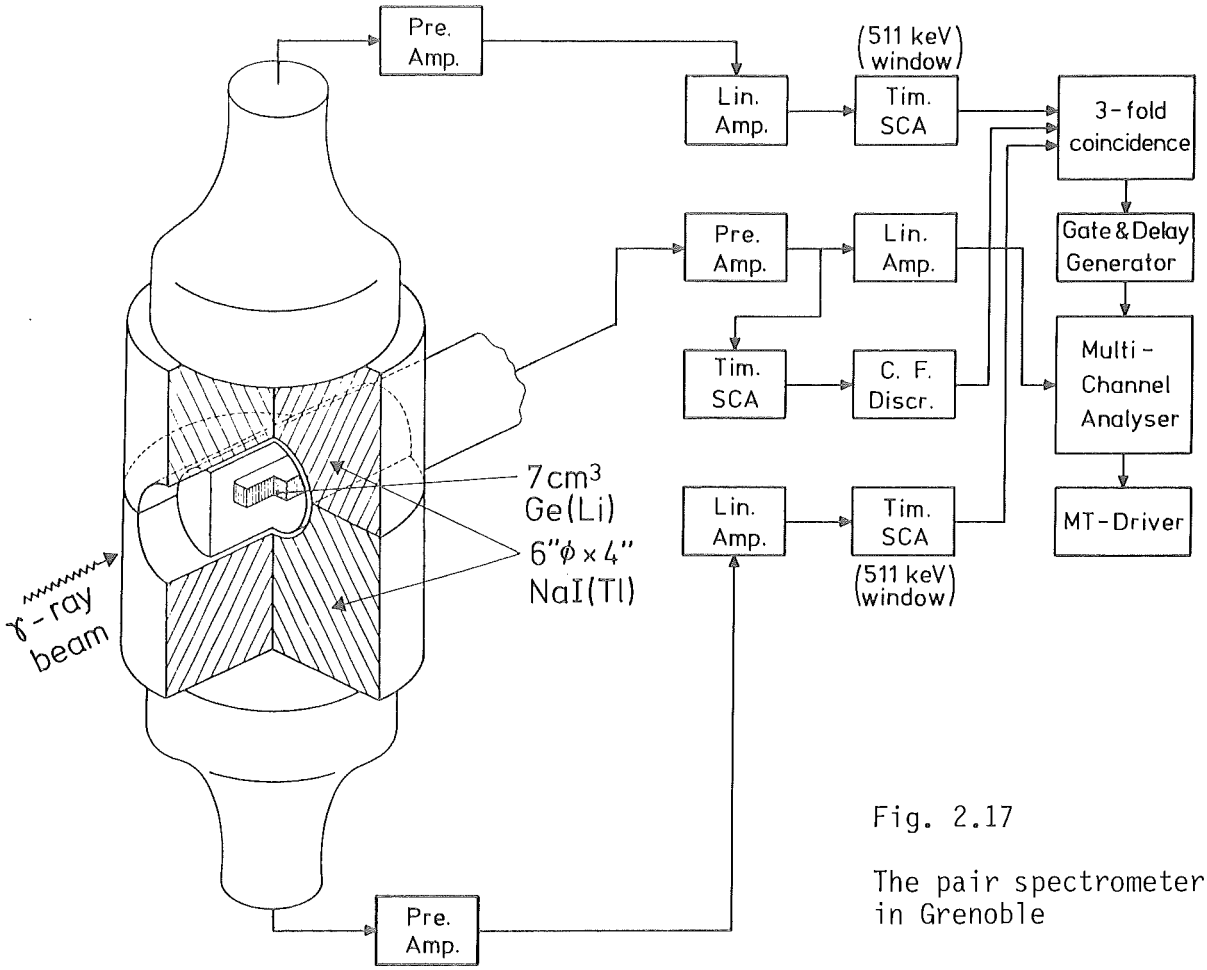

Fig. 2.17

The pair spectrometer in Grenoble

The target used is common with the GAMS spectrometers and placed near the reactor core (internal geometry). The same γ-ray beam tube with the GAMS spectrometers is used for the Grenoble pair spectrometer, which is situated behind the GAMS 1 spectrometer (see Fig. 2.2). The pair spectrometer is operated when the NaI-detector and its surrounding shielding-material of GAMS1 do not block the γ-rays from the target.

Fig. 2.13 shows also a portion of γ-ray energy spectrum taken with the Grenoble pair spectrometer. The resolution observed in this spectrum was 7.0 keV(FWHM) at 6 MeV.

2.4 Targets

In the present work two Selenium isotopes were used as targets for the investigation of the (n,γ) reactions, i. e. $^{74}_{34}Se$ and $^{76}_{34}Se$. Both selenium isotopes were delivered in a form of metal powder. The $^{74}_{34}Se$-metal powder was supplied by U.S.S.R. and the $^{76}_{34}Se$-metal powder by the Oak Ridge National Laboratory/U.S.A. The enrichments of both Se-isotopes specified in their certificates are the following:

Natural Selenium

Isotope	^{74}Se	^{76}Se	^{77}Se	^{78}Se	^{80}Se	^{82}Se
Abundance(%)	0.9	9.0	7.5	23.5	50.0	9.0
(n,γ)-cross section(barns) †	51.8±1.2	85±7	42±4	0.4±0.4	0.610±0.045	0.045±0.003
Contribution to the (n,γ) reaction(%)	4.0	65.6	27.0	0.8	2.6	0.04

$^{74}_{32}Se$ enriched metal powder

Isotope	^{74}Se	^{76}Se	^{77}Se	^{78}Se	^{80}Se	^{82}Se
Abundance(%)	98.85±0.1	1.11	<0.02	<0.02	<0.02	<0.02
Contribution to the (n,γ) reaction(%)	98.2	1.8	<0.016	$<1.5\times10^{-4}$	2.3×10^{-4}	1.7×10^{-5}

$^{76}_{32}Se$ enriched metal powder

Isotope	^{74}Se	^{76}Se	^{77}Se	^{78}Se	^{80}Se	^{82}Se
Abundance(%)	0.14±0.1	96.88±0.1	0.85±0.02	0.99±0.05	0.95±0.03	0.18±0.01
Contribution to the (n,γ) reaction(%)	0.09	99.46	0.43	0.005	0.007	0.0001

† Ref./Mu73/

Table 2.2 Comparison of Natural Selenium and the enriched isotopes (Natural Selenium was not used for the experiment)

For the measurements in Jülich the enriched Selenium metal powder was used without special treatment or processing of the powder, since the external geometry is exploited (no serious γ- and β-heating in the target). In contrast the experiments in Grenoble are done adopting the internal geometry. Temperature as high as $\sim 300^{\circ}C$ in the GAMS target position and $\sim 250^{\circ}C$ in the BILL target position /Bö79,Sc79a, Ma81/ do not permit the use of metallic Se-targets, because Se-metal melts at $217^{\circ}C$ and boils at $685^{\circ}C$ in a atmospheric pressure, while SeO_2 sublimates at $\sim 315^{\circ}C$. Further this problem might be more serious in vacuum at the BILL-target position and in low pressure (3 Torr He-gas) at the GAMS-target position. Therefore a special treatment was required for the targets used in Grenoble. The use of Selenium in the form of Pb-Se(50%-50%) binary alloy was thought to be best suited to overcome this problem from the following reasons,

- High melting temperature of $\sim 1076^{\circ}C$ /Ha58/.
- Low neutron capture cross section of Pb (σ_{γ} = 0.17b,natural Pb) and the very simple γ-ray energy spectrum from the Pb(n,γ) reaction (practically only one γ-line could be observed, see Fig. 2.26) /Ma72/.

The ^{74}Se- and ^{76}Se-enriched metal powder were transformed into the Pb^{74}Se- and Pb^{76}Se-alloy respectively, and those alloys were again ground into powder for the use as GAMS- and BILL-targets.

In the following sections the shape of the targets used in Grenoble and in Jülich are described.

2.4.1 Target for the experiments with the GAMS crystal spectrometers and the Grenoble pair spectrometer

The targets used in GAMS- and pair spectrometer experiments consist of three basic materials: target powder, Al-wrapping foil and carbon holder. The targets are prepared in the following order,

1. wrap the target powder with thin Al-foil(0.025mm thick and 6.7mg/cm^2)
2. press the wrapped target
3. sandwich with two graphite holders (see Fig. 2.19)

After pressing the target material (powder) packed in a highly pure aluminium (99.99 %) foil has a size of 50 mm (length) x 4 mm (width). The total thickness was $\sim$ 0.15 mm and depends also on the quantity of target powder. The thickness of the part of target powder was $\sim$ 0.08 mm for both Pb ^{74}Se- and Pb ^{76}Se-targets. The actual and effective thickness of the part of target powder can be later calculated using a γ-ray line width in the γ-ray energy spectrum taken with the GAMS1 and GAMS 2/3 crystal spectrometers.

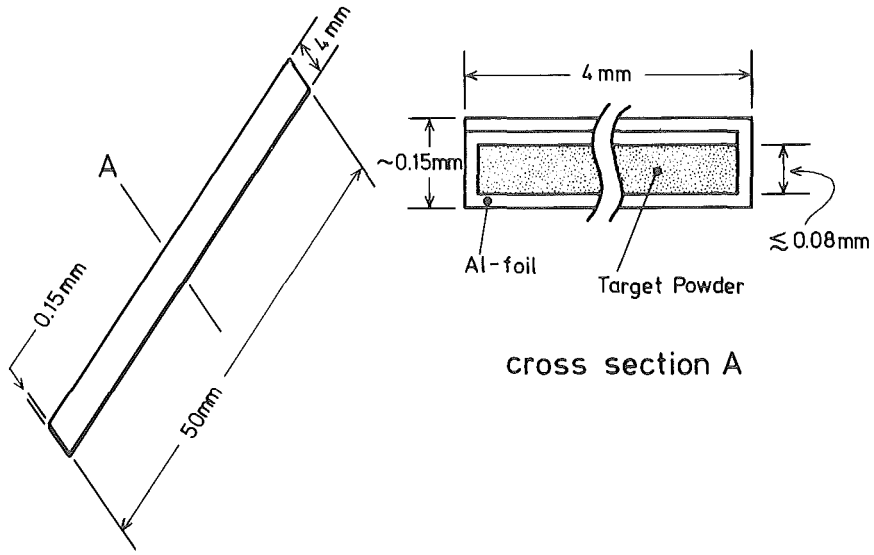

Fig. 2.18 Target used in the experiments with GAMS- and pair spectrometer in Grenoble.

The quantity of Pb ^{74}Se powder in the experiment of the ^{74}Se(n,γ) reaction was 75 mg, and 43.2 mg Pb ^{76}Se powder was used for the experiment of the ^{76}Se(n,γ) reaction.

The target shown in Fig. 2.18 is sandwiched by two graphite holders (Fig. 2.19). This target is transferred to the irradiating position by the source changer from the side of GAMS 2/3 (Fig. 2.2).

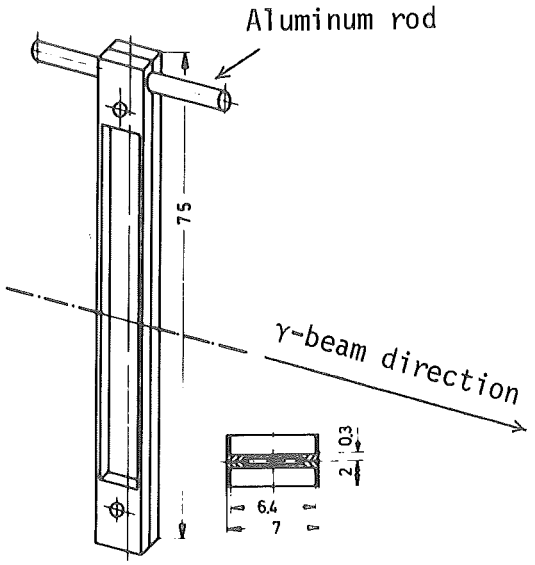

Fig. 2.19 A graphite target holder used in the experiments with GAMS and pair spectrometer in Grenoble

The total γ-ray spectrum does, therefore, contain not only the γ-rays from the (n,γ) reaction of the target sample but also the γ-rays from the target holder and the wrapping material of the target powder.
However, as one can easily see from this target shape, the γ-lines arising from the Al(n,γ) and C(n,γ) reactions can be very easily distinguished from the other (n,γ) reactions. These γ-rays have always very broad line widths and the γ-lines from the Al(n,γ) reaction are strongly asymmetric in the spectrum taken with GAMS 1 and GAMS 2/3 crystal spectrometers (see also § 3). The effect of the γ-ray self absorption in the target is not negligible in the lower energy. The γ-ray attenuation by this self absorption was corrected by the following coefficient assuming an isotropic distribution of the target powder in the target.

In the case of a binary alloy of PbSe the mass attenuation coefficient is the average of two mass attenuation coefficients of Pb and Se, and this averaged attenuation coefficient is given as

$$\mu_{\text{average}} = \frac{\mu_{Pb} M_{Pb} + \mu_{Se} M_{Se}}{M_{Pb} + M_{Se}} \qquad \ldots\ldots \text{ eq. 2.8}$$

where μ_{Pb} and μ_{Se} are the mass attenuation constants of Pb and Se, respectively and M_{Pb} and M_{Se} are the atomic weights of the elements Pb and Se, respectively.

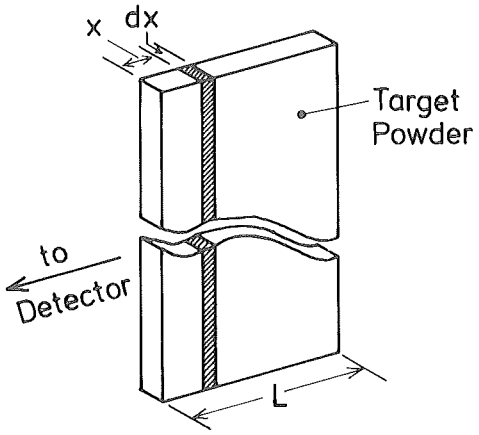

(see also Fig. 2.18)

ρ : density

μ : mass attenuation coefficient

Gamma rays from the small slice dx suffer an attenuation of

$$e^{-\mu \int_0^x \rho \, dx}$$

This must be averaged over the whole target region,

$$\frac{\int_0^L \rho \, e^{-\mu \int_0^x \rho \, dx}}{\int_0^L \rho \, dx} = \frac{1-e^{-\mu \rho L}}{\mu \rho L}$$

(In the case of isotropic distribution of powder)

Fig. 2.20 Calculation of the coefficient of the γ-ray self attenuation

Actually inhomogeneity of target powder distribution and other target material affect the attenuation coefficient calculated above. Therefore, the value of μ was used as a parameter to provide the best result (best fit) in the intensity calibration procedure (§ 3.1).

2.4.2 Target for the experiments with the ß-spectrometer BILL

There are two methods to prepare targets for the measurements with BILL spectrometer, i. e. the evaporation method and the precipitation method. The precipitation method provides stronger electron sources, but generally worse energy resolution in the low energy region ($\lesssim$ 500 keV). In the present work the evaporation method was used.

Target material (Pb ^{74}Se or Pb ^{76}Se) was evaporated onto a extraordinarily thin Al-foil ($\sim$0.22 mg/cm^2). The size of the foil is about 14 cm x 4 cm and the evaporated area is 11 cm x 2 cm (Fig. 2.21). For the target of the experiment on the ^{74}Se(n,γ) reaction 12.9 mg of Pb ^{74}Se was evaporated onto the Al-foil and 5.0 mg of Pb ^{76}Se for the experiment on the ^{76}Se(n,γ) reaction.

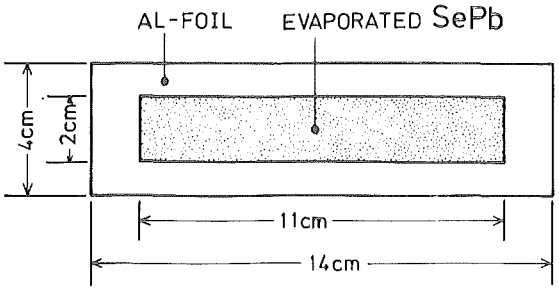

Fig. 2.21 Target made by evaporation for the measurements with BILL

This target is fixed in the graphite target holder (see /Bl81/) and brought down to the irradiating position through a vacuum tube using the source carrier system (see Fig. 2.11).

The observed background electrons and undesired electron lines were the following

- electrons observed as smooth continuous background which originates in the β^--decay of ^{28}Al after neutron capture in ^{27}Al
- external conversion electrons of γ-rays from the $Zr(n,\gamma)$ reaction by Pb (Pb Se target). The γ-rays of the $Zr(n,\gamma)$ reaction come from the wall of zircalloy tube (see Fig. 2.11)
- external conversion electrons of γ-rays from the $Se(n,\gamma)$ reaction by Pb (Pb Se target)

Elimination of the external conversion lines and the contaminant lines were achieved during the procedure of data analysis.

2.4.3 Target for the experiments with the Jülich pair spectrometer

For the measurements with the Jülich pair spectrometer four different targets were prepared, i. e. two targets of ^{74}Se and ^{76}Se metal powder for the $^{74}Se(n,\gamma)$ and $^{76}Se(n,\gamma)$ reactions respectively, and two targets for the γ-ray energy calibration of these two reactions.

In the case of the targets for the $^{74}Se(n,\gamma)$ and $^{76}Se(n,\gamma)$ reactions metal powder of ^{74}Se ($\sim$ 60 mg) and ^{76}Se ($\sim$ 50 mg) were enclosed in thin mylar foil, then these are fixed to a graphite rod and suspended from the middle

of the target holder (see Fig. 2.22). The clearly observed contaminant γ-rays were only from the Cl(n,γ) reaction (§ 3). These γ-rays were later identified as contamination of the outer surface of mylar foil and the graphite rod because the same target powder was used for the experiment in Grenoble and there were found much less contaminant γ-lines.

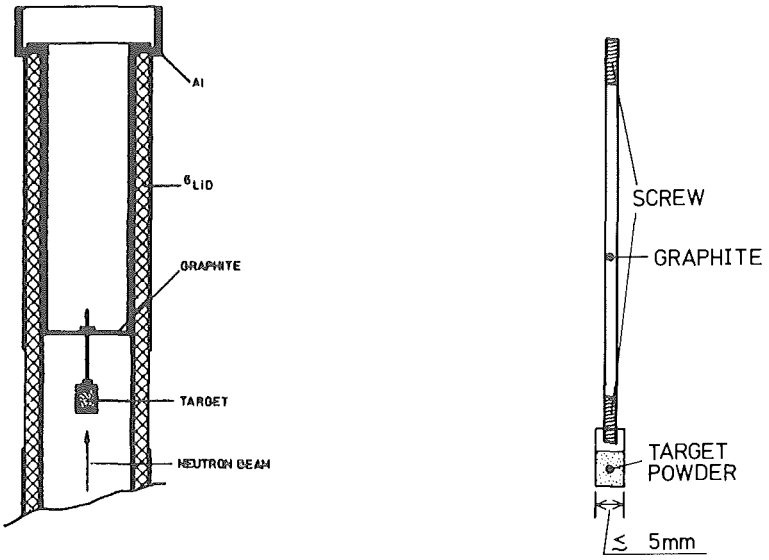

Fig. 2.22 Target and Target holder for the measurements with the pair spectrometer in Jülich (see also § 2.3.1)

For the energy calibration measurements ca. $\frac{1}{3}$ - $\frac{1}{2}$ of the selenium metal powder used in the above mentioned $^{74}Se(n,\gamma)$ and $^{76}Se(n,\gamma)$-measurements was irradiated together with urea which was packed in a small graphite box (see the left figure in Fig. 2.22). The γ-rays from the $^{1}H(n,\gamma)$ and $^{14}N(n,\gamma)$ reactions were used for the energy calibration (§ 3.3).

2.5 Summary of all the experiments carried out in Jülich and in Grenoble

Three types of measurements were performed in different lengths of periods, with different targets and under different conditions using the GAMS, BILL and pair spectrometers. Table 2.4 (see next page) summarizes all experiments done in Jülich and in Grenoble, and shows a quick review of them.
In addition, an experiment for the detection efficiency calibration of the Grenoble pair spectrometer was done by C. Hofmeyr in Feb. 1980 using a target of Melamine + Aluminum (§ 3.3)

Below the additional informations on the resolutions of the GAMS spectrometers are given,

$^{74}Se(n,\gamma)$

$$\text{GAMS 1}: \quad \Delta E = \frac{4.8 \times 10^{-6} \times E\gamma(keV)^2}{n} \quad keV$$

$$\text{GAMS 2}: \quad \Delta E = \frac{1.9 \times 10^{-6} \times E\gamma(keV)^2}{n} \quad keV$$

$$\text{GAMS 3}: \quad \Delta E = \frac{2.0 \times 10^{-6} \times E\gamma(keV)^2}{n} \quad keV$$

$^{76}Se(n,\gamma)$

$$\text{GAMS 1}: \quad \Delta E = \frac{7.9 \times 10^{-6} \times E\gamma(keV)^2}{n} \quad keV$$

$$\text{GAMS 2}: \quad \Delta E = \frac{2.3 \times 10^{-6} \times E\gamma(keV)^2}{n} \quad keV$$

$$\text{GAMS 3}: \quad \Delta E = \frac{2.9 \times 10^{-6} \times E\gamma(keV)^2}{n} \quad keV$$

Table 2.3 Energy resolution(FWHM) of GAMS spectrometers observed in the $^{74}Se(n,\gamma)$ and $^{76}Se(n,\gamma)$ reactions.

Target	Instrument	Resolution (FWHM)	Total measuring time	Term of experiment	Spectra code name
$Pb^{74}Se$	GAMS 1, 2/3	2.8 steps(GAMS 1)[a]	22 days	Jan. 1980	C4
$Pb^{74}Se$	BILL	0.2 keV at 160 keV	16 days(2 runs)	March 1980	B4
$Pb^{74}Se$	Pair(Grenoble)	7.2 keV at 6 MeV	5 days(3 runs)[b]	Jan. 1980	PG4
^{74}Se(ca.50mg)	Pair(Jülich)	5.5 keV at 6 MeV	∿ 100 hours[c]	Nov. 1979	PJ4
^{74}Se + Urea	Pair(Jülich)	5.3 keV at 6 MeV	63 hours	Nov. 1979	PC4
$Pb^{76}Se$	GAMS 1, 2/3	4.6 steps(GAMS 1)[a]	40 days	July-Aug. 1979	C6
$Pb^{76}Se$	BILL	0.2 keV at 160 keV	16 days(2 runs)	Sep. 1979	B6
$Pb^{76}Se$	Pair(Grenoble)	7.0 keV at 6 MeV	2 days	July-Aug. 1979[d]	PG6
^{76}Se(ca.60mg)	Pair(Jülich)	4.2 keV at 6 MeV	70 hours	Oct. 1979	PJ6
^{76}Se + Urea	Pair(Jülich)	4.2 keV at 6 MeV	71 hours	Oct. 1979	PC6

a) 1 step=2 interferometer step number ∿ 1" angular resolution ∿ 0.2 keV at 484 keV of 2nd order reflection

b) See §2.6. Only the 3rd spectrum is partly analysed(1.5 MeV - 3 MeV and 5.1 MeV - 11.2 MeV). The measuring time of 3rd spectrum is ca.70 hours.

c) System stopped because of current shutdown.

d) This spectrum was anlysed but the results are not quoted in the present work, because the pair spectrum taken in Jülich has shown much better quality.

Table 2.4 List of experiments performed in the present work

2.6 Double neutron capture in the ^{74}Se nucleus

The product nucleus after single neutron capture in ^{74}Se has a half life of ca. 120days and decays to ^{75}As by electron capture. No evidence for the neutron capture reaction on this β-unstable ^{75}Se has been reported until now. However, one might expect that this reaction would occur for the following reasons,

1. From the systematics of the thermal neutron capture cross section σ, one may conclude that the ^{75}Se nucleus also has a cross section of the order of σ = 10 - 100 b .

Isotope	^{74}Se	^{75}Se	^{76}Se	^{77}Se	^{78}Se	^{79}Se	^{80}Se	^{81}Se	^{82}Se
Cross section(b)	51.8	?	85	42	∿0.5	?	0.61	-	0.045

Table 2.5 Cross sections of selenium isotopes (Data from /Mu73/)

2. Even with a small neutron cross section of ^{75}Se one might observe the γ-rays from the neutron capture in ^{75}Se rather clearly, due to the high resolution and high sensitivity of the GAMS crystal spectrometers, and in the pair spectrum due to the fact that the neutron binding energy of ^{76}Se is about 3 MeV higher than that of ^{75}Se (see Fig. 2.23 and 2.24). So even if these γ-rays are very weak, they might be identified clearly in the low energy region by the GAMS spectrometers and with very low background in the high energy region above the neutron binding energy of ^{75}Se by the pair spectrometer.

In order to clarify these things the related reactions are shown in the schematic diagram given in Fig. 2.23.

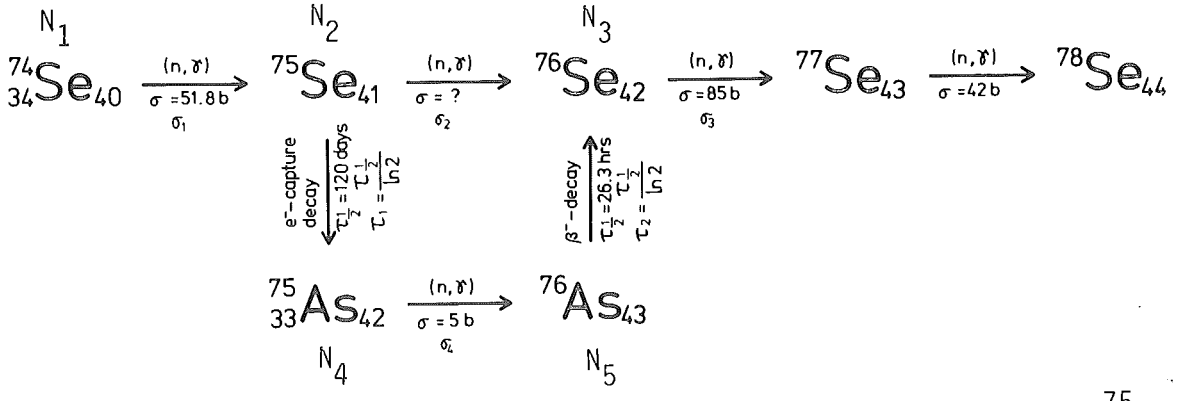

Fig. 2.23 Flow chart of the reactions which are relevant to the $^{75}Se(n,\gamma)$ process following the $^{74}Se(n,\gamma)$ reaction in Grenoble (as for $N_1 \ldots N_5$, $\sigma_1 \ldots \sigma_5$ and $\tau_1 \ldots \tau_5$ see text)

The reason why the high energy γ-rays may be seen in the experiment is shown in Fig. 2.24.

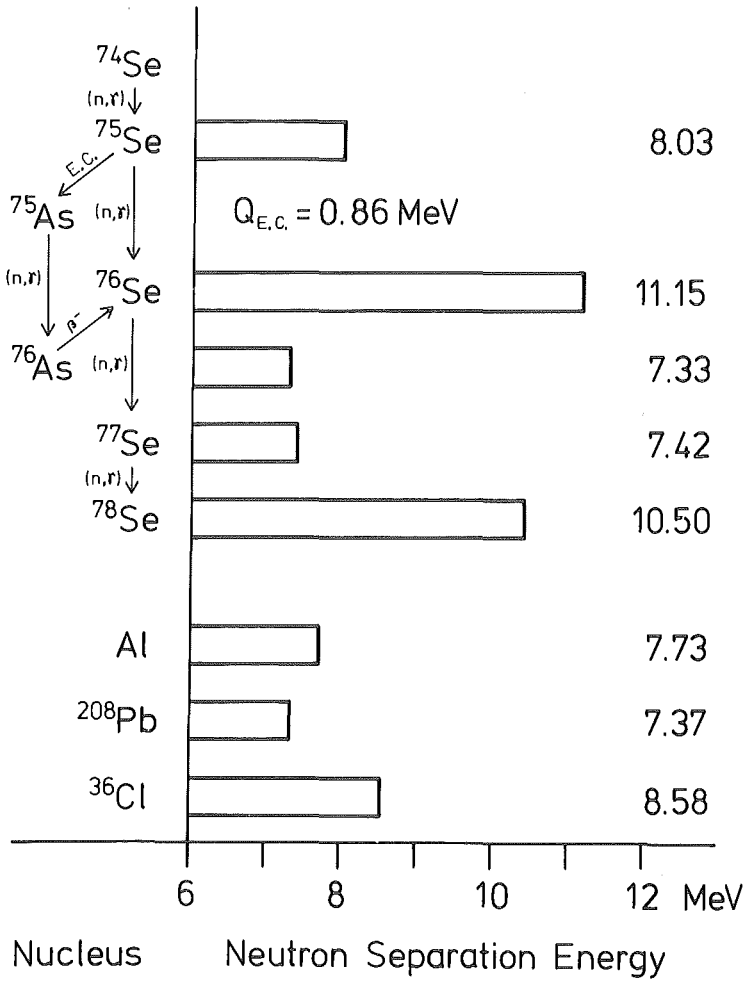

Fig. 2.24

Neutron binding energies of relevant nuclei in the experiment on the $^{74}Se(n,\gamma)$ reaction. The binding energy in ^{76}Se was predicted by the model calculation of Wapstra et al. /Wa77/.

The γ-rays after neutron capture in ^{77}Se may be understood as double capture in ^{76}Se (isotopic impurity, see §2.4). Anyway the γ-rays which belong to ^{78}Se are expected to be not so strong as will be discussed later and their energy spectrum is simple in the high energy region. So these γ-rays do not obstruct the observation of the γ-rays from the $^{75}Se(n,\gamma)$ reaction. Consequently one can easily see in Fig. 2.24 that above 8 MeV almost only the γ-rays from the $^{75}Se(n,\gamma)$ reaction may be expected. This idea proved to be true and is clearly demonstarted in Fig. 2.25 - 2.27. The effect of the binding-energy-difference which enables the easy identification of the double capture γ-rays was already observed in the experiment on the $^{76}Se(n,\gamma)$ reaction (see Fig. 2.13).

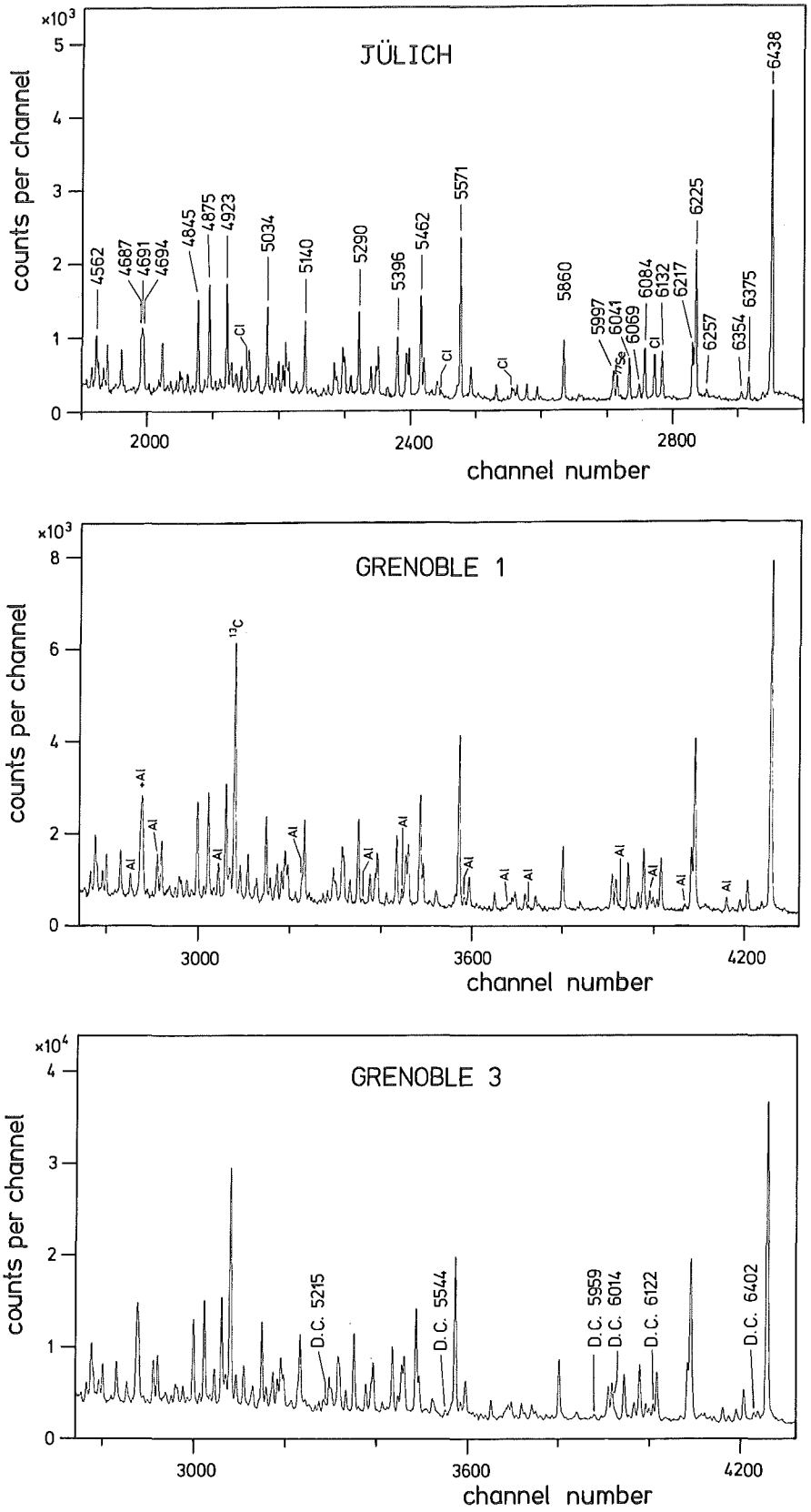

Fig. 2.25 High energy portions of the spectra of the $^{74}Se(n,\gamma)$ reaction taken in Jülich and in Grenoble. The middle spectrum is after one week neutron irradiation at the target position and the bottom one is after four weeks irradiation.

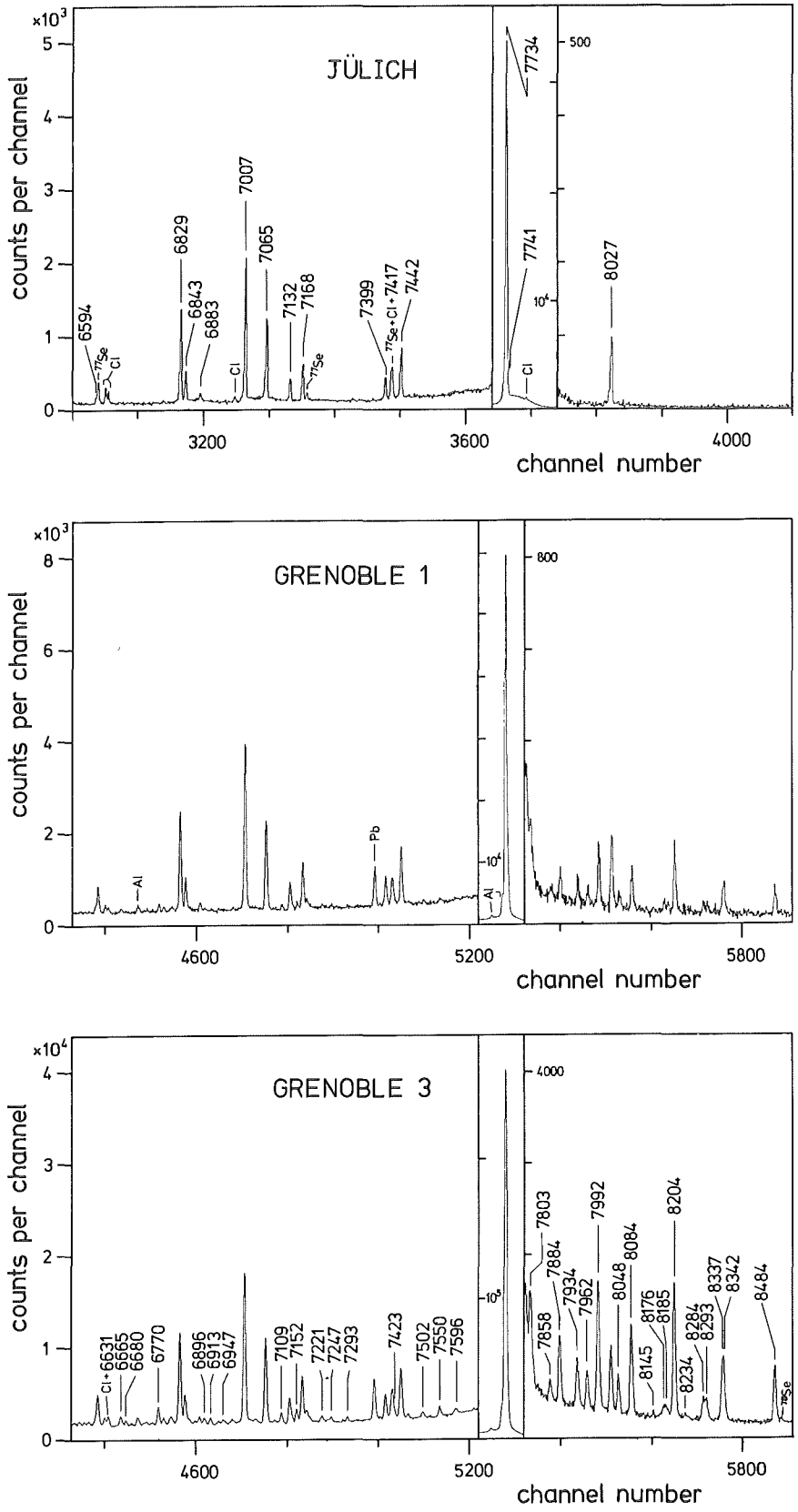

Fig. 2.26 Continuation of Fig. 2.25

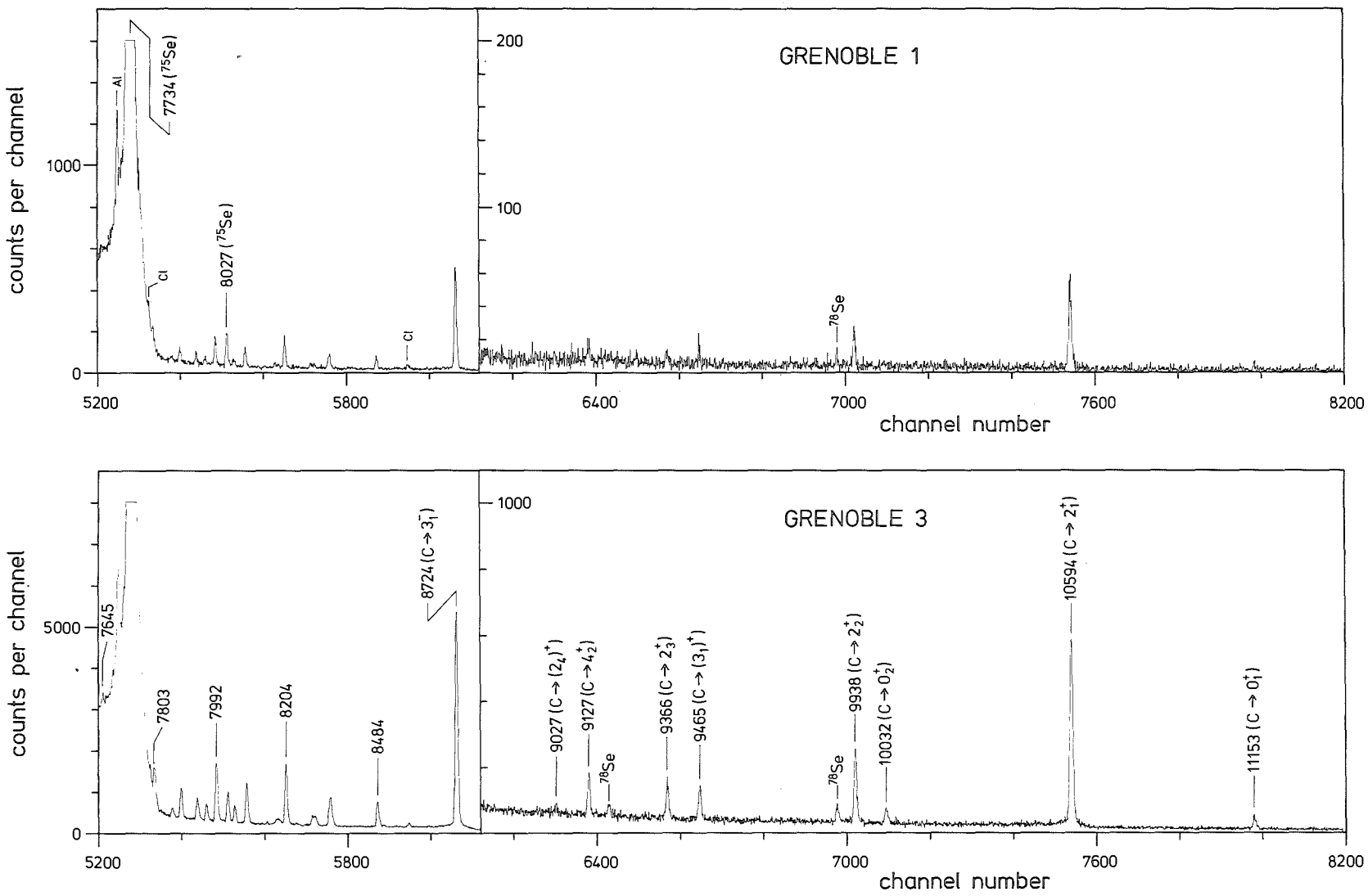

Fig. 2.27 Upper part of the spectrum of the $^{74}Se(n,\gamma)$ and $^{75}Se(n,\gamma)$reactions taken in Grenoble

The identification of the γ-rays after double neutron capture in ^{74}Se as well as the γ-rays after E.C.-decay of ^{75}Se is further facilitated because of their intensities growing with time. Actually this time-growing intensity has played a crucial role in identifying low energy γ-rays in the spectrum taken by the GAMS spectrometers. In order to clarify this situation and to help the later calculation of the thermal neutron capture cross section of ^{75}Se - until now this was unknown - , the change of the intensities of the γ-rays are calculated and shown in the following.
As shown in Fig. 2.23, for simplicity , the quantities of ^{74}Se, ^{75}Se, ^{76}Se, ^{75}As and ^{76}As are symbolized as N_1, N_2, N_3, N_4 and N_5, respectively. The mean lives of ^{75}Se and ^{76}As are replaced by τ_1 and τ_2. We get the following conditions for N_1, N_2, N_3, N_4 and N_5,

$$\frac{dN_1}{dt} = -\sigma_1 \phi N_1 \qquad \ldots\ldots \text{ eq. 2.9}$$

$$\frac{dN_2}{dt} = \sigma_1 \phi N_1 - \left(\sigma_2 \phi + \frac{1}{\tau_1} \right) \cdot N_2 \qquad \ldots\ldots \text{ eq. 2.10}$$

$$\frac{dN_3}{dt} = \sigma_2 \phi N_2 - \sigma_3 \phi N_3 + \frac{1}{\tau_2} \cdot N_5 \qquad \ldots\ldots \text{ eq. 2.11}$$

$$\frac{dN_4}{dt} = \frac{1}{\tau_1} N_2 - \sigma_4 \phi N_4 \qquad \ldots\ldots \text{ eq. 2.12}$$

$$\frac{dN_5}{dt} = \sigma_4 \phi N_4 - \frac{1}{\tau_2} \cdot N_5 \qquad \ldots\ldots \text{ eq. 2.13}$$

ϕ : Neutron flux at the target position of HFR/Grenoble
$= 5.5 \times 10^{14}$ n/cm^2·s (GAMS spectrometer)

The reaction rate R_d of the $^{75}Se(n,\gamma)$ reaction or the double neutron capture in ^{74}Se is defined as $R_d = \sigma_2 \phi N_2$, and the reaction rate $R\beta$ of the electron capture decay of ^{75}Se is given as $R\beta = (1/\tau_1) \cdot N_2$, thus providing an important relationship between R_d and $R\beta$,

$$R_d/R_\beta = \sigma_2 \phi \cdot \tau_1 \qquad \ldots\ldots \text{ eq. 2.14}$$

Eq. 2.14 was used to calculate σ_2 (§ 4.2). In order to evaluate the time-evolution of R_d and R_β the eq. 2.9 and 2.10 should be solved, and the results are,

$$N_1 = N_0 \exp(- \sigma_1 \phi t) \qquad \ldots\ldots \text{ eq. 2.9a}$$

$$N_2 = \frac{N_0 \sigma_1 \phi}{\sigma_1 \phi - \sigma_2 \phi - \frac{1}{\tau_1}} \left\{ \exp(- \sigma_2 \phi - \frac{1}{\tau_1})t - \exp(- \sigma_1 \phi t) \right\} \qquad \ldots\ldots \text{ eq. 2.10a}$$

where N_0 is the initial quantity of N_1 at t=0.

Using the expressions of eq. 2.9a and 2.10a the reaction rate R_d was calculated for the ^{74}Se target, and for several other nuclei (Fig. 2.28).

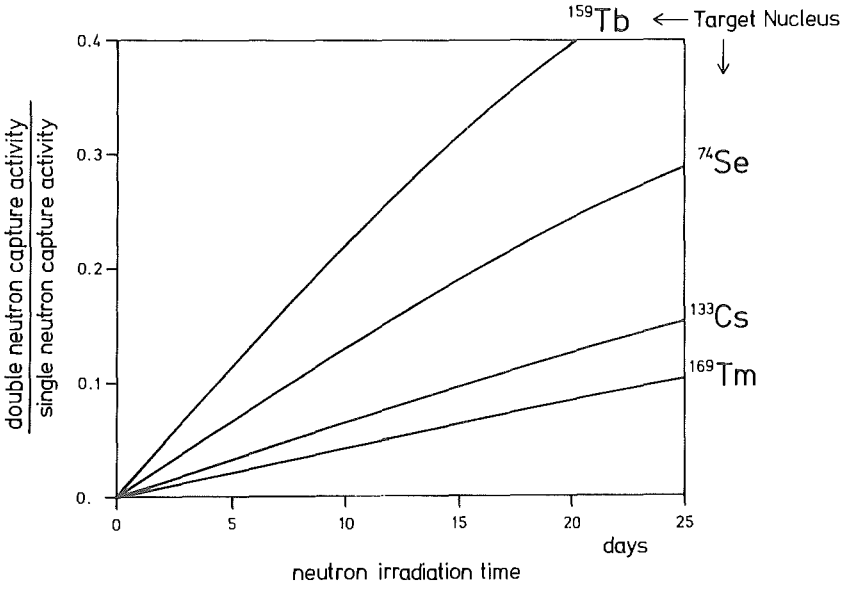

Fig. 2.28

Ratio of the (n,γ)- and $(n,\gamma)^2$-reaction rates. The capture cross section of ^{75}Se was assumed to be σ = 300barns (§ 4.2).

The actual evaluation of equations 2.9 - 2.13 was done by the computer program "BURNUP" /Na75/.

As can be easily seen in Fig. 2.28, the intensities of γ-rays from the $^{75}Se(n,\gamma)$ reaction and the electron capture decay of ^{75}Se increase almost linearly with time duration during the experiment with the GAMS crystal spectrometer and the pair spectrometer at the HFR/Grenoble. This enables the easy identification of theses γ-rays from the other γ-rays of the single neutron capture reaction.

The eq. 2.14 will be used for the estimation of the cross section of the $^{75}Se(n,\gamma)$reaction (§ 4.2). In order to make the situation of the experiment in Grenoble clearer , an (n,γ)-cross section equivalent to the half life of ^{75}Se ($\tau_{1/2}$ = 119.76 ± 0.05 days /Sc80b/) is calculated with,

$$\frac{\ln 2}{\tau_{\frac{1}{2}}} = \sigma_2 \phi \rightarrow \frac{0.69315}{119.76\times24\times3600} = \sigma_2 \times 5.5 \times 10^{14} \ (cm^{-2}.s^{-1})$$

$$\sigma_2 = 1.22 \times 10^{-22} \ cm^2 \qquad \ldots\ldots \text{ eq. 2.15}$$

120 days of half life → 122 barns of (n,γ) cross section

One can estimate with eq. 2.10a and 2.14, whether the observation of the neutron capture reaction in other β-unstable nuclei is possible or not. This kind of experiment provides much more precise determination of neutron binding energy and neutron capture cross section, which will contribute to the calculation of atomic mass formula and to astrophysics, respectively. Astrophysics needs precise neutron capture cross sections of neutron-rich, neutron-deficient and β-unstable nuclei in order to calculate the origin of elements.

3. Data Analysis

The three instruments GAMS, BILL and pair spectrometer have different measuring systems and different characteristics (resolution, efficiency, energy, response, peak line shape, etc.). Thus these three instruments have their own data evaluation systems. Each evaluation system has many processes and programs, which are grouped into two major processes.

1. Spectrum analysis
   - peak fit
   - intensity calibration
   - energy calibration

2. Data check
   - impurity γ-lines
   - spurious peaks

In this chapter the outlines of each data evaluation system are discussed.

3.1 Evaluation of data taken with the curved crystal spectrometers GAMS 1 and GAMS 2/3

The process of data analysis of GAMS spectrometers is rather complex. Fig. 3.1 shows a schematic diagram of the flow of the data analysis procedure. For peak-fitting (FITSP, FITL5) a simple Gaussian is used to define the peak shape. If the reflections have strange shapes or if they are close doublets, peak-fitting was carefully done. One can always quite easily differentiate , if a peak is a doublet or only strange shaped using the following procedures,

- compare peak with other higher order of reflection
- compare the peak shapes of GAMS 1, GAMS 2 and GAMS 3 and see whether the γ-peak is commonly found in the spectrum (see Fig. 3.2, 3.3).

In the higher order of reflection the resolution is much better. If a γ-line is a doublet, it changes its shape or it is resolved into single peaks. There are two types of asymmetrical peak shape (even for individual γ-lines) arising

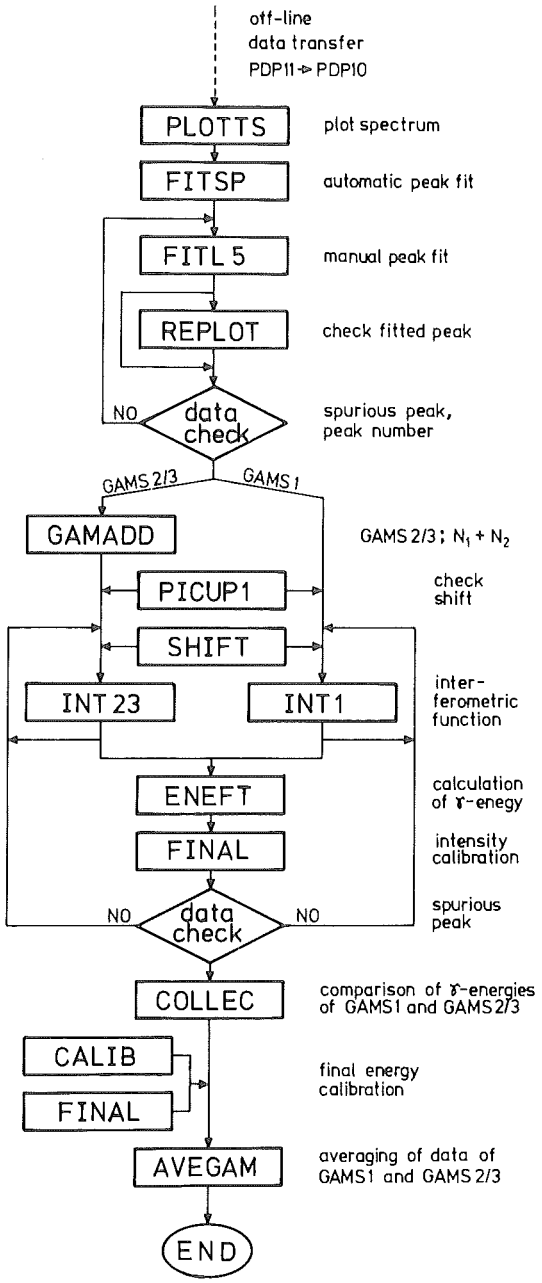

Fig. 3.1 A schematic diagram of the data handling procedure. Program names are written in capital letters.

from two different origins, i. e. the target shape and the target movement. If the asymmetrical peak-shape originates in the target shape, all peaks are asymmetrical and the peak shape of GAMS 3 is just a mirrored peak-shape of GAMS 2 (see Fig. 3.2). However, in the present work the asymmetry arising from the target shape was very small and single peaks are well fitted by a simple Gaussian.

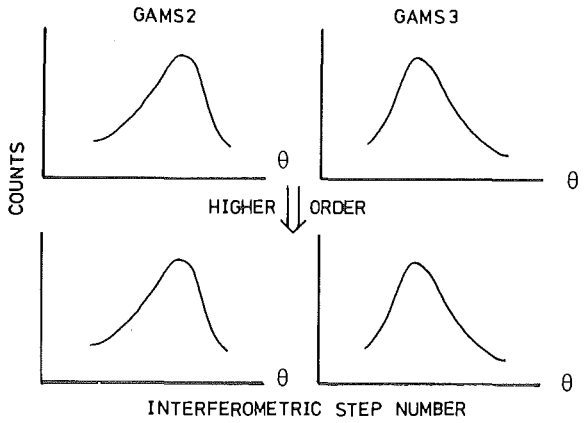

Fig. 3.2

Peak asymmetry due to the target shape.

If the asymmetry comes from the target movement the shape is time-dependent and one will not see such an asymmetry in the other orders of diffraction or in neighboring peaks. The γ-ray peaks having this kind of asymmetry are often accompanied by a strange interferometer step number. Such erroneous points are easily found in the energy averaging procedure of different orders, and they are then discarded (program ENEFT and "data check").

There exist in the spectra the following impurity γ-lines and spurious-peaks which are easily found in the peak-fit routine before going into the next procedure of determining the interferometric function.

- γ-lines from the $Al(n,\gamma)$ reaction
- γ-line from the $^{12}C(n,\gamma)$ reaction (E_γ=1262keV)
- spurious peaks from Compton scattering of higher energy γ-rays (see Fig. 3.4)
- spurious peaks from pile-up effect of lower energy γ-rays (see Fig. 3.4)

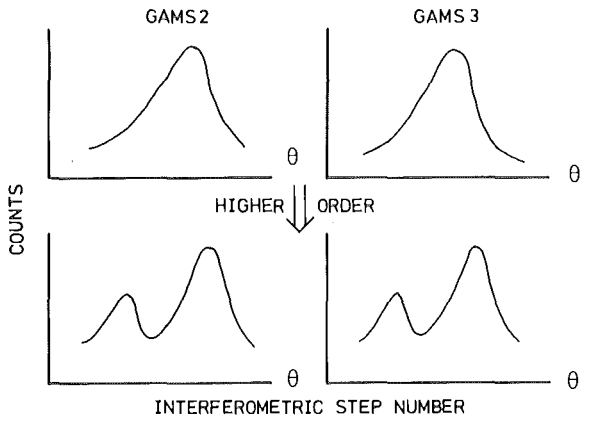

Fig. 3.3

A doublet which looks like an asymmetric peak in low reflection order.

The γ-lines from the Al(n,γ) reaction are readily identified from broad and asymmetrical peak shape (see also § 2.1), and their energies are well known /To78,Sc80a/. The 1262 keV γ-ray and the 511 keV annihilation γ-ray have very broad peak width and they are thus easily recognized. Spurious peaks from Compton scattering and pile-up peaks occur at the same interferometer step number as the original γ-rays (Fig. 3.4).

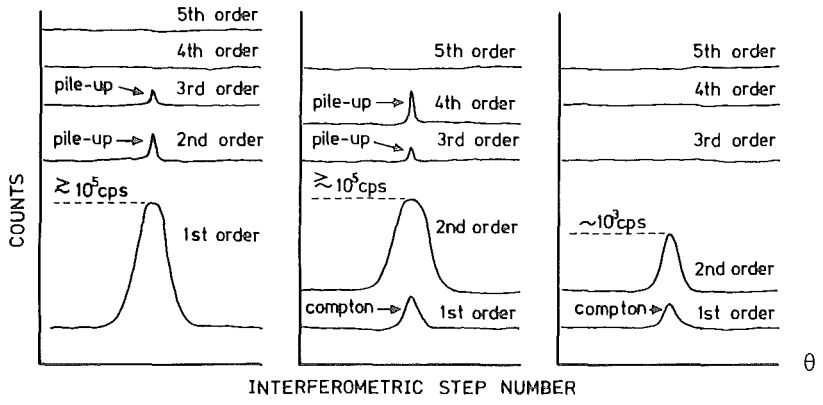

Fig. 3.4

Sketch of the spectrum taken with the GAMS spectrometers, when there are strong peaks in the spectrum. The peak-width of a pile-up spurious peak is narrower than its original γ-ray.

In order to distinguish the Compton peak clearly, one should look into another diffraction order. For example, a peak in the second order which has 100% intensity originating from Compton scattering of a high energy γ-ray does not appear in the third order of diffraction. A pile-up spurious peak is much easier to identify, because this peak has a narrower line width than the other γ-peaks due to the fact that pile-up is strong only in the maximum region of one γ-line. Further identification and elimination of spurious peak is done in the procedure of energy averaging of different diffraction orders. After elimination of spurious peaks and identification of doublets, positions of fitted γ-peaks are again

drawn in the spectrum (REPLOT) and checked visually. All in all, peak-fitting was done without fixing the line-width. This is because the line-width changes slightly from time to time due to source movement and the line-widths of higher orders are slightly narrower than those of lower orders due to the crystal effect /Ko80b/. Only in case of a very close doublet the line-width is fixed at the most appropriate value found in the peak-fitting of neighboring γ-lines.

After data-checking as discussed above, some fifteen strong γ-rays ($\sim$ several tens of γ-lines in different orders in the spectrum) are selected to determine the interferometric function (eq. 2.4a or 2.5b) with the program INT1 and INT23. Then energies of γ-rays are roughly calculated by the program ENEFTS using this interferometric function. This does not mean that the calculated energy is not precise, but that only the absolute value is uncertain. The energies for one γ-ray determined in different orders of reflection are grouped by the program ENEFTS and averaged by the program FINAL to define the representative energy-value for this γ-ray. By use of these tabulated γ-rays one can easily identify spurious peaks.

In the experiments with the GAMS spectrometers every 1 - 2 days the spectrum data are transfered to a DEC tape, so the whole spectrum is divided into some ten data files. Sometimes one finds small systematic differences of interferometric steps between two successive data files. In such a case the difference is corrected by the program SHIFT, and again a new interferometric function is found (lowest χ^2-value). Several trial calculations of the interferometric function are performed. When the overlap between two spectrum data contains many common γ- peaks, the program PICUP1 is applied to calculate the mean difference between two different data files.

As standard for the energy calibration of GAMS 1 the well-known energies of Pb-X-rays /La77/ (see § 4.6) were used as is discussed in § 2.1. The γ-energies of GAMS 2/3 are calibrated by the γ-rays common in GAMS 1 and GAMS 2/3 (program CALIB + FINAL) after comparing their energy differences with the help of the program COLLEC. After the energy calibration of GAMS 1 and GAMS 2/3, both results are averaged and mixed by the program AVEGAM, and the final γ-ray energies are obtained.

The program ENEFTS also performs the intensity calibration. The total efficiency curves for each order are included in this program. The self absorption coefficients (see § 2.4.1) were calculated by the interpolation using the input data

set of the empirical $\mu\rho$ L-value, which is calculated by use of well-known μ (eq. 2.5) /Ve73/ and the previous experimental data /Ra71,Ak73a/. The averaged intensity of GAMS 1-and GAMS 2/3-data is again calculated by the program AVEGAM.

The final output from the program AVEGAM is used for the next step : the construction of decay scheme (§ 5.1).

3.2 Data evaluation of the β-spectrometer BILL

The minicomputer used for the measuring system of BILL is similar to that used for GAMS 1, and again data taken with BILL are transfered to the central computer PDP10. Fig. 3.5 shows the data analysis procedure.

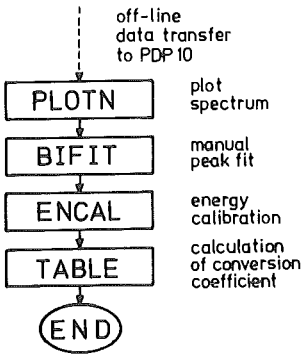

Fig. 3.5

Flow of data analysis of the β-spectrometer BILL. The system adopted in the present work is slightly different from the standard routine (see text).

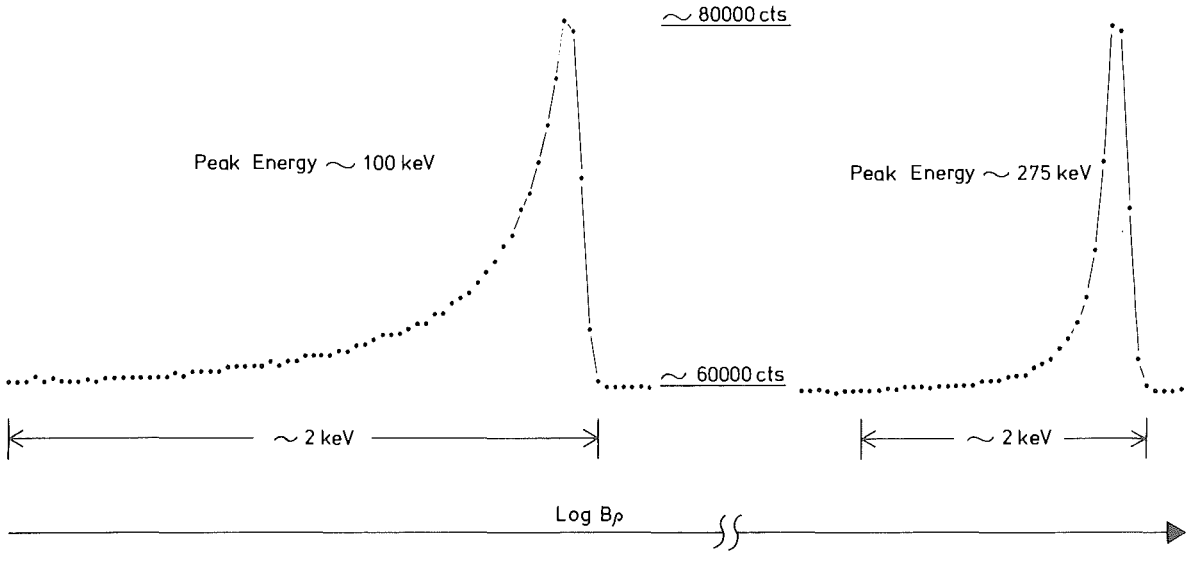

Fig. 3.6 Comparison of peak shapes between low energy and high energy electron lines. Data are taken from the $^{76}Se(n,e^-)$-experiment in the present work.

The line-shape of electron-peaks found in the spectrum are always asymmetrical. This is due to the energy loss of electrons in the target and internal or external excitation of atoms. The existence of a long low energy tail, which is nearly of the same length for low energy ($\sim$ 80keV) and for relatively high energy ($\sim$ 300keV),implies the importance of an atomic process of inelastic electron-atom collision (Fig. 3.6).

The peak-fit program BIFIT defines the peak-shape of an electron line combining three different functions /Eg68/,

shape : Gaussian + exponential decay curve × inversed Gaussian

$$f(x) = H \cdot \exp\left(-(x-x_0)^2 \cdot \frac{4\ln 2}{G^2}\right) + H \cdot S \cdot \exp\left(-(x-x_0+GG) \cdot \frac{\ln 2}{A}\right) \cdot \left(1-\exp\left(-(x-x_0)^2 \cdot \frac{\ln 2}{GG^2}\right)\right) \quad \cdots\cdot \text{ eq. 3.1}$$

x_0 : defined peak position

The meaning of each parameter is schematically shown in Fig. 3.7.

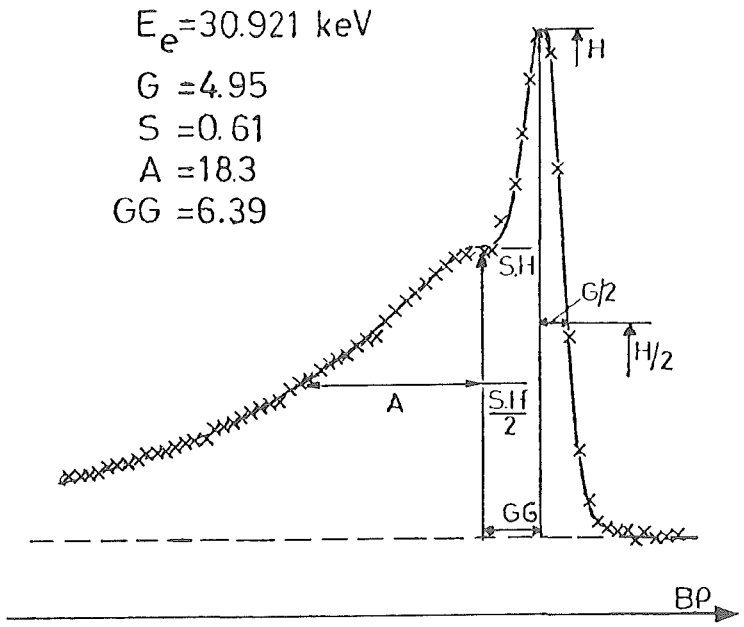

Fig. 3.7

Example of the peak-shape observed in the experiment with BILL. All characters written in the figure are the parameters which define the peak-shape (see text).

All parameters are slowly varying function of energy (Bρ or momentum) and depend on the target (see /Br79b/). As the variations of these parameters according to energy are well defined by a suitable function, one can use another semiautomatic peak-fit program SFIT fixing each parameter in order to speed up the data evaluation. However in the present work only a few conversion electron lines were observed, so peak-fitting was done peak by peak with appropriate variation of the parameters.

After peak-fitting, energy calibration was achieved with the use of the program ENCAL with a second order polynomial, i.e. $f(x) = \sum_{i=0}^{2} a_i x^i$, as stated in § 2.2. Calibrated γ-energies of the GAMS spectrometers serve as reference energies.

In the experiment with BILL absolute intensities of electron lines are not obtained experimentally. Absolute electron intensities are determined empirically by the program TABLE using theoretical conversion coefficients of known transitions of pure multipolarities (E2 or E3) and their γ-ray intensities from the GAMS-measurements. Then the program TABLE determines the conversion coefficients for other electron lines simultaneously. The program TABLE also calculates the corresponding theoretical conversion coefficients using the subroutine written by Hager and Seltzer /Ha68/. By comparing both the experimental and theoretical conversion coefficients the multipolarities of transitions are deduced.

3.3 Evaluation of data taken with the pair spectrometers in Jülich and in Grenoble

Both data taken in Jülich and in Grenoble were analysed and evaluated in Grenoble. Fig. 3.8 shows a schematic diagram of data evaluation procedure.

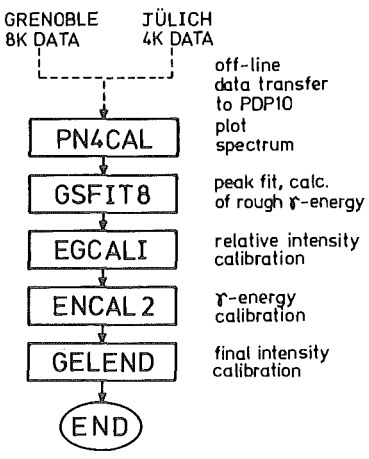

Fig. 3.8

Flow of data evaluation for the pair spectrometers in Jülich and in Grenoble.

The peak-fit program GSFIT8, which is originally developed in Karlsruhe and is adapted to the Grenoble computer with little improvement, defines a peak-shape with Gaussian + tail. The tail-shape is defined by the following function,

$$f(x) = (c_0 + c_1 x + c_2 x^2) \cdot \exp(- \frac{x_0 - x - \sigma}{\sigma})$$

σ : Gaussian peak width

x_0 : peak position

The energy dependence of the coefficients c_i as well as the Gaussian shape parameters are determined beforehand using several γ-lines, which are singlets and well isolated from other γ-lines in the relevant spectrum. The tail can either be on the high energy side or on the low energy side. In the present work the low energy tail was adopted. The background shape can be approximated either by straight line or an exponential curve. A simple straight line was sufficient for our purposes.

Apparent impurity γ-lines, which are from the Cl(n,γ) reaction in the Jülich-spectrum and from the Al(n,γ) and Pb(n,γ) reactions (see Figs. 2.25 - 2.27), are checked during the work of peak-fitting using the data of refs./Ba67,St78/.

The program EGCALI contains a function defining the relative efficiency curve of the pair spectrometer. This function was calculated individually for both pair spectrometers using the following expressions,

Jülich pair spectrometer : $$\varepsilon(E) = \sum_{i=0}^{n} a_i E^{-i} \qquad \cdots\cdots\cdots \text{ eq. 3.2}$$

Grenoble pair spectrometer : $$\varepsilon(E) = \exp(\sum_{i=0}^{n} a_i (\log E)^i) \qquad \cdots\cdot \text{ eq. 3.3}$$

Both functions eq. 3.2 and 3.3 provide quite similar results. As for the physical meaning of these formulas, one should refer to the theory of pair formation /He57,Da54,Ov68/. The intensities of the γ-lines from the ^{14}N(n,γ) reaction which was investigated by Thomas et al./Th67/ were used for the calibration lines. The data of the ^{14}N(n,γ) reaction are compiled by Ajzenberg-Selove /Aj76/ and the results by three investigators on this reaction are compared there. The data of Thomas et al. provided the smoothest curve of relative detection efficiency in the present work (see also the discussion in § 4.3.1).
A standard least-squares method was used to determine the coefficients a_i of eqs. 3.2 and 3.3. The best-fit was obtained with n = 4,5 for eq. 3.2 and n = 2 for eq. 3.3, respectively.

Energy calibration was done with the program ENCAL2, which is a universal least-

squares-fit program for polynomial functions and was developed in the present work. Normally in the routine of energy calibration, the position error (channel error) of a reference line coming from the peak-fit process is transfered to the energy and is quadratically added in the error of reference energy. Then the χ^2 is defined using the residuum calculated from the reference energy and the fitted energy. However the program ENCAL2 can handle the errors of reference energy and the channel error independently. ENCAL2 also performs standard calculation and further can choose any combinations of polynomials. The best-fit function was chosen from both the normal and special method of ENCAL2. For both methods of curve-fitting the standard variance-covariance matrix was exploited to minimize the χ^2 (the principal algorithm is shown in § 5.1). In the present case the third order polynomial has provided the best-fit for both the Jülich-data and Grenoble-data.

$$E\gamma = a_o + a_1 x + a_2 x^2 + a_3 x^3 \qquad \cdots \text{ eq. 3.4}$$

x : channel number

The error of a γ-line calibrated by the eq. 3.4 is defined by quadratic addition of position error Δx (channel error) transfered to energy by the coefficient a_1 in eq. 3.4 and calibration error Δc calculated by variance-covariance matrix (error matrix),

$$\Delta E\gamma = \sqrt{(a_1 \Delta x)^2 + (\Delta c)^2} \qquad \cdots \text{ eq. 3.5}$$

In order to calculate the coefficients a_i in eq. 3.4, the γ-energies of the reactions $^{14}N(n,\gamma)$ /Gr80/, $^{1}H(n,\gamma)$ /Gr78/ and $^{12}C(n,\gamma)$ /Gr78,Wa80/ were used for reference γ-energies, which are shown in Table 3.1 in the next page.

The γ-ray energies in the $^{74}Se(n,\gamma)$ and $^{76}Se(n,\gamma)$ reactions investigated with the Jülich pair spectrometer are calibrated by the mixed target method (§ 2.5) using the γ-rays in Table 3.1. The accuracy of γ-energies from the $^{14}N(n,\gamma)$ reaction /Gr80/ was also demonstrated in the report of Kennett et al./Ke81/.

The energies of several prominent γ-lines from the GAMS-measurement were also used for the energy calibration, when there was an overlap region between the GAMS- and pair-data (Fig. 3.9)

E_γ(keV)	ΔE_γ(eV)	Origin	
1884.820	47	$^{14}N(n,\gamma)$	a)
2223.247	16	$^{1}H(n,\gamma)$	b)
3531.964	87	$^{14}N(n,\gamma)$	a)
3677.748	57	$^{14}N(n,\gamma)$	a)
3683.921	23	$^{12}C(n,\gamma)$	c)
4508.665	110	$^{14}N(n,\gamma)$	a)
4945.319	20	$^{12}C(n,\gamma)$	d)
5269.122	35	$^{14}N(n,\gamma)$	a)
5297.795	35	$^{14}N(n,\gamma)$	a)
5533.401	35	$^{14}N(n,\gamma)$	a)
5562.073	35	$^{14}N(n,\gamma)$	a)
6322.474	60	$^{14}N(n,\gamma)$	a)
7288.980	90	$^{14}N(n,\gamma)$	a)
8310.218	104	$^{14}N(n,\gamma)$	a)

a) ref./Gr80/
b) ref./Gr78/
c) ref./Wa80/
d) ref./Gr78/

Table 3.1 Reference γ-energies adopted for the energy calibration of the data taken with the Jülich pair spectrometer

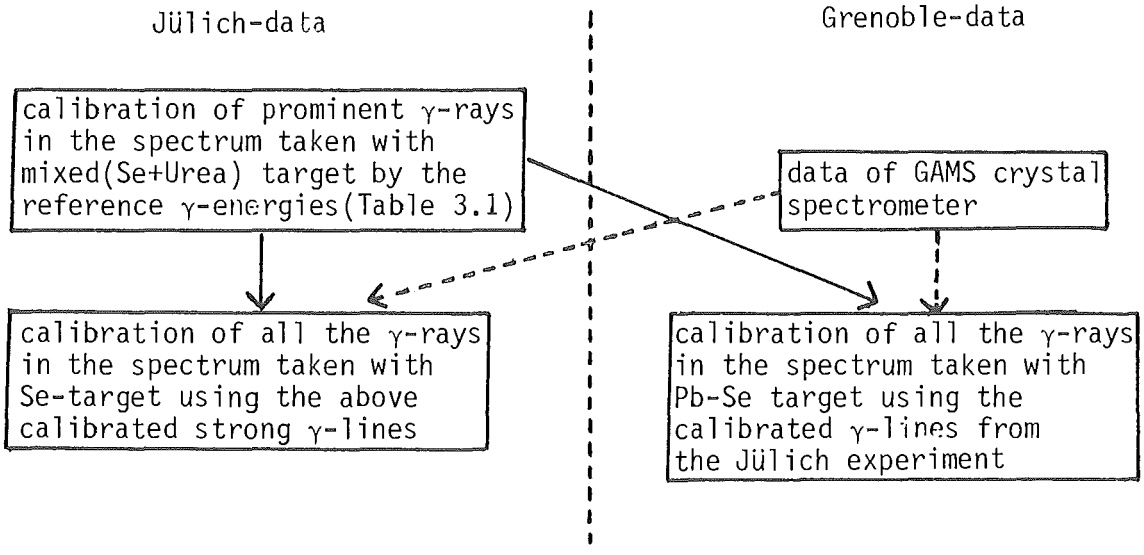

Fig. 3.9 Energy calibration of the pair spectrometer

The data taken in Grenoble could be calibrated by the data taken in Jülich. However for the γ-rays with energies higher than 8.1 MeV in the experiment with the ^{74}Se-target (see § 2.5), there were no good reference γ-rays. In this case the energies of two weak γ-rays (9884keV and 9189keV) from the ^{77}Se(n,γ) reaction /Br79a/ with a small correction (in that work previous data of the ^{14}N(n,γ) reaction were used) were taken, though naturally the energy errors provided by the error matrix for very high energy γ-rays ($\lesssim$ 10MeV) are not very small.

3.4 Absolute intensity calibration

The absolute γ-ray intensity calibration (per 100 neutrons captured) is often difficult to perform with the desired accuracy. In the present work absolute γ-ray intensities are given using results of previous experiments. However one should always aim at a self-consistent solution. In this section methods to obtain the absolute intensity calibration are described, and the problems accompanying each method are discussed.
There exist three methods to perform absolute intensity calibration based on decay schemes,

$$1)\quad \sum_i I_i \text{ (primary transition)} = 100 \qquad \cdots\cdot \text{ eq. 3.6.a}$$

$$2)\quad \sum_i I_i \cdot E_i \text{ (all transitions)} = 100 \cdot Q \qquad \cdots\cdot \text{ eq. 3.6.b}$$

$$3)\quad \sum_i I_i \text{ (ground state transition)} = 100 \qquad \cdots\cdot \text{ eq. 3.6.c}$$

I_i : transition intensity/100n E_i : transition energy
Q : neutron binding energy($=B_n$)

Principally, consistence of the absolute γ-ray intensities calculated by these three methods implies that the "exact" absolute intensity calibration was accomplished. However all these three methods have the same difficulty : "all γ-rays cannot be found". One can easily see this fact from the Table 3.2 (next page).
The γ-rays found for the first time in the present work have all weak intensities. However, quite many unfound weak lines yield a considerable difference for the absolute intensity calibration. It is needless to say that the relative γ-ray intensity must be always calibrated from low energy to high energy, when one

Gross results from the analysis of the γ-spectra

reaction	number of identified γ-rays	
	Present	Previous
$^{74}Se(n,\gamma)$	ca. 1400	149 a)
$^{76}Se(n,\gamma)$	ca. 1300	334 b)
$^{76}Se(n,\gamma)$ (pair spectrum)	ca. 670	236 c)

a) ref./Ak73a/ b) ref./Ra71/ c) ref./Br79a/

Table 3.2 Comparison of numbers of identified γ-rays with the previous experiments(data from §4)

wants to adopt any method in eq. 3.6.
After construction of the decay scheme as far as possible, the 3rd method (eq. 3.6.c) provides the most reliable intensity calibration because most of the intensities, even of weak transitions with high and intermediate energies which are not detectable in the spectrum, are accumulated by the low energy transitions between low-lying states.

Besides the three methods shown above there is another method to obtain absolute γ-intensities. The mixed-target method determines the γ-intensities in comparison with the well-known (n,γ)-cross section and the well-known absolute γ-intensities of the mixed sample. In order to apply this method one must know the contents and the composition of the target precisely, and further the neutron flux should be homogeneous everywhere in the target. This can be easily performed with the internal target geometry. However in Grenoble, no experiment especially prepared for this purpose was carried out. Several γ-lines from the $Al(n,\gamma)$ reaction were too weak to provide reasonable intensity normalization.

In conclusion the γ-ray intensities were normalized to the previous experiments. No self-consistent γ-ray absolute intensity calibration was done in the present work.

4. Results of spectrum analysis

In § 2 and §3 the experimental procedure was described, and so far the following overall results were obtained (Table 4.1).

Reaction	Instrument	Energy range MeV	Number of identified γ-or e^-lines	Spectra code name
$^{74}Se(n,\gamma)^{75}Se$	GAMS 1, 2/3	0.05 - 1.80	ca. 600	C4
$^{74}Se(n,e^-)$	BILL	0.10 - 0.80	24†	B4
$^{74}Se(n,\gamma)$	Pair(Jülich)	1.91 - 8.03	ca. 750	PJ4
$^{74}Se(n,\gamma)$	Pair(Grenoble)	1.53 - 3.02 5.12 - 8.03	ca. 400	PG4
$^{75}Se(n,\gamma)^{76}Se$	GAMS 1, 2/3	0.43 - 1.80	ca. 50	C4
$^{75}Se(n,e^-)$	BILL	0.55	1	B4
$^{75}Se(n,\gamma)$	Pair(Grenoble)	5.12 - 11.15	ca. 50	PG4
$^{75}Se(E.C.,\gamma)^{75}As$	GAMS 1, 2/3	0.06 - 0.40	9	C4
$^{75}Se(E.C.,e^-)$	BILL	0.10 - 0.30	7	B4
$^{76}Se(n,\gamma)^{77}Se$	GAMS 1, 2/3	0.05 - 2.42	ca. 700	C4
$^{76}Se(n,e^-)$	BILL	0.04 - 0.76	40†	B6
$^{76}Se(n,\gamma)$	Pair(Jülich)	1.62 - 7.42	ca. 670	PJ6

† including subshell lines

Table 4.1 Review of the results of the spectrum analysis. The complete data lists C4, PJ4, PG4, C6, and PJ6 are given elsewhere/To82/.

Also the level schemes of ^{75}As and ^{78}Se are shown here. They were much more precisely determined in the present work and they are very simple due to small numbers of observed γ-rays.

4.1 Results of the experiments on the $^{74}Se(n,\gamma)$ and $^{74}Se(n,e^-)$ reactions

The primary γ-rays which populate the levels up to 2 MeV excitation energy are shown in Table 4.2. The remaining lines are tabulated separately elsewhere /To82/. In the low energy region only the strong γ-rays which are commonly seen in the spectra taken with the GAMS and BILL spectrometers are shown in Table 4.3. The full list C4 is given elsewhere. Low energy γ-rays so far placed in the decay

scheme are contained in Fig. 5.2. (p.93)
The absolute γ-intensity calibration of primary transitions as well as low energy transitions is based on the experiment by Akhmed et al./Ak73a/. However, the intensities shown in /Ak73a/ seemed to be overestimated, so that the intensities in the present work were first reduced by an amount of 30%, and then the reduced values were again revised after further investigation of the decay scheme. Recently nearly the same γ-intensity reduction compared to the intensity of Akhmed et al. has been reported independently by Engler et al./En81/.

4.1.1 Primary γ-rays observed by the pair spectrometer

In Table 4.2 shown are the primary γ-rays in the $^{74}Se(n,\gamma)$ reaction (next page). The recoil energies from the γ-emission, $E_{\gamma r}$, is calculated from the following equation and added to the γ-energy in Table 4.2 to obtain the transition energies.

$$E_{\gamma r} = \frac{E_\gamma^2}{2Mc^2} \qquad \ldots\ldots \text{ eq. 4.1}$$

E_γ : γ-ray energy M : Mass of product nucleus

The ground state E2 transition from the capture state ($J^\pi=1/2^+ \rightarrow J^\pi=5/2^+$, E_γ=8027keV) has been observed in the present work for the first time.
Another E2 primary transition of E_γ = 7998.6 keV /Ak73a,He75,Ek81/ has been also confirmed.
The very close doublet γ-line at 7.74 MeV has been identified from its large asymmetric peak-shape in the spectrum. This doublet was expected to be observed since Agarwal et al./Ag73,Ag74/ had proposed low-lying levels at 286.6 keV ($J^\pi=3/2^-$) and at 293.1 keV ($J^\pi=1/2^-$).

4.1.2 Strong low energy transitions in ^{75}Se

In Table 4.3 are shown the strong low energy transitions which are found commonly by the GAMS and BILL spectrometers (see the page after next).

The self absorption correction in the GAMS-measurements was done by the data of the previous (n,γ)-experiment /Ak73a/.

E (trans. energy) in keV	I_γ /1000n	Populating level E_x in keV	J^π a)
8027.61(34)	0.70(4)	0.	$5/2^+$
7741.0(11)	9.1(29)	286.6	$3/2^-$
7734.55(28)	250.(13)	293.1	$(1/2)^-$
7461.6(8)	0.32(9)		
7441.63(16)	5.02(25)	585.9	$(3/2)^-$
7417.(2)	0.71(22)	610.7	$1/2^+$
7399.03(16)	2.31(21)	628.4	$5/2^+$
7187.9(5)	0.037(5)	839.9	$3/2^+$
7167.95(19)	3.57(21)	859.5	$3/2^-$
7132.35(14)	2.24(11)	895.3	$1/2^-,3/2^-$
7065.00(11)	7.76(39)	962.6	$3/2^-$
7007.09(11)	13.8(7)	1020.5	
6882.99(20)	0.63(5)	1144.5	
6843.44(11)	2.54(13)	1184.2	
6829.05(9)	8.0(4)	1198.5	
6782.4(8)	0.19(5)	1245.2	
6594.77(34)	0.423(35)	1432.4	
6450.9(7)	0.26(6)		
6438.10(7)	27.3(14)	1589.5	
6424.8(10)	0.27(5)		
6374.80(8)	2.35(27)	1652.9	
6360.5(7)	0.17(4)		
6354.57(27)	0.74(7)		
6257.19(22)	0.491(28)		
6225.55(7)	12.7(6)	1802.o	
6216.89(8)	4.50(23)	1810.7	
6132.61(7)	3.89(20)	1894.9	
6084.25(9)	4.47(22)	1943.3	
6069.25(14)	1.27(7)	1958.3	
6054.8(6)	0.178(39)		
6041.56(7)	3.52(19)	1986.2	

a) Data taken from ref./Ek81/. See §5.2 for further information.

Table 4.2 Primary γ-rays in the $^{74}Se(n,\gamma)$ reaction

TABLE 4.3 CONVERSION ELECTRON LINES IN THE 74SE(N,γ) REACTION
THE FIRST FOUR COLUMNS ARE GAMMA-RAY DATA

E (trans.) KEV	ERROR KEV	I_γ /100N	ERROR %	E_e* KEV	ERROR KEV	I_e /100N	ERROR %	SHELL	CONVERSION COEFF.	ERROR %	MULTIPOL. & COMMENTS
839.887	0.006	3.66	4.	827.25	0.05	1.58E-3	13.	K	4.32E-4	13.	M1
733.898	0.004	3.82	4.	721.25	0.07	1.68E-3	13.	K	4.42E-4	13.	E1 OR M1
610.714	0.003	5.99	6.	598.076	0.018	7.14E-3	12.	K	1.19E-3	13.	(E2)
608.701	0.002	2.05	6.	596.08	0.04	2.0E-3	26.	K	9.6E-4	27.	M1
516.044	0.002	2.78	11.	503.371	0.017	4.40E-3	10.	K	1.58E-3	15.	M1(+E2)
484.214	0.003	0.58	5.	471.59	0.03	2.1E-3	20.	K	3.7E-3	21.	E2(+M3?)
431.653	0.002	1.90	4.	418.981	0.023	4.06E-3	10.	K	2.15E-3	11.	M1
427.885	0.002	2.88	5.	415.200	0.021	2.98E-3	12.	K	1.03E-4	13.	E1
377.386	0.002	2.41	5.	364.713	0.011	7.01E-3	10.	K	2.90E-3	11.	M1
319.766	0.002	0.53	5.	307.12	0.03	2.76E-3	12.	K	5.25E-3	13.	M1(+E2, δ^2=0.15±0.14)
299.377	0.002	0.64	7.	286.71	0.03	3.33E-3	15.	K	5.17E-3	17.	M1
292.844	0.002	5.76	5.	280.182	0.011	3.14E-2	5.	K	5.44E-3	8.	M1(+E2)
				291.188	0.015	3.89E-3	9.	L1	6.76E-4	11.	
286.572	0.004	53.54	10.	273.914	0.005	1.88E-1	3.	K	3.50E-3	10.	E1
				284.922	0.006	1.79E-2	4.	L1	3.35E-4	11.	
236.075	0.003	0.44	11.	223.466	0.016	5.17E-3	14.	K	1.19E-2	18.	M1(+E2, δ^2=0.12±0.14)
229.178	0.002	0.38	13.	216.62	0.04	4.3E-3	20.	K	1.14E-2	24.	M1(+E2)
141.315	0.001	4.00	8.	128.656	0.003	2.02E-1	2.	K	5.06E-2	9.	M1+E2
				139.68	0.03	2.19E-2	5.	L1	5.49E-3	10.	δ^2=0.11±0.03
133.041	0.001	0.089	14.	120.378	0.005	3.50E-2	8.	K	3.95E-1	17.	E2(+M3?)
112.388	0.001	5.97	8.	99.729	0.002	7.32E-1	2.	K	1.23E-1	8.	M1+E2
				110.730	0.003	8.63E-1	6.	L1	1.45E-2	10.	@ δ^2=0.17±0.03
				110.920	0.013	1.37E-2	14.	L2+L3	2.29E-3	16.	@
				112.153	0.007	1.66E-2	6.	M TOTAL	2.79E-3	10.	

ELECTRON BINDING ENERGIES IN EV : K=12657.8,L1=1653.9,L2=1476.2,L3=1435.8,
TAKEN FROM REF. /La77/ M1=231.5,M2=168.2,M3=161.9

* RECOIL ENERGY IS ADDED
@ NOT USED FOR THE CALCULATION OF MIXING RATIO

The electron energy in Table 4.3 includes the recoil energy. The recoil energy from electron emission E_r is calculated as following :

$$E_r = \frac{E_e^2}{2Mc^2} + \frac{E_e \cdot mc^2}{Mc^2} \qquad \ldots\ldots \text{ eq. 4.2}$$

E_e : Electron kinetic energy
m : Electron rest mass
M : Mass of product nucleus

The second term is the only difference from the case of γ-emission, and this second term is important from the low energy region (non-relativistic) up to intermediate energy region ($\lesssim$ 2MeV).

4.2 Primary γ-rays and low energy γ-rays in the $^{75}Se(n,\gamma)$ reaction

As discussed in § 2.6, this is the reaction which is observed as two successive neutron captures in ^{74}Se. The absolute γ-ray intensity calibration in this reaction is especially difficult because

- All γ-rays are not found in the spectrum, because these γ-rays are relatively weak and buried in the complex spectrum of single neutron capture γ-rays.
- The intensities should be calibrated by the absolute γ-intensities in the $^{74}Se(n,\gamma)$ reaction, because the γ-ray intensities in the $^{75}Se(n,\gamma)$ reaction are related to the $^{74}Se(n,\gamma)$ reaction by eq. 2.6.

However, after the determination of precise absolute γ-intensities in the $^{74}Se(n,\gamma)$ reaction, an attempt will be made to obtain the absolute intensities in the $^{75}Se(n,\gamma)$ reaction. Here relative intensities are given only for the primary γ-rays.

4.2.1 Primary γ-rays in the $^{75}Se(n,\gamma)$ reaction

In the pair spectrum taken in Grenoble there were more than 50 peaks which were not found in the Jülich spectrum, and they are believed to belong to the $^{75}Se(n,\gamma)$ reaction. In Table 4.4 only the γ-rays of energy above 7.74 MeV are shown. These γ-rays are very clearly seen in the spectrum due to the low background (see § 2.6).

E (trans.) in keV	I_γ a)	Populating level E_X in keV	J^π c)
11153.7(40) b)	1.01(11)	0.	0^+
10595.3(35) b)	16.0(9)	559.4	2^+
10032.2(16) b)	1.22(10)	1122.3	0^+
9938.3(14) b)	4.75(31)	1216.1	2^+
9465.5(9) b)	2.06(14)	1688.9	(3^+)
9366.5(10) b)	2.07(14)	1787.6	2^+
9127.9(7) b)	2.45(16)	2026.0	4^+
9028.0(13)	0.40(10)	2127.3	(2^+)
8724.9(5)	100.(5)	2429.1	3^-
8640.1(10)	0.61(11)	2515.	
8484.16(41)	11.2(6)	2670.3	(2^-)
8342.3(5)	8.1(9)	2812.1	
8337.0(5)	8.0(9)	2817.3	
8293.66(44)	3.83(26)	2860.7	
8284.49(43)	4.09(27)	2869.9	
8265.6(17)	0.34(11)	2888.7	
8243.6(18)	0.47(14)	2910.7	
8234.1(10)	0.90(16)	2920.2	
8205.05(35)	25.7(13)	2950.3	
8185.6(7)	1.77(23)	2968.7	
8176.8(8)	2.31(26)	2977.5	
8145.7(11)	0.63(14)	3008.7	
8084.61(34)	15.7(9)	3069.8	
8048.66(37)	5.96(39)	3105.7	
7892.56(32)	23.7(12)	3161.8	
7962.53(35)	6.5(4)	3191.8	
7934.87(33)	8.5(5)	3219.5	
7885.31(31)	11.8(6)	3269.1	
7858.92(40)	3.48(27)	3295.5	
7803.54(32)	10.5(6)	3350.8	

a) Values relative to the intensity of the 8725 keV line.

b) Errors calculated in the extrapolation region by the error matrix seem to be overestimated.

c) Data taken from ref./Le78/ and /We80/. See §5.3 for further information.

Table 4.4 The primary γ-rays in the $^{75}Se(n,\gamma)$ reaction

The spin and parity of the neutron capture state is $J^{\pi} = 2^+$ or 3^+ due to the ground state $J^{\pi} = 5/2^+$ of the ^{75}Se nucleus. It should be noted that there are two γ-rays which populate the two 0^+ states in ^{76}Se. The multipolarities of these two γ-rays ought to be E2 ($2^+ \rightarrow 0^+$). However, these two E2 transitions do not directly mean that the spin and parity of the capture state is 100% $J^{\pi} = 2^+$ (see § 5.2).

4.2.2 Low energy γ-rays in the ^{75}Se(n,γ) reaction

The following γ-rays have been identified as candidates for the γ-rays which belong to the ^{75}Se(n,γ) reaction (Table 4.5, next page).

Most of the γ-lines clearly identified as arising from the ^{75}Se(n,γ) reaction are also placed in the decay scheme (Fig. 5.4, p.107).
An attempt to obtain reliable values of the intensities for these γ-rays will be made after calculation of more precise γ-ray intensities in the ^{74}Se(n,γ) reaction. However, one can estimate the intensity of the 559 keV transition ($2^+_1 \rightarrow 0^+_1$) from the γ-ray intensities of the $2^+_1 \rightarrow 0^+_1$ transitions in the neighbouring nuclei. The intensity of this 559 keV transition may be $I\gamma(559\text{keV}, 2^+ \rightarrow 0^+) \gtrsim 60$ (per 100 neutron captured). This estimate is used to extract the information about the cross section of the ^{75}Se(n,γ) reaction using eq. 2.14 with the neutron flux of $\phi = 5.5 \times 10^{14}$ n/cm^2·s, and the estimated cross section σ was

$$\sigma\,(^{75}\text{Se}(n,\gamma)^{76}\text{Se}) \sim 300 \pm 100 \text{ b}$$

In order to obtain this estimate one needs a value for the intensity of any γ-rays from the ^{75}As nucleus (^{75}Se electron capture decay). For this calculation the intensity of the 280 keV γ-ray from ^{75}As was used (see Fig. 4.1, page after next, and see § 4.6). This γ-line is seen in the spectrum (Fig. 4.1) in the same interferometric region as the 559 keV γ-line(^{76}Se), so that there any ambiguities arising from the time-growing intensities of these γ-rays are excluded.

E (trans.) in keV	Placement in the decay scheme	E (trans.) in keV	Placement in the decay scheme
339.5641(21)†	2127 → 1788	830.30(14)	
358.0932(24)†	1609 → 1331	868.12(12)†	2656 → 1788
358.639(5)		882.23(17)†	2670 → 1788
382.900(8)†	2170 → 1788	885.846(30)	
395.660(4)†	2825 → 2429	954.50(5)	2170 → 1216
403.089(6)†	2429 → 2026	980.47(10)	2670 → 1689
430.6325(27)†		1031.46(10)†	(2363 → 1331)
438.2464(29)†	2127 → 1689	1058.07(8)	
456.77(5)	1788 → 1331	1129.841(16)†	1689 → 559
464.640(21)†		1147.52(14)	
472.8049(28)†	1689 → 1216	1159.72(5)	
540.357(16)†		1212.903(36)†	2429 → 1216
548.022(12)†		1216.096(20)†	1216 → 0
559.0939(25)†	559 → 0	1228.611(38)†	1788 → 559
563.1688(28)†	1122 → 559	1283.90(23)	
568.055(11)		1285.55(30)	
571.490(8)†	1788 → 1216	1286.78(19)	
575.298(11)†	2363 → 1788	1332.53(9)†	
598.779(6)†		1359.10(10)	
657.0313(35)†	1216 → 559	1378.70(21)	
665.753(5)†	1788 → 1122	1453.61(11)	2670 → 1216
695.127(8)†	2026 → 1331	1470.62(17)	
697.40(10)†		1474.36(6)	
727.001(9)†	2515 → 1689	1493.99(10)	2825 → 1331
740.172(25)†	2429 → 1689	1528.96(8)	
771.747(8)†	1330 → 559	1568.02(7)†	2127 → 559
796.06(6)	(2127 → 1216)	1596.34(23)	
798.82(6)†	2825 → 2026	1611.8(4)	2170 → 559
800.49(6)†		1624.2(6)	
809.817(7)†	2026 → 1216	1787.82(26)†	1788 → 0

† These γ-lines are clearly identified to be from the $^{75}Se(n,\gamma)$ reaction.

Table 4.5 Low energy γ-lines from the $^{75}Se(n,\gamma)$ reaction observed with the GAMS spectrometers. The placements of γ-transitions are shown for those which depopulate the levels up to 2.8 MeV(see Fig.5.4).

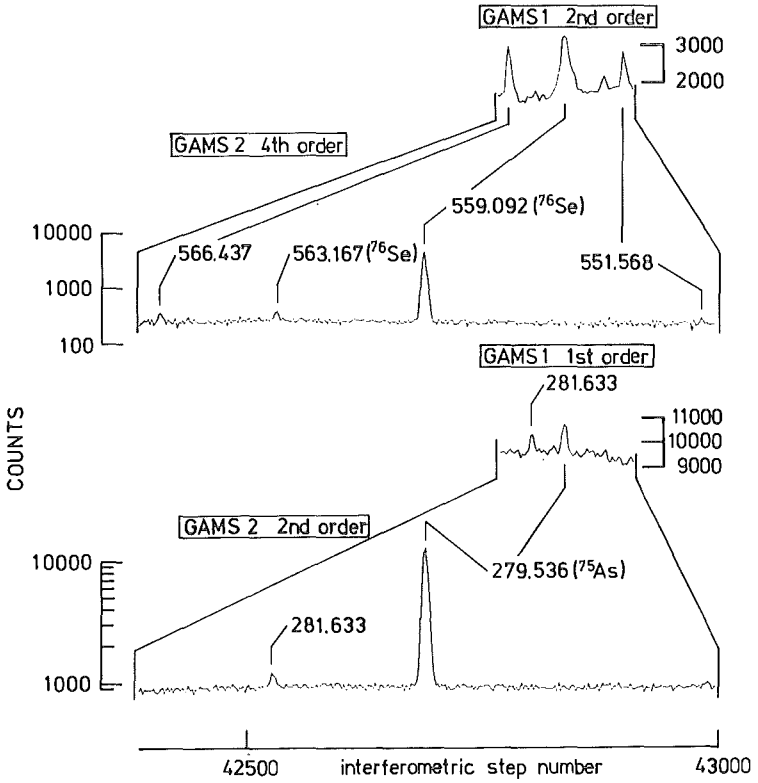

Fig. 4.1

Portions of spectra taken with the GAMS spectrometer. Two γ-lines at 279keV and 559keV were used to calculate the cross section of the $^{75}Se(n,\gamma)$ reaction (see text).

4.3 Results of the spectrum analysis of the $^{76}Se(n,\gamma)$ reaction

Absolute intensity calibration of the γ-lines in the pair spectrum as well as in the GAMS-spectra of the $^{76}Se(n,\gamma)$ reaction was done using the previous data of Rabenstein and Vonach /Ra71/. Present γ-ray intensities show excellent agreement with those of /Ra71/ (Table 4.6 , see also § 3.4).
Again the complete list of γ-rays found in the present study is given elsewhere /To82/. Only the primary γ-rays which populate the low-lying levels up to 2 MeV are shown in § 4.3.1, and the low energy transitions which are commonly seen in the GAMS- and BILL-spectra are shown in § 4.3.2.

4.3.1 Primary γ-transitions in the $^{76}Se(n,\gamma)$ reaction

In Table 4.6 the list of primary γ-rays in the $^{76}Se(n,\gamma)$ reaction is shown together with the results of other authors /Ra71,Br79a/.

Table 4.6 Primary γ-rays in the $^{76}Se(n,\gamma)$ reaction

Present				Rabenstein et al.[b]		Brewster [c]	
$E_{trans.}$(error) in keV	I_γ(error) /1000N	Populating level E_x in keV	J^π [a]	$E_{trans.}$(error) in keV	I_γ(error) /1000N	$E_{trans.}$(error) in keV	I_γ(error) /1000N
7418.85(22)	55.4(29)	0.	$1/2^-$	7418.4(8)	60.4(70)	7418.45(19)	67.8(28)
	< 0.05			7241.9(20)	1.5(4)		
7179.85(16)	38.8(20)	239.0	$3/2^-$	7179.6(11)	38.6(45)	7179.78(13)	47.9(19)
6906.7(10)	0.08(3)						
6898.23(17)	0.82(6)	520.6	$3/2^-$	6896.0(15)	1.6(3)	6898.43(8)	1.2(1)
6887.8(12)	0.06(3)						
6601.03(8)	94.(5)	817.8	$1/2^-$	6600.8(10)	94.(13)	6601.17(9)	120.(4)
6507.32(11)	2.54(15)	911.5	$3/2^+$	6506.9(12)	2.2(4)	6507.48(9)	3.3(1)
6413.68(7)	28.3(15)	1005.2	$3/2^-$	6413.1(10)	28.(4)	6414.11(10)	37.3(12)
6291.15(22)	0.76(7)	1128.1	$1/2^+$	6291.1(15)	5.1(7)	6291.16(11)	1.3(1)
6231.84(7)	14.9(8)	1187.0	(3/2)	6231.3(15)	15.(5)	6232.16(11)	19.1(6)
6054.84(15)	1.24(10)	1363.9		6052.3(20)	3.(1)	6053.76(23)	2.3(1)
6016.41(7)	15.0(8)	1402.5	$3/2^\pm(1/2^-)$	6016.6(13)	14.4(20)	6016.64(12)	21.6(6)
6007.22(6)	43.4(22)	1411.6	$3/2^-$	6006.7(10)	45.(6)	6007.54(12)	58.9(16)
5930.56(16)	1.11(9)	1488.2	$3/2^-$	5930.6(15)	1.3(4)	5930.65(12)	1.6(1)
5907.79(9)	3.00(17)	1511.0	(3/2)	5907.2(10)	2.3(6)	5907.72(12)	4.0(1)
5838.8(10)	0.10(6)						
5810.91(14)	0.99(9)	1607.7	(3/2)			5811.08(12)	1.2(1)
5795.69(6)	18.7(10)	1623.1	$3/2^-$	5795.0(10)	17.3(40)	5795.44(12)	26.1(7)
5773.5(7)	0.20(6)						

Table 4.6 Continued

Present				Rabenstein et al.[b]		Brewster [c]	
$E_{trans.}$(error) in keV	I_γ(error) /1000N	Populating level E_x in keV	J^π [a]	$E_{trans.}$(error) in keV	I_γ(error) /1000N	$E_{trans.}$(error) in keV	I_γ(error) /1000N
5717.0(7)	0.23(6)						
5704.15(8)	4.08(23)	1714.7	$1/2^-,3/2^-$	5704.2(10)	6.9(17)	5703.86(11)	5.6(2)
5628.9(5)	0.37(8)						
5601.21(6)	45.8(24)	1817.6	$1/2^-$	5600.4(10)	43.(10)	5601.00(11)	64.2(17)
5588.04(24)	1.64(17)	1830.8				5587.60(11)	2.6(1)
	< 0.1					5527.74(22)	0.4(1)
5502.68(9)	2.31(14)	1916.0		5502.3(10)	2.8(7)	5502.25(11)	3.3(1)
5483.6(7)	0.17(5)						
	< 0.1					5447.14(11)	0.4(1)
5432.6(5)	0.30(6)					5430.82(11)	0.5(1)

a) Present data compilation(see §5.4 for further information)

b) Ref./Ra71/

c) Ref./Br79a/

Except for weak lines the agreement between the three measurements is very good. The 7242 keV γ-ray was found in the report of Rabenstein et al. and in the recent paper of Engler et al./En81/. This γ-ray may establish a low-lying level at 176 keV. However, this γ-ray was seen neither in the present work nor in the report of Brewster /Br79a/. Further in the present work no low energy transition which establishes the 176 keV level was observed (§ 4.3.2 and ref./To82/). One can easily see from the energy combination of primary γ-rays and their corresponding level energies that the energy calibration of the primary transition in the present work is excellent.

The relative γ-ray intensities in the present work are in excellent agreement with those of Rabenstein et al.. The present relative γ-intensities are calibrated with the data of the $^{14}N(n,\gamma)$ reaction which was investigated by Thomas et al. /Th68/, while the γ-ray intensities of Brewster were calibrated with the data of the $^{14}N(n,\gamma)$ reaction investigated by Bellmann /Be71/. The γ-ray intensities in the work of Rabenstein et al. were calibrated with the data of the $^{53}Cr(n,\gamma)$ reaction studied by Kane et al./Ka67/. The data of Kane et al. are in excellent agreement with the newest compiled data /Ve78a/ as for the relative γ-ray intensities (see also § 3.3).

4.3.2 Strong low energy transitions in ^{77}Se

The list of strong low energy transitions is shown in Table 4.7 (next page).

The intensities of low energy γ-rays were calibrated relatively as well as absolutely using the data of Rabenstein et al./Ra71/ (see § 3.1). This intensity seemed to be quite satisfactory, because the calculated conversion coefficients, which were normalized to give the best agreement with the theoretical values /Ha68/ for the transitions of known pure multipolarities (51keV E1, 126keV E2, 162keV E3 and 250keV E2), are consistent with the theoretical values. The relative intensities of electron -lines were obtained with the use of the measured detection efficiency curve of BILL (see § 3.2).

The extracted multipolarities of the transitions are in good agreement with the known spins and parities of the levels (see § 5.3).
The 88 keV transition is once reported to have a multipolarity of E1 with small admixture of M2 /Br74/ from the $\gamma\gamma$- angular distribution measurement, and this admixture of M2 has a very much enhanced transition rate (11 s.p.u. < B(M2) < 214 s.p.u.) /Si80/. This admixture of M2 in E1 was also seen in the present

TABLE 4.7 CONVERSION ELECTRON LINES IN THE 76SE(N,γ) REACTION
THE FIRST FOUR COLUMNS ARE GAMMA-RAY DATA

E (trans.) KEV	ERROR KEV	I_γ /100N	ERROR %	E_e* KEV	ERROR KEV	I_e /100N	ERROR %	SHELL	CONVERSION COEFF.	ERROR %	MULTIPOL. & COMMENTS
755.387	0.003	2.69	5.	742.68	0.07	1.5E-3	51.	K	-------	---	(M1)
645.824	0.002	1.43	4.	633.18	0.07	1.3E-3	27.	K	8.9E-4	27.	M1
578.851	0.005	3.30	9.	566.198	0.021	3.65E-3	11.	K	1.10E-3	14.	M1
520.632	0.003	14.3	9.	507.972	0.008	1.76E-2	4.	K	1.24E-3	10.	M1
				518.973	0.025	1.56E-3	15.	L1	1.10E-4	18.	
518.171	0.004	3.26	9.	505.513	0.013	4.04E-3	8.	K	1.24E-3	12.	M1
484.639	0.006	1.34	14.	471.895	0.040	2.37E-3	12.	K	1.77E-3	18.	M1
439. ?	0.005	3.72	12.	426.737	0.007	1.42E-2	5.	K	3.81E-3	13.	E2
331.215	0.001	0.590	5.	318.526	0.012	3.96E-3	12.	K	6.71E-3	13.	M1+E2 δ^2=1.0±0.5
303.779	0.005	0.649	5.	291.116	0.013	3.50E-3	10.	K	5.40E-3	12.	M1
297.208	0.008	4.14	5.	284.549	0.007	2.31E-2	3.	K	5.57E-3	6.	M1(+E2)
				295.541	0.020	3.43E-3	16.	L1	8.3E-4	17.	δ^2=0.04±0.08
281.633	0.002	1.49	5.	268.988	0.015	1.03E-3	5.	K	6.95E-3	7.	M1(+E2)δ^2=9±6×E-2
249.782	0.002	6.71	6.	237.120	0.004	1.70E-1	2.	K	2.53E-2	6.	E2
				248.140	0.008	1.74E-2	3.	L1	2.60E-3	7.	
				248.362	0.021	3.49E-3	18.	L2+L3	5.2E-4	19.	
				249.546	0.017	3.81E-3	14.	M TOTAL	5.7E-4	16.	
238.989	0.003	24.3	4.	226.324	0.004	0.260	2.	K	1.02E-2	5.	M1+E2
				237.336	0.005	2.58E-2	2.	L1	1.06E-3	5.	δ^2=0.065±0.023
				237.53	0.06	2.8E-3	51.	L2+L3	-------	---	
				238.749	0.012	4.23E-3	10.	M TOTAL	1.74E-4	11.	
231.422	0.001	1.53	5.	218.753	0.006	1.60E-2	11.	K	1.05E-2	13.	M1(+E2)
200.448	0.002	3.26	4.	187.787	0.010	4.74E-2	3.	K	1.46E-2	5.	M1(+E2)
				198.774	0.010	6.77E-3	10.	L1	2.08E-3	11.	
180.743	0.003	0.415	3.	168.086	0.010	7.91E-3	14.	K	1.91E-2	14.	M1
161.920	0.001	12.4	4.	149.266	0.003	9.48	2.	K	0.764	5.	E3
				160.269	0.003	0.890	2.	L1	7.17E-2	5.	
				160.466	0.003	0.691	6.	L2+L3	5.82E-2	7.	
				161.696	0.008	0.146	22.	M TOTAL	1.18E-2	22.	

* RECOIL ENERGY IS ADDED

TABLE 4.7 CONTINUED

E (TRANS.) KEV	ERROR KEV	I_γ /100N	ERROR %	* Ee KEV	ERROR KEV	Ie /100N	ERROR %	SHELL	CONVERSION COEFF.	ERROR %	MULTIPOL. & COMMENTS
139.224	0.001	8.97	6.	126.565	0.003	0.942	2.	K	0.105	7.	M1+E2
				137.571	0.004	8.40E-2	4.	L1	9.36E-3	8.	δ^2=0.553 ±0.041
				137.774	0.003	2.22E-2	8.	L2+L3	2.48E-3	10.	
				139.008	0.004	1.72E-2	4.	M TOTAL	1.91E-3	8.	
125.842	0.001	1.09	4.	113.186	0.002	0.274	2.	K	0.252	5.	E2
				124.179	0.005	3.20E-2	5.	L1	2.94E-2	7.	
				124.398	0.009	1.40E-2	12.	L2+L3	1.32E-2	13.	
87.866	0.001	3.3	11.	75.203	0.001	0.432	2.	K	0.130	11.	E1+M2
				86.205	0.004	4.99E-2	5.	L1	1.51E-2	12.	δ^2=0.031 ±0.010
				86.413	0.013	9.8E-3	14.	L2+L3	2.97E-3	18.	
51.361	0.001	0.475	10.	38.706	0.002	0.295	3.	K	0.622	11.	E1 (+M2?)

ELECTRON BINDING ENERGIES IN EV : K=12657.8, L1=1653.9, L2=1476.2, L3=1435.8,
TAKEN FROM REF. /La77/ M1=231.5, M2=168.2, M3=161.9

* RECOIL ENERGY IS ADDED

work. The conversion coefficient for this transition is considerably large compared with the theoretical value. The mixing of M2 is calculated to be 3±1% and its corresponding transition probability is B(M2) = $3.4\pm1.1\times10^{2}$ s.p.u..(§ 6.4)

4.4 Low energy γ-rays in the $^{77}Se(n,\gamma)$ reaction and the level energies in ^{78}Se

The γ-rays from the $^{77}Se(n,\gamma)$ reaction were observed as double neutron capture in ^{76}Se, and so far the following γ-lines in the spectrum taken with the GAMS spectrometers are identified as possibly arising from this reaction (see Table 4.8, next page).

Despite of the weak intensities of these γ-lines in the present work, the high sensitivity of the GAMS spectrometers has resulted in a performance comparable with the measurements by a semiconductor detector /Ra71/.
Three γ-lines (1005keV, 1199keV and 1852keV), which were misassigned in the work of Rabenstein and were not placed in the decay decay scheme in the study of Brewster /Br79a/, were identified to depopulate the level at 2508 keV with spin and parity of $J^{\pi} = 3^{-}$.
More precise energy-values are calculated for several levels in ^{78}Se using the data in Table 4.8, and they are shown in Table 4.9.

Table 4.8 Low energy γ-rays in the $^{77}Se(n,\gamma)$ reaction

Present† $E_{trans.}$ (error) in keV	Assignment§	Rabenstein et al.[a] $E_{trans.}$ (error) in keV	I_γ (error) /100N
354.735(24)	2682 → 2327	355.1(3)	0.2(1) [b]
497.295(7)	1995 → 1499	497.0(10)	0.4(2)
545.302(12)	1854 → 1309	545.37(10)	2.0(3)
570.905(9)	2898 → 2327		
		575.0(10)	< 1.0
613.7280(29)	614 → 0	613.78(10)	64.5(70)
651.576(11)		651.3(4)	0.4(2)
687.257(6)	1996 → 1309	687.41(20)	2.1(4)
694.9192(35)	1307 → 614	694.82(12)	13.4(20)
716.679(43)			
733.92(19)		733.7(3)	0.55(20)
		768.0(10)	< 0.3 [c]
778.211(29)			
828.194(13)	2682 → 1854	828.2(4)	1.0(2)
		840.5(5)	0.4(2) [c]
843.22(13)		843.1(3)	0.5(2)
884.867(15)	1499 → 614	884.8(10)	4.(1) [d]
889.105(12)	1503 → 614	889.0(10)	1.3(5) [d]
		912.0(10)	< 0.4
		943.0(10)	< 0.3
		958.7(8)	0.15(10)
		1005.(1)	< 0.5
		1010.4(8)	0.35(20)
		1019.2(4)	0.3(1)
		1025.6(3)	0.5(1)
		1080.0(3)	0.65(10)
1144.968(17)	1759 → 614	1145.1(2)	2.45(20)
1199.39(13)	2508 → 1309	1199.2(5)	1.0(2)
1229.16(11)	2538 → 1309	1230.1(6)	0.3(1)
1240.142(29)	1854 → 614	1240.5(2)	3.1(3)
		1293.2(4)	0.8(4)

Table 4.8 Continued

Present†		Rabenstein et al.[a]		
$E_{trans.}$(error) in keV	Assignment§	$E_{trans.}$(error) in keV	I_γ(error) /100N	
1308.600(45)	1309 → 0	1308.5(2)	9.4(8)	
		1339.3(3)	1.0(2)	
		1373.0(10)	0.5(2)	
		1382.1(4)	1.9(4)	
		1387.5(5)	0.3(2)	
		1530.1(3)	< 1.0	
		1620.2(5)	0.4(2)	c)
		1654.2(7)	0.4(2)	
		1672.8(4)	0.5(2)	
		1714.1(3)	4.0(5)	
(1721.12(20))		1720.(1)	< 1.0	
		1744.2(5)	0.4(2)	c)
		1791.1(4)	0.8(2)	
		1852.0(3)	0.7(3)	
		1894.1(5)	0.6(2)	
		1924.4(10)	1.5(4)	
1995.96(34)	1995 → 0	1996.0(3)	3.9(5)	

† Due to the low reaction rate of double neutron capture in ^{76}Se (cf. §2.6) only the strong γ-lines were observed.

§ The assignments of Rabenstein et al., which agree well with the present data, are shown.

a) Ref./Ra71/

b) Intensity is estimated to be much less (< 0.04) in the present work.

c) Existence is questionable /Ra71/

d) The intensity ratio for these two γ-lines in the present work is 1:5 (885keV : 889keV).

Low-lying level		Primary transitions and energy-sums in keV			
Present		Brewster [b]		Engler et al. [c]	
E_x in keV	J^π [a]	$E_{trans.}$	Energy sum	$E_{trans.}$	Energy sum
0.	0^+	10497.55(20)	10497.55(20)	$10497.7_6(3)$	$10497.7_6(3)$
613.7278(30)	2^+	9884.11(69)	10497.84(69)	$9883.8_7(1)$	$10497.6_0(1)$
1308.645(5)	2^+	9189.19(35)	$10497.83_5(35)$	$9189.0_8(1)$	$10497.7_3(1)$
1498.603(9)	(0^+)	8999.35(31)	10497.95(31)	$8998.7_6(1)$	$10497.3_6(1)$ †
1502.833(19)	(4^+)				
1758.715(24)	$(0^+,1,2)$	8738.99(27)	$10497.70_5(27)$	$8739.1_3(4)$	$10497.8_4(4)$
1853.935(13)	$(2^+,3^+)$				
1995.900(7)	(2^+)	8501.76(25)	10497.66(25)	$8501.8_0(1)$	$10497.7_0(1)$
		Average	10497.72(13)	Average	10497.7(1)
			$\chi^2 = 0.22$		$\chi^2 = 0.89$

a) Data taken from Nucl. Data Sheets ref./Si81/.

b) Ref./Br79/ with small correction (see text).

c) Ref./En81/. Recoil energy is added.

† Omitted from the averaging.

Table 4.9 Level energies in ^{78}Se and the calculation of the neutron separation energy

4.5 Neutron separation energies in the nuclei ^{75}Se, ^{76}Se, ^{77}Se and ^{78}Se

In the present work more precise values of the neutron separation energies in the nuclei ^{75}Se, ^{76}Se, ^{77}Se and ^{78}Se could be deduced after level energy calculation (§ 5.1). These values are listed in Table 4.10 together with the previous values for comparison (see next page).

Generally the agreement between the results by different investigators are reasonably good. Only in the case of the ^{76}Se nucleus the present value of 11154.38 keV is much less than the value from the model calculation by Wapstra and Bos /Wa77/. This large difference is not unnatural because the direct determination of the neutron binding energy by the $^{75}Se(n,\gamma)$ reaction has never been achieved before. Wapstra et al. have calculated the neutron binding energy in ^{76}Se in the following manner,

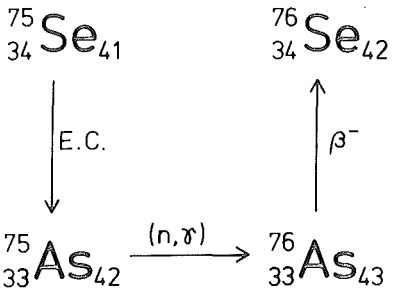

Fig. 4.2

Data link which was used to calculate $B_n(^{76}Se)$ by Wapstra et al./Wa81/.

Using the total binding energies in ^{75}Se, ^{75}As, ^{76}As and ^{76}Se, they have obtained the neutron separation energy B_n in ^{76}Se,

$$B_n = \text{total B.E.}(^{76}Se) - \text{total B.E.}(^{75}Se) \qquad \ldots\ldots \text{ eq. 4.4.1}$$

Wapstra has pointed out that one of the values in the data link shown above (Fig. 4.1) might be wrong /Wa81/. It is rather difficult to point out exactly, which reaction energy is possibly incorrect. However by the present examination of the previous reports on these reactions, the data of the $^{75}As(n,\gamma)$ reaction /Jo68, Gr69/ are reliable and do not explain the large difference. Thus the value $Q_{E.C}$ of ^{75}Se or Q_{β^-} of ^{76}As should be revised. The value of $Q_{E.C.}$ of ^{75}Se is calculated in the following way,

Neutron Seperation Energies in keV

Nuclei	Present†	Rabenstein et al.[a]	Akhmed et al.	Brewster [d]	Engler et al.[e]	Wapstra and Bos [f]
^{75}Se	8027.603(19)	———	8021.3(10) [b]	———	8027.5(4)	8027.7(14)
^{76}Se	11154.38(17)	———	———	———	———	11161.7(22)
^{77}Se	7418.841(15)	7418.0(8)	———	7418.97(13)	7418.8(2)	7418.4(8)
^{78}Se	10497.72(13) [g] 10497.7(1) [h]	10497.4(12)	10497.6(12) [c]	10497.59(14)	10497.8(3)	10496.8(10)
^{208}Pb	7367.70(21)	———	———	———	———	7367.7(7) [i]

a) Ref./Ra71/

b) Ref./Ak73a/. This value was adjusted to be 8027.4(15) keV by Horen et al./Ho75/.

c) Ref./Ak73b/

d) Ref./Br79a/

e) Ref./En81/

f) Ref./Wa77/

g) When the data of Brewster are adopted (see Table 4.9).

h) When the data of Engler et al. are adopted (see Table 4.9).

i) Original data from ref./Ma72/.

† Only the errors from the level energy optimization process (§ 5.1) are shown for ^{75}Se, ^{76}Se and ^{77}Se. The systematic error due to the absolute energy calibration is estimated from the data listed in Table 3.1 as $\sim 10^{-5} \cdot E_\gamma$ and should be included in an absolute energy calibration.

Table 4.10 Neutron separation energies reported by various investigators.

$$Q(^{75}\text{Se electron capture decay}) = -Q(^{75}\text{As(p,n)}) + 511.0\text{keV} - (M_n - M_p) \quad \text{..... eq. 4.4.2}$$

$$\begin{cases} Q(^{75}\text{As(p,n)}) = -1647.3 \pm 0.9 \text{ keV} \\ M_n = \text{Neutron mass} \\ M_p = \text{Proton mass} \\ M_n - M_p = Q_\beta(\text{Neutron}) + 511.0 \\ Q_\beta(\text{Neutron}) = 782.4 \text{ keV} \end{cases}$$

$$= 1647.3 - 782.4 = 864.9 \pm 0.9 \text{ keV}$$

The $Q(^{75}\text{As(p,n)})$-value is determined by the measurement of the threshold energy of the $^{75}\text{As(p,n)}$ reaction /Jo64,Wa77/. Thus, if $Q_{E.C.}$ is incorrect, then

$$Q(^{75}\text{Se electron capture decay}) = 857.7 \text{ keV}$$

and

$$Q(^{75}\text{Se(p,n)}) = -1640.1 \text{ keV}$$

as we have calculated together with Q-values of the $^{75}\text{As}(n,\gamma)$ reaction and the β^--decay of ^{76}As /Wa77/ (see Fig. 4.2).
If the Q_{β^-} of ^{76}As should be corrected, the adopted value (Q_{β^-} =2968.6±1.8 keV /Wa77/) should be further lowered to Q_{β^-} = 2961.4 keV.

The neutron binding energy in ^{208}Pb was obtained from the 7367.57 keV (+ recoil energy 0.14 keV) ground state transition, which has almost 100% of all the intensity in the $^{208}\text{Pb}(n,\gamma)$ reaction /Ma72/. The present value agrees quite well with that of ref./Ma72/.

4.6 Precise level energies in ^{75}As

In the course of the measurement with the $Pb^{74}Se$ target in Grenoble, several γ-rays, which belong to the ^{75}As nucleus, were observed in the spectra taken with the GAMS 1 and 2/3 spectrometers (see § 2.6 and § 4). These γ-rays are shown in Table 4.11 and the calculated level energies are in Fig. 4.3.

γ-Transition Energies

Present E_γ(error) in keV	Vylov [1] E_γ(error) in keV	Nucl. Data [2] E_γ(error) in keV	Schötzig et al. [3] I_γ(error) /100 decay
400.6406(17)	400.646(8)	400.658(6)	11.56(15)
303.9090(28)	303.908(10)	303.924(3)	1.34(2)
279.5360(39)	279.535(6)	279.538(3)	25.2(4)
264.6470(12)	264.652(5)	264.656(4)	59.1(8)
198.5996(10)	198.603(5)	198.596(6)	1.47(3)
135.9960(7)	136.000(3)	136.002(3)	59.0(8)
121.1094(8)	121.117(3)	121.119(3)	17.3(3)
96.7307(13)	96.734(4)	96.734(2)	3.48(9)
66.0514(31)	66.050(3)	66.060(7)	1.14(2)

1) Ref./Vy77/
2) Ref./Ek81,He78/
3) Ref./Sc80/

Table 4.11 γ-rays after electron capture decay of ^{75}Se

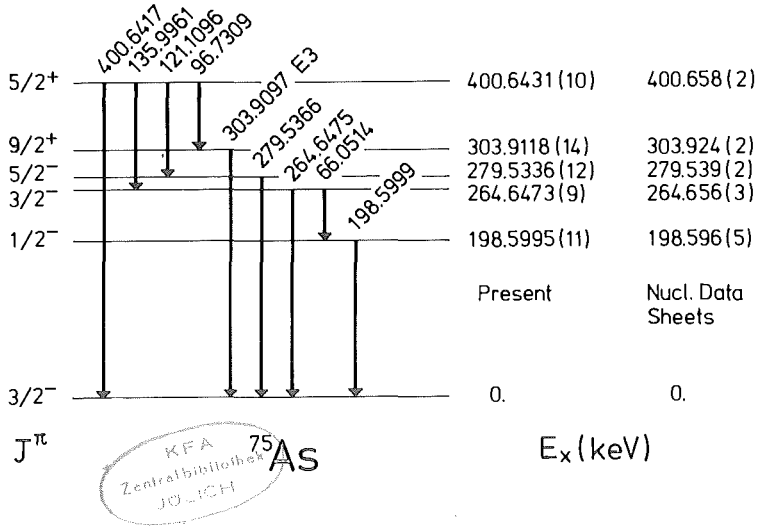

KFA Zentralbibliothek JÜLICH

Fig. 4.3
Decay scheme of ^{75}As. Energies shown in the figure are transition energies.

The present values of γ-rays are in good agreement with those of Vylov /Vy77/. However, there is considerable discrepancy between the present data and the values compiled in Nucl. Data Sheets /Ek81/. The difference is more than five standard deviations for the levels at 303.9 keV and at 400.6 keV.

The precision of the present work is much better than the previously obtained with semi-conductor detectors. The present data will provide a new standard set of γ-energies for ^{75}As.

4.7 Pb X-ray natural energy width from the measurement with the GAMS 1 spectrometer.

The natural width of a X-ray is directly ralated to the life time of the atomic level, i.e. atomic transition rate. From measurements of these widths one can examine the validity of atomic models. However experimental data on X-ray widths are fairly scarce, and for Pb only one report could be found /Ne69/. Further, there exist small discrepancy between the previous experimental value of Nelson et al./Ne69/ and the value which was calculated by interpolation with many other X-rays of different atoms /Sa76b/.
Because a Pb-Se alloy target was used for the measurements in Grenoble, all K-X-rays except K-P X-ray were clearly observed. The K-P X-ray was too weak to be detectable in the present work ; The K-$N_{IV,V}$ X-ray was clearly observed; however, no satisfactory peak-fit was obtained due to its weak intensity /Sc74/. In this section the data evaluation process is shortly presented and the results for the observed nine K X-rays ($KL_{III}(K\alpha_1)$, $KL_{II}(K\alpha_2)$, KM_{III}, KM_{II}, KM_{IV}, KM_{V}, KN_{II}, KN_{III}, $KO_{II,III}$) are shown.

4.7.1 X-ray data evaluation

In Fig. 4.4 an example is shown of X-ray lines. Due to the high resolution of the GAMS 1 spectrometer, an X-ray has a Lorentzian peak-shape arising from its natural width.
The actual X-ray width in a experimental spectrum has a small component of the intrinsic line width or instrumental resolution which is convoluted with the Lorentzian shape. Thus a peak-shape must be described by the following function,

$$f(x) = A \int_{-\infty}^{\infty} \frac{\exp\left((x-x')^2 \cdot \frac{4\ln 2}{\sigma^2}\right)}{(x-x_0)^2 + \frac{1}{4}\Gamma^2}\, dx' \qquad \text{..... eq. 4.3}$$

σ : intrinsic resolution of the detector
x_0 : peak position
Γ : Lorentzian width

The value of σ was taken as the representative value of γ-line width which was calculated by the program FITL5 (see § 3.1) assuming a Gaussian peak-shape.

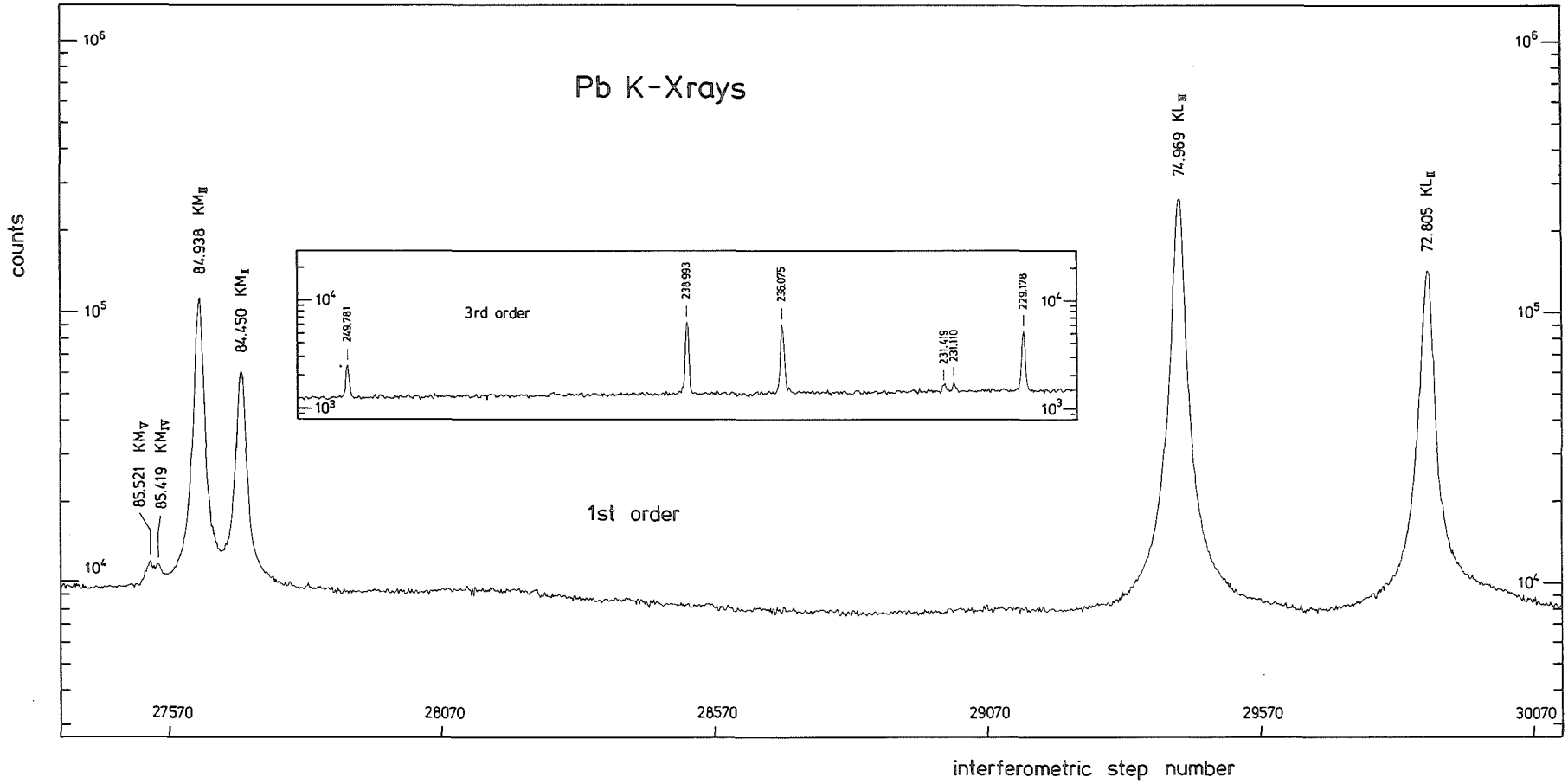

Fig. 4.4 X-ray spectra. This figure is taken from the 1st order diffraction in the spectra taken with ^{76}Se-Pb target (spectra code name C6, see Table 2.3). The inset figure is taken from the 3rd order diffraction and shows γ-ray line widths.

Using this σ, the X-ray peak was fitted by the program XRAYDB /Ba81/, which adopts eq. 4.3 for peak-shape approximation, and the Lorentzian width Γ of the X-ray was extracted from this fitting (see Fig. 4.5)

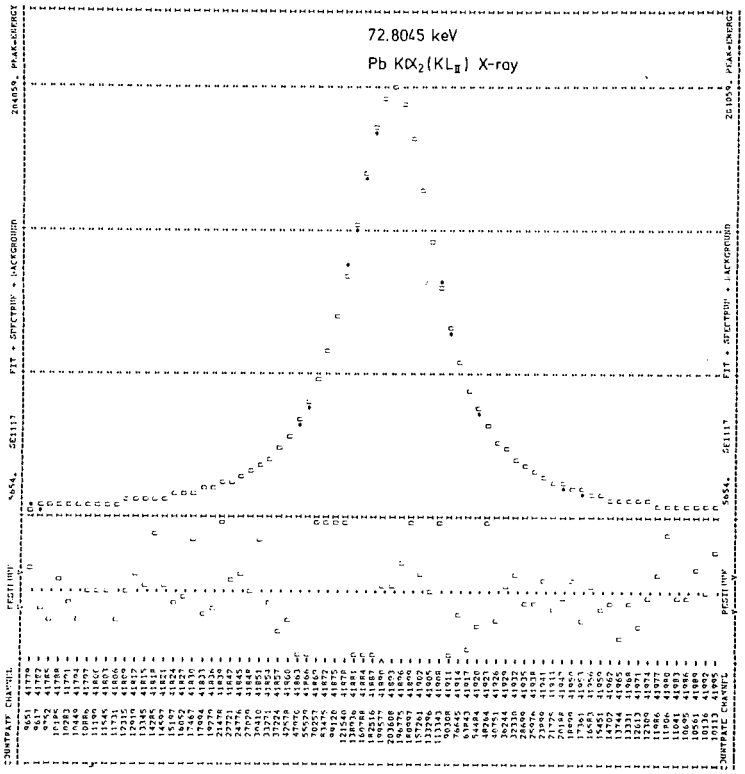

Fig. 4.5

An example of X-ray line-fit. ✱ shows the measurement and ⌀ shows the fitted value.

4.7.2 Results and discussion

The final results of K X-ray natural widths are shown in Table 4.12 (next page). Adopted instrumental σ was 6 steps and 7 steps (interferometric step, see Table 2.4 and § 2.1) for 1st and 2nd order diffractions of ^{74}Se-Pb target, respectively, and were 9.2 steps and 10 steps for 1st and 2nd order diffractions of the ^{76}Se-Pb target, respectively.

A considerable discrepancy exists between the experimental values of Nelson et al./Ne69/ and the expected values which were calculated by Salem et al./Sa76/. The present data are closer to the values of Salem et al., and the widths of α_1(KL III) and β_3(KM II) X-rays are in good agreement with those of Salem et al.. However, present values of α_2(KL II) and β_1(KM III) X-rays are considerably smaller than those of Salem et al.. Also the present widths of the Kα X-rays are both larger than those semiempirical values of Krause et al./Kr79/.

Energy of X-ray[1] in keV	X-ray width in eV Present	Salem[2] et al.	Nelson[3] et al.	Krause[4] et al.
87.9† ($KO_{II,III}$)	68.3(35)			
87.3600(KN_{III})	72.4(23)			
87.2406(KN_{II})	64.5(23)			
85.5205(KM_{V})	63.6(28)			
85.4189(KM_{IV})	56.2(52)			
84.9381(KM_{III})	67.8(15)	72.2		
84.4503(KM_{II})	76.8(23)	74.9		
74.9693(KL_{III})	69.2(17)	68.3	77.9	66.2
72.8045(KL_{II})	73.2(27)	79.0	73.9	66.8

† 87.8997keV(KO_{II})-87.9215keV(KO_{III}) doublet

1) Ref./La77/

2) Ref./Sa76b/

3) Ref./Ne69/. The uncertainty of each values is $\sim \pm 10\%$.

4) Ref./Kr79/

Table 4.12 K X-ray natural width in lead

Several effects may be considered for broadening of X-ray lines, and the largest contribution may arise from multiplet splitting and multiple ionization /Kr79/. A nice example of theoretical prediction for such multiplet splitting is given by Borchert et al. for Au $K\alpha_1$ X-ray /Bo81/. However, most of the lines in a example of Borchert et al. have intensities less than 1% of "main" $K\alpha_1$ X-ray line, and mostly they are within 2 eV away from the main line. This effect may explain the small difference between the present experimental value and the semiempirical values of Krause et al.. However, the large discrepancy seen in the $K\alpha_2$ X-ray should be from other origins, for ex. unaccounted atomic processes. In order to help understanding the situation a simple description about the X-ray width is given below.

The natural line width of an X-ray is given, for example, by the following equation /Ke74/,

$$\Gamma(K\alpha_1, L_{III} \rightarrow K) = \Gamma(K) + \Gamma(L_{III}) \qquad \ldots\ldots \text{ eq. 4.4}$$

where $\Gamma(K\alpha_1, L_{III} \rightarrow K)$ is the natural line width and $\Gamma(K)$, $\Gamma(L_{III})$ are the total level widths of K and L_{III} electrons, respectively. The total level width is decomposed into three terms (or more ?) Γ_R, Γ_A and Γ_C, i.e.;

$$\Gamma = \Gamma_R + \Gamma_A + \Gamma_C \qquad \ldots\ldots \text{ eq. 4.4.a}$$

Γ_R : Radiative width Γ_A : Auger width
Γ_C : Coster-Kronig width

In the case of K-level the width Γ_C does not exist, because the K-shell has no subshell. The Coster-Kronig process is not possible for all elements (see for example /Bu72/), however in the case of Pb-atom this effect exists.
As one can easily see from eq. 4.4, in the case of K X-rays the term of $\Gamma(K)$ is common for all K X-rays, and the other terms should explain the wide variety of line-widths in Table 4.12. Purely theoretical total widths for atomic levels are given by Keski-Rahkonen et al./Ke74/. These predicted level widths show a similar trend to experimental X-ray line widths. However there seem to exist some small discrepancies. For example the present data show that the width of the KM_V X-ray is larger than the width of the KM_{IV} X-ray, whereas the predicted level width of Keski-Rahkonen et al. may indicate a just inversed relation.

In conclusion, the experimental X-ray widths are still not fully explained theoretically, and further detailed study on these kinds of measurements is clearly needed.

5. Decay schemes and level properties

The decay schemes and level energies of the nuclei ^{75}Se, ^{76}Se and ^{77}Se are based on the γ-ray energies presented in § 4. and ref./To82/. In this chapter the method of constructing a decay scheme is described , and then the decay schemes and level properties of each nucleus are discussed.

5.1 Construction of the decay scheme

For construction of the decay scheme two computer programs LEVEL and RITZ were utilized. The program LEVEL/Sc75/ provides possible γ-ray placements in the level scheme using already known level energies, and then optimizes the level energies with the help of the least-squares method including all placed γ-rays. With the program RITZ one can try to find a new level using the RITZ combination principle(energy combination). The possible existence of a new level is searched for step by step with a mesh-search routine in this RITZ program. Both programs LEVEL and RITZ are used in a cyclic way (Fig. 5.1) in order to try to construct a complete decay scheme.

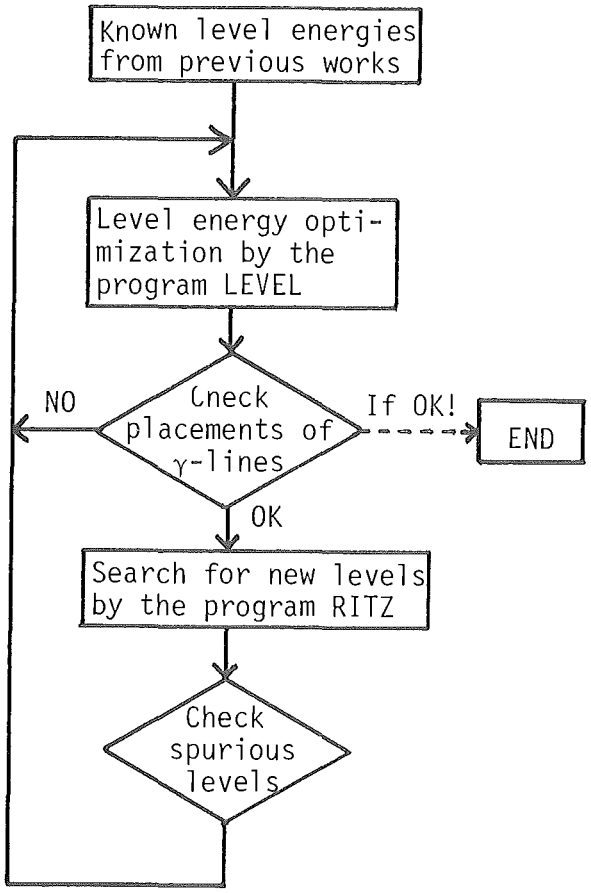

Fig. 5.1 Flow chart of the process of decay scheme construction. If there exists no previous scheme, one should start with the program RITZ.

The program LEVEL is based on the least-squares method using a variance-covariance matrix(error matrix). This kind of method can be commonly used for various optimizations(for ex. curve fitting, see § 3.). In the next page the principle algorithms are described of the method adopted in the program LEVEL. The mathematical verification of the following formula was given by Mitsunari/Mi80/. The most important step in this kind of calculation is to obtain a linearized expression of eq. 5.2.

First, we define the chi-square χ^2 of level energy fit,

$$\chi^2 = \sum_{i<j} (E_{\gamma ij} - |E_{xi} - E_{xj}|)^2/\sigma_{E_{\gamma ij}}^2 + \sum_i (E_{\gamma io} - E_{xi})^2/\sigma_{E_{\gamma io}}^2 \quad \text{..... eq. 5.1}$$

$E_{\gamma ij}$: Transition γ-ray energy from level j to level i

E_{xi} : i^{th} excited level energy(excluding the ground state)

$\sigma_{E_{\gamma ij}}$: Error of transition γ-ray energy $E_{\gamma ij}$

$E_{\gamma io}$: Ground state transition from i^{th} excited state

$\sigma_{E_{\gamma io}}$: Error of $E_{\gamma io}$

The summation should be performed for all γ-rays. The minimization of χ^2 is done by the following condition,

$$\frac{\partial \chi^2}{\partial E_{xi}} = 0 \qquad i = 1, \ldots\ldots, N \text{ (N excited levels)} \qquad \text{..... eq. 5.2}$$

One of the simultaneous equations defined by eq. 5.2 has the following form,

$$\left(\sum_{i \neq j} \frac{1}{\sigma_{E_{\gamma ij}}^2} + \frac{1}{\sigma_{E_{\gamma io}}^2} \right) E_{xi} + \left(- \sum_{i \neq j} \frac{1}{\sigma_{E_{\gamma ij}}^2} \right) E_{xj}$$

$$= \frac{E_{\gamma io}^2}{\sigma_{E_{\gamma io}}^2} + \sum_{j<i} \frac{1}{\sigma_{E_{\gamma ij}}^2} E_{\gamma ij} - \sum_{j>i} \frac{1}{\sigma_{E_{\gamma ij}}^2} E_{\gamma ij} \qquad \text{..... eq. 5.3}$$

For the excited state i. Summations are done by the suffix j.

Performing partial differentiation by E_{xi} for all the levels like in eq. 5.3, the simultaneous equations defined by eq. 5.2 can be written in a matrix formula,

$$A \vec{E} = \vec{C} \qquad \text{..... eq. 5.4}$$

where $A = (A_{ij})$, $A_{ij} = A_{ji} = - \frac{1}{\sigma_{E_{\gamma ij}}^2}$

and $A_{ii} = \sum_{m \neq i} \frac{1}{\sigma_{E_{\gamma im}}^2} + \frac{1}{\sigma_{E_{\gamma io}}^2}$

(summation by the suffix m)

and, $\vec{E} = \begin{pmatrix} E_{X_1} \\ \vdots \\ E_{X_N} \end{pmatrix}$, $\vec{C} = \begin{pmatrix} C_1 \\ \vdots \\ C_N \end{pmatrix}$

$$C_i = \frac{E_{\gamma io}}{\sigma^2_{E_{\gamma io}}} + \sum_{j<i} \frac{1}{\sigma^2_{E_{\gamma ij}}} E_{\gamma ij} - \sum_{j>i} \frac{1}{\sigma^2_{E_{\gamma ij}}} E_{\gamma ij}$$

$\vec{E}$ is the vector which contains the level energies $E_{X_1}, \ldots, E_{X_N}$, and the above equation can be solved by the matrix inversion,

$$\vec{E} = A^{-1}\vec{C} = RC \quad \text{(replacing the matrix } A^{-1} \text{ by } R\text{)} \qquad \ldots\ldots \text{ eq. 5.5}$$

As can be easily seen from eq. 5.4, the matrix R is also a symmetrical matrix and it is often called "Error Matrix". The uncertainty of each level energy ΔE_{Xi} is given by the diagonal element of the matrix R, i.e.

$$\Delta E_{Xi} = \sqrt{R_{ii}} \qquad \ldots\ldots \text{ eq. 5.6}$$

Sometimes ΔE_{Xi} is multipled with the square root of χ^2. However in the present case one should not apply this procedure, because χ^2 is calculated from all γ-rays and the total decay scheme. Instead the value of the local reduced χ^2, which is calculated only from the relevant γ-rays and levels, should be used, because the influence of γ-rays, which are not connected directly or indirectly to the relevant level, should be eliminated from the calculation. Then,

$$\Delta E_{Xi} = \sqrt{\frac{\chi^{2'}}{N_\gamma' - N'}} \cdot \sqrt{R_{ii}} \qquad \ldots\ldots \text{ eq. 5.6.a}$$

where $\chi^{2'}$ is the value calculated with the relevant N_γ' γ-rays and N' levels. Using the above representation one can further calculate the mean value of the transition energies $\overline{E_{\gamma ij}}$ between two levels E_{Xi} and E_{Xj}, and its associated error $\Delta\overline{E_{\gamma ij}}$,

$$\overline{E_{\gamma ij}} = \left| E_{Xi} - E_{Xj} \right|$$

$$\Delta\overline{E_{\gamma ij}} = \sqrt{R_{ii} + 2R_{ij} + R_{jj}} \qquad \ldots\ldots \text{ eq. 5.7}$$

or

$$\Delta\overline{E_{\gamma ij}} = \sqrt{\frac{\chi^{2'}}{N_\gamma' - N'}} \sqrt{R_{ii} + 2R_{ij} + R_{jj}}$$

Because the values E_{Xi} and E_{Xj} are correlated, it cannot be written as

$$\Delta\overline{E_{\gamma ij}} = \sqrt{R_{ii} + R_{jj}}$$

The program RITZ finds a new level with the level energy $E_{x,new}$, if there are more than m (the number of γ-lines, an input parameter) γ-lines($E_{\gamma j}$), which satisfy the following condition,

$$\left| |E_{x,new} - E_{xi}| - E_{\gamma j} \right| < \text{const.} \sqrt{\Delta E_{xi}^2 + \Delta E_{\gamma j}^2} \qquad \ldots\ldots \text{ eq. 5.8}$$

where E_{xi} is the already known level energy and $E_{\gamma j}$ is the energy of a γ-ray which is not yet placed in the decay scheme. ΔE_{xi} and $\Delta E_{\gamma j}$ are the associated errors of E_{xi} and $E_{\gamma j}$ respectively. The constant factor in the right hand side of eq. 5.8 is used to relax or strengthen the condition. The value $E_{x,new}$ is changed step by step in order to find a new level which fulfils all conditions stated above. If there are already many levels used as input, then, even with the high energy precision of the GAMS spectrometers the program RITZ finds many spurious levels. These non-existing levels must be checked and eliminated by the investigator with the use of criteria that are not included in the program.

One should recall that the decay scheme construction in the present study is mainly based on the γ-ray energy combination. Therefore we cannot exclude with 100% safety an erroneous placement of a line, which might lead to an incorrect J^{π} assignment.

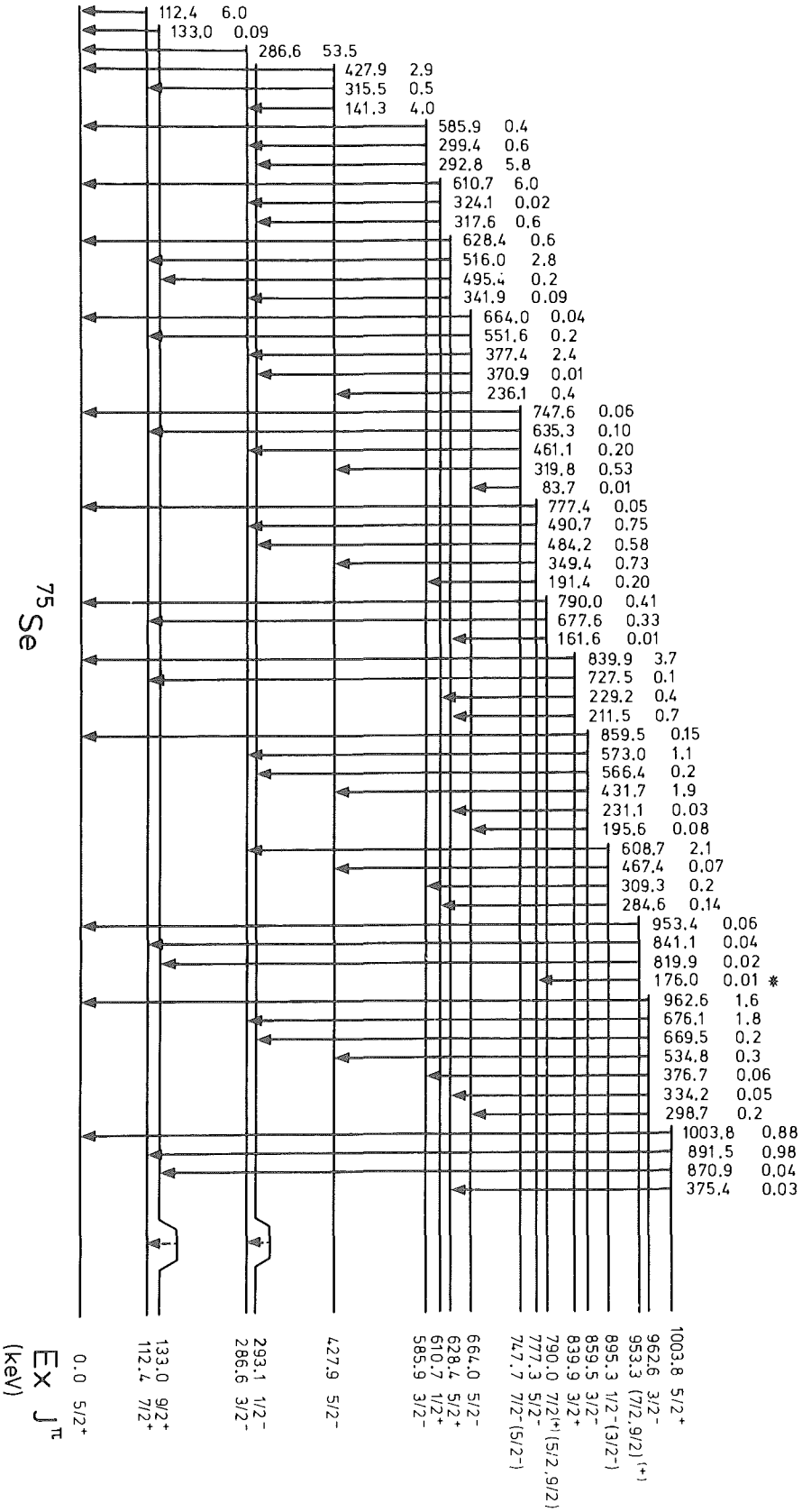

Fig. 5.2 ^{75}Se level scheme (* shows a tentative assignment)

5.2 The level scheme and the level properties of ^{75}Se

Fig. 5.2 shows the γ-decay scheme of levels up to 1 MeV in ^{75}Se. The precise level energies are given in Table 5.1 at the end of this section.
Assignments of spins and parities of each levels were performed by its γ-decay mode, the multipolarities of transitions determined in the conversion electron measurements, the (n,γ)-level population (Fig. 5.3) and the previous results which are discussed in §5.2.1.

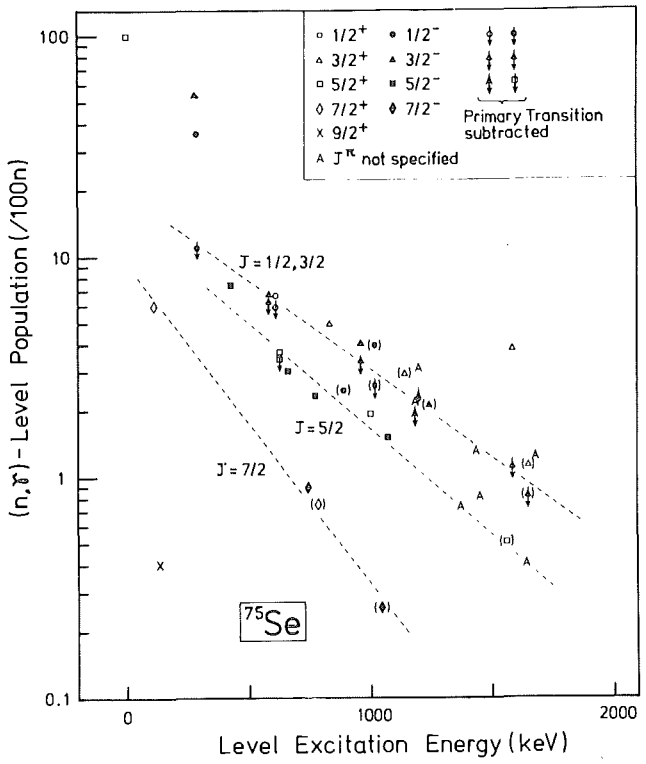

Fig. 5.3

(n,γ)-level population for ^{75}Se

Clear evidence of the existence of the levels is nicely demonstrated in the (p,n) reaction investigated by Finckh et al./Fi70/ and in some other neutron transfer reactions /Sa73,Sh78,Ba79/. In the next section detailed arguments for each level are given.

5.2.1 Levels up to 1 MeV excitation energy in ^{75}Se

The $5/2^+$ groundstate

The groundstate spin J=5/2 is established by the measurements of the hyperfine structure of $OC^{75}Se$ using the microwave method /Aa55/. The parity was determined to be π=+ by the various measurements : electron capture decay to the 400.6keV $5/2^+$ state in ^{75}As with log ft = 6.1 /Pa66/, angular momentum transfer l_n=2 in the reactions ^{76}Se(d,t) /Sa73/, ^{74}Se(d,p) /Sh78/ and ^{76}Se(p,d) /Ba79/.
In the present work, a weak E2 primary γ-transition to this state was observed for the first time (see Table 4.2, and Fig. 2.26, 5.2).
This ground state is believed to be deformed due to its large electric quadrupole moment (+1.0±0.2 barn/Aa55,Fu69/). The small spectroscopic factor in the particle transfer reactions mentioned above may also indicate that this state is highly collective.
The magnetic dipole moment is known to have a value of μ= 0.67 ± 0.04 μ_N /Ca74/.
The half life of the electron capture decay to ^{75}As is $\tau_{1/2}$ = 119.76 ± 0.05 days /Sc80b/.

The 112.4 keV $7/2^+$ level

This level was firstly recognized in the (p,n) and (p,nγ) reactions /El58,Lo60, Fi70/. The spin and parity of $J^\pi = 7/2^+$ was proposed /Pa66/ from ① the high log ft - value in the β-decay of ^{75}Br /Pa66,Co72,Ek81/, ② the short life time (latest value $\tau_{1/2}$ = 0.69±0.12ns /Ag73,Ag74/) and ③ the systematics of neighboring nuclei. This J^π-assignment was confirmed by the following experiments:

- $\gamma(\theta)$- measurements in the ^{75}As(p,nγ) /La74,Ag74/ and ^{72}Ge(α,nγ) reactions
- measurements of the internal conversion of the 112.4 keV groundstate transition /Ag74,Su74,present/.

In the particle transfer reactions the results are still ambiguous (l_n=3,4) /Sa73/ but this level is not well resolved from the close-lying $9/2^+$ level at 133 keV and possibly only weakly excited /Sh78,Ba79/. The present (n,γ)-population is consistent with J = 7/2 (Fig. 5.3).
The (E2/M1)-mixing ratio of the 112.4 keV transition is found to be δ^2 = 0.17±0.03 in the present work, which is in good agreement with that of Sugimitsu et al. /Su74/ (δ^2 = 0.12±0.04), supporting the smaller value of δ of sanderson et al. /Sa76a,Kr74/ (δ = +0.25 or +2.1).
A primary γ-transition (E_γ=7909keV, I_γ=0.20/100n) to this level has been reported

in the previous (n,γ)-study /Ak73a/. The present work shows no trace of this primary transition (sensitivity of present work at this energy ; $I_\gamma > 0.002/100n$). With the present mixing ratio and the half life given above, the reduced transition rate of the 112.4 keV γ-ray is calculated to be
$B(M1) = (2.0 \pm 0.4) \times 10^{-2}$ W.u. and $B(E2) = (3.4 \pm 0.9) \times 10^{2}$ W.u..

The 133.0 keV $9/2^+$ level

Due to the large spin difference between the $1/2^+$ neutron capture state and this level, the population of this level in the (n,γ)-reaction is very weak. In the previous (n,γ)-studies of the ^{75}Se nucleus, no lines were reported concerning this $9/2^+$ level /Ru70,Ak73a/. However the high sensitivity of GAMS 1,2/3 enabled the identification of several γ-rays in connection with this level (Fig. 5.2).
The spin and parity $J^\pi = 9/2^+$ is well established through studies of the particle transfer reactions (l_n=4,/Sa73,Sh78,Ba79/) and the conversion electron measurement of the E2 ground state transition /Ag73,Ag74,Su74,present/.
This level is strongly excited by the particle transfer reactions mentioned above. The sum of the spectroscopic factor from the pick-up /Sa73,Ba79/ and the stripping /Sh78/ reactions provide a theoretical limit of 10 for the $g_{9/2}$ single particle state.
The half life of this level was measured to be $\tau_{1/2}$ = 5.3 $\pm$ 0.6 ns by the (657.7keV) - e^-(133.0keV) coincidence. This half life shows that this 133.0 keV E2-ground state transition is enhanced (42$\pm$11 W.u.) compared with the single-particle estimate , as well as well as the 112 keV ground state transition /Ag74/.

The 286.6 keV, $3/2^-$ - 293.1 keV, $1/2^-$ doublet

Agarwal et.al. /Ag73,Ag74/ have proposed this doublet of levels in order to solve the following problems,

(1) different half lives are reported for the 286.6 keV level $\tau_{1/2}$ = 30.0 $\pm$ 0.4 ns /Ri68/ by a pulsed beam method in the ^{75}As(p,nγ) reaction, and 1.23 $\pm$ 0.15 ns /Ra69/ when gated with 511 keV-annihilation photons.
Coban et al. /Co72/ have shown that the 286 keV γ-ray, when gated by the 511 keV-line, has a time distribution which is a superposition of a shorter life time and a longer life time (29.6 $\pm$ 3.2 ns). They also showed that the 286.6 keV line with shorter life time is coincident with 141.3, 373.4, 573.4, 573.0, 608.7, 733.9, and 912.0 keV γ-rays, and that the component of longer life time is coincident with 292.8 and 952.1 keV γ-rays.

(2) In total 7 doublet-lines were seen with the same energy difference of 6.5 keV /Co72/ namely lines with 579.5-586.0, 852.9-859.4, 1067.6-1073.7, 1177.8-1184.3, 1238.6-1245.5 and 1554.4-1561.0 keV.

③ The low-lying $J^{\pi}=1/2^{-}$ state, which is commonly seen in the neighbouring nuclei, was missing.

The present results are in agreement with the observation of Agarwal et al.. Within the sensitivity of the GAMS spectrometers no γ-lines were observed with lower energies that would extend the number 7 of the doublets mentioned above. A primary γ-transition to the 286.6 keV (E =7741.0 keV) level was firstly identified because of the large asymmetry of the strong 7734.55 keV-line, supporting a close doublet of levels (see table 4.2).

The spin and parity ($J^{\pi}=3/2^{-}$) of the 286.6 keV level is well established by ① the E1-multipolarity of the ground sate transition from the measurements of conversion electrons /Co72,Su74,Ag74,present/, and ② the neutron angular momentum transfer $l_n=1$ in the ^{76}Se(d,t) experiment /Sa73/. Agrawal et al. have proposed $J^{\pi}=1/2^{-}$ for the 293.1 keV level from the absence of the ground-state transition. The γ-ray decay scheme and the multipolarities of the transitions in the present work are in agreement with the assumption of $J^{\pi}=1/2^{-}$. In the Nuclear Data Sheets /Ek81/, this spin and parity assignment is still in brackets. However, within the detection limit ($\gtrsim$ 0.005) of the GAMS spectrometers the 293.1 keV ground state transition was not found. This means that the allowed E1-ground state transition is hindered by a factor of more than 6×10^{11} compared with the single particle estimate, if we assumed $J^{\pi}=3/2^{-}$ for the 293.1 keV level. Thus the assignment of $J^{\pi}=3/2^{-}$ for the 293.1 keV level is very improbable. On the other hand the hindrance factor for the M2-ground state transition is $\gtrsim 10^4$, which is reasonable for $J^{\pi}=1/2^{-}$ if one considered that the 6.5 keV M1-transition from the 293.1 keV level to the 286.6 keV level (pure M1 assumed) is already retarded by a factor of 16 /Ag74/. In the (d,p)-study /Sh78/ the 293.1 keV level is strongly excited ($l_n=1$). On the other hand, the (d,t)- and (p,d)-reactions /Sa73,Ba79/ provide evidence for strong excitation of the 286.6 keV level. These facts show that these two close-lying levels have rather pure single-particle nature.

For the half life of the 286.6 keV-level a value of 1.29 ± 0.11 ns is listed in Nucl. Data Sheets as an average of two different measurements /Ra69,Ag74/. Using this half life, the hindrance factor of the 286.6 keV E1-transition is calculated to be 7.8×10^4.

The 427.9 keV $5/2^{-}$ level

This level was seen for the first time in the (p,n)- and (p,nγ)-reactions /El58, Lo10,Pa66,Fi70/, and its spin and parity $J^{\pi}=5/2^{-}$ is well established by the following experimental facts,

- direct β-feeding from ^{75}Br ($J^{\pi}=3/2^{-}$ ground state) with log ft = 6.22 /Ra69, Co75,Ek81/

- E1-multipolarity of the 427.9 keV ground state transition /Ag74,Su74,present/ determined by the conversion electron measurement
- M1+E2 (δ^2=0.11 $\pm$ 0.03 present) 141.3 keV transition to the 286.6 keV $3/2^-$ level
- Presence of 315.5 keV transition to the 112.4 keV $7/2^+$ level
- The value of neutron angular momentum l_n= 3 for this level /Sa73,Sh78,Ba79/
- $\gamma(\theta)$-measurements in the (p,nγ) reaction /La74/ and in the (α,nγ) reaction /Sa76a/

The present (E2/M1)-mixing ratio of 141.3 keV transition is in reasonable agreement with the value of Sugimitsu et al. /Su74/ (δ^2= 0.09 $\pm$ 0.04) and of Sanderson et al./Sa76a/ (δ = -0.19 $\pm$ 0.10), but it slightly deviates from the value of Zell et al. /Ze75,Kr77/ (δ = -0.13 $\pm$ 0.03).
This level is populated in the particle transfer reactions with a fairly large spectroscopic factor /Sa73,Sh78,Ba79/, which is consistent with the assumption of a rotational band built on this level /Ze75/.

The 585.9 keV $3/2^-$ level

Though only a clean single reaction peak is seen in the spectrum of the (p,n) reaction /Fi70/, this level was misassigned as a 579-586 keV doublet as discussed before in the argument of the 286.6 keV-293.1 keV doublet.
The spin and parity of this level is uniquely determined to be $J^\pi=3/2^-$ by:
① l_n=1 in the (d,t)- /Sa73/, /(d,p)- /Sh78/ and (p,d)-reactions /Pa79/,
② existence of the ground state transition, ③ (M1+E2)-multipolarity of the 292.8 keV transition to the 293.1 keV $1/2^-$ level /Ag73,Ag74,Su74,present/.
A large E2 admixture has been reported (δ^2(E2/M1)= 0.6 $\pm$ 0.3),/Su74/) for the 292.8 keV transition. However other investigations and the present work show only a small admixture of E2 in M1.

The 610.7 keV $1/2^+$ level

This level and the next $5/2^+$ level at 628.4 keV are not seen in the β-decay studies of ^{75}Br /Co72,Ho75,Le78,Ek81/, and they are weakly excited by the transfer reactions /Sa73,Sh78,Ba79/. However this level is clearly found in the present (n,γ)-work as well as in the (p,n)- and (p,nγ)-reactions /Pa66,Fi70, Ag73,Ag74,Su74/, due to the non-selectivity of these reactions.
$J^\pi=1/2^+$ is unambiguously determined by the above mentioned transfer reactions (l_n=0). The present data are consistent with this spin-parity assignment.

The 628.4 keV $5/2^+$ level

$J^\pi=5/2^+$ is clearly determined by the following arguments;
- Transfer reactions are showing l_n=2 /Sa73,Sh78,Ba79/
- Three depopulating γ-rays to the levels ground state $5/2^+$, 112.4 keV $7/2^+$ and

133.0 keV $9/2^+$ /Ag73,Ag74,present/

- The 516.0 keV transition to the 112.4 keV $7/2^+$ level has a multipolarity of M1 (+E2) /Ag74,present/

In the reevaluated previous (n,γ)-study /Ak73a,Ho75,Ek81/, existence of a primary E2 transition to this level was indicated. The present study clearly confirms this argument.

The 664.0 keV $5/2^-$ level

Like for most of the levels in ^{75}Se, the existence of this level was cleary established by the (p,n) reaction /Fi70/ (also /Lo61/). The spin and parity $J^\pi=5/2^-$ is unambiguously determined by:

- log ft = 6.05 in the β-decay of ^{75}Br /Ra68,Co72,He75,Ek81/
- Neutron transfer reaction /Sa73,Sh78,Ba79/, showing $l_n=3$
- γ(θ)-measurements /La74,Ag74,Sa76a/ of the 377.4 keV transition to the 286.6 keV $3/2^-$ level
- The multipolarity of the 377.4 keV transitions is M1 /Su74,Ag74,present/
- γ-decay mode, presence of a transition to the 112.4 keV $7/2^+$ level

In the present work five γ-rays are found to depopulate this level (see Fig.5.2), which, together with the multipolarity of the 377.4 keV transition, alone fix the only possible spin and parity $J^\pi=5/2^-$.

The 747.7 keV $7/2^-$ ($5/2^-$) level

The most probable spin and parity of this level is $J^\pi=7/2^-$, which is deduced from:

- The multipolarity of the 319.8 keV transition to the 427.9 keV $5/2^-$ level is M1 /Su74,present/, and that of the 461.1 keV transition to the 286.6 keV $3/2^-$ level is E2 /Ag74/.
- γ(θ)-measurement in the ^{72}Ge (α,nγ) reaction showed two possible spins J = 3/2, 7/2 /Sa76a/.
- The present study shows that the (n,γ)-level population is apparently favouring J = 7/2 (see Fig.5.3).

This level is only weakly excited in the transfer reactions /Sa73, Sh78,Ba79/. Sanderson et al. /Sa73/ proposed a l_n-value of 1+4. The present data (γ-decay mode, (n,γ)-population,etc.) strongly favour $J^\pi=7/2^-$, but do not completely exclude the possibility of $J^\pi=5/2^-$.

This level is assigned as a member of a rotational band based on the $5/2^-$ 427.9 keV level /Ze75,Sa76a/. A small spectroscopic factor for this level in the transfer reaction is consistent with such an assumption.

Coban et al. /Co72,Ek81/ have reported a direct β-feeding (log ft = 7.34 in

/Ek81/) from the $3/2^-$ ground state of ^{75}Br of this level. It is unlikely that a $\Delta J = 2$ transition has such a small log ft -value. According to the present γ-decay scheme two populating γ-rays from the levels at 1374.5 keV and 1073.8 keV (not shown in Fig.5.2) have already enough intensities ($I\gamma$=0.07 and 0.17) to cancel the intensity of direct β-feeding. Therefore, the existence of this β-feeding is questionable. This fact is again favouring $J^\pi = 7/2^-$.

The 777.3 keV $5/2^-$ level

Sanderson et al. /Sa73/ and Barbopoulos et al. /Ba79/ have shown that the transfered angular momentum of picked-up neutrons in the (d,t)- and (p,d)-reactions feeding this state is l_n=3, restricting possible spin and parity assignments to $J^\pi = 5/2^-$, $7/2^-$. The existence of the 484.2 keV transition to the $1/2^-$ 293.1 keV level eliminates the possibility of $J^\pi=7/2^-$. The E2 multipolarity of the 484.2 keV transition, which is estimated by the measurements of conversion electrons /Su74,present/, is consistent with this assignment. The (n,γ)-level population of this level is also favouring $J = 5/2^-$.
The log ft -value given in the Nuclear Data Sheet (log ft = 6.73) /Ek81/ should be somewhat smaller, because, according to the present decay scheme, 35% more intensity is estimated to depopulate this level. This fact is consistent with the assumption $J^\pi=5/2^-$.

The 790.0 keV $7/2^{(+)}$ (5/2, 9/2) level

Essentially two depopulating γ-rays ($E\gamma$ = 790.0, 677.6 keV) established this level /Su74,Ag74,present/. Another depopulating γ-ray ($E\gamma$ = 657 keV) is also reported by several authors /Ak73a,Su74,Ag74,Sa76a/. These investigators have given rather different informations on this γ-ray, e.g. intensity, coincidence, threshold energy (p,n) etc.. This γ-ray was expected at 656.950 keV in the present work and if it existed, it could be well resolved from the neighbouring strong 657.031 keV double capture γ-line, using the 2nd and 3rd order reflection of GAMS 2/3. However, within the sensitivity of GAMS 2/3 ($I\gamma > 0.01$) this γ-ray was not found.
From the γ-ray decay mode the possible spin and parity of this level is $J^\pi = 3/2^+$, $5/2^\pm$, $7/2^\pm$ and $9/2^+$. However, the level population (Fig.5.3) shows that $3/2^+$ may be excluded and $J = 7/2$ may be most likely. Further, positive parity for this level is more favourable, because the three depopulating γ-rays in the present work are all populating the low-lying positive parity states.

The 839.9 keV $3/2^+$ level

This level was proposed in the ^{75}As (p,nγ)-studies /Su74,Ag74/ based on the energy combination and the excitation function of the three depopulating γ-rays 211.5 keV, 229.2 keV and 839.9 keV. In the present work, further, the 727.5 keV γ-line is found to agree well with the energy difference between this level and the 212.4 keV $7/2^+$ level. A level reported at 832 keV in the (p,n) reaction /Fi70/ may be identical with this level.

The spin and parity are unambiguously determined to be $J^\pi=3/2^+$ in the present study by the following results;

- The four depopulating transitions stated above restrict possible spin-parity assignment to $J^\pi=3/2^+$, $5/2^+$.
- The multipolarities of the transitions with 211.5, 229.2 and 838.9 keV are all M1 /Su74,present/ requiring $J^\pi=3/2^+$, which is consistent with the (n,γ)-level population.

The 859.5 keV $3/2^-$ level

The present γ-decay mode of this level is in good agreement with that of β-decay study /Co72,Ek81/. Additionally one weak transition ($E\gamma$=231.1 keV, $I\gamma$=0.03/100n) is assigned to depopulate this level in the present study.

The assignment of the spin and parity $J^\pi= 3/2^-$ is unambiguous from the following results;

- $l_n=1$ is obvious in the neutron transfer reactions /Sa73,Sh78,Ba79/.
- Two depopulating transitions, 859.5 keV /Co72,Ak73a,Ek81,present/ and 231.1 keV /present/, to the ground state $5/2^+$ and the level at 628.4 keV $5/2^+$ eliminate the possibility of $J^\pi=1/2^-$ for this level.
- The multipolarity of the 431.7 keV transition to the 427.9 keV $5/2^-$ level is M1 (+E2) /Su74,Ag74,present/.
- $\gamma(\theta)$ measurement of the 431.7 keV transition favours J = 3/2 than J = 1/2 /Sa76a/.

A log ft -value of 5.74 /Ek81/ is consistent with $J^\pi=3/2^-$.

The 895.3 keV $1/2^-$ ($3/2^-$) level

Coban et al. /Co72,Ek81/ have reported three depopulating γ-rays with 608.7, 467.4 and 309.3 keV. The log ft -values of 6.22 /Ek81/ may indicate that the spin and parity of this level are $J^\pi=(1/2, 3/2, 5/2)^-$. The transfered angular momentum $l_n=1$ /Sa73,Sh78,Ba79/ eliminates $5/2^-$.

In the present study the 284.6 keV transition, which was misassigned in the work of Agarwal et al. /Ag74/, has been additionally assigned to depopulate this level. The multipolarity of the 608.7 keV transition has been determined

to be M1, which is consistent with the spin and parity assignment $J^{\pi}=1/2^{-}$ or $3/2^{-}$. However, the absence of the ground-state transition leads one to prefer $1/2^{-}$ over $3/2^{-}$.

The 953.3 keV $(7/2,9/2)^{+}$ level

Agarwal et al./Ag74/ have suggested the existence of this level from the excitation function of the 953.4 keV ground state transition. Sanderson et al./Sa76a/ have reported two possible depopulating γ-lines, i.e. the 953.4 keV and 841.1 keV transition.
In the present study this level was found by the Ritz combination program (§ 5.1). Four transitions, 953.4, 841.1, 819.9 and 176.0 keV, are tentatively assigned to depopulate this level. The first three transitions are all populating low-lying positive parity states (ground state $5/2^{+}$, 112.4keV $7/2^{+}$, 133.0keV $9/2^{+}$), favouring positive parity. The 176.0 keV transition is assumed to populate the 777.3 keV $5/2^{-}$ level. If this placement is correct the possibility of $J^{\pi} = 9/2^{+}$ is eliminated. The (n,γ)-level population is somewhat lower than expected for $J = 7/2$ (population $\sim$ 0.1, see Fig. 5.3).

The 962.6 keV $3/2^{-}$ level

The neutron transfer reactions /Sa73, Sh78, Ba79/ have shown that the transfered angular momentum is $l_n = 1$ restricting the possible spin and parity of this level to $(1/2, 3/2)^{-}$. The $\gamma(\theta)$-measurement on the 962.6 keV γ-ray favours $J = 3/2$, and its intensity to the $5/2^{+}$ ground state excludes $1/2^{-}$.
The $(p,n\gamma)$ reactions /Su74, Ag74, Ho75, Ek81/ have shown three depopulating γ-rays 962.6, 676.1 and 534.8 keV , which are all doubly placed in the decay scheme /Ho75/. The high resolution of the GAMS 2/3 spectrometer has shown that these three γ-lines are all close doublets, and all three double assignments have been confirmed. Further additional four transitions (669.5, 376.7, 334.2 and 298.7 keV) have been assigned to depopulate this level (Fig. 5.2). The 334.2 keV transition which populates the 628.4 keV $5/2^{+}$ level favours $J^{\pi} = 3/2^{-}$ for this level. A γ-line of energy at 121.8 keV has once been reported to depopulate this level /Su74,also Ho75,Ek81/. However this is a misassignment of a γ-line of ^{75}As. Within the sensitivity of the GAMS spectrometer no other γ-line was found at this energy.

The 1003.8 keV $5/2^{+}$ level

The neutron transfer reactions /Sa73, Sh78, Ba79/ have unambiguously shown a typical $(l_n = 2)$-pattern, which limits the possible spin and parity for this level to $(3/2, 5/2)^{+}$.
The $(p,n\gamma)$-reactions /Su74, Ag74, Ho75, Ek81/ have revealed three depopulating

γ-lines 1003.8, 891.5 and 870.9 keV (present γ-ray energies). The 891.5 keV line was found to be a close doublet (891.47 - 891.09) in the present work, and the 891.09 keV γ-line was placed to depopulate a higher-lying level(1144.5keV). The intensity of this γ-line is in good agreement with the result of β-decay studies /Lo72, Ho75, Ek81/, where this γ-line is the only depopulating transition of this level, thus providing no evidence of direct γ-feeding to this level from ^{75}Br. Together with an additional γ-line of 375.4 keV, in total four transitions to the $5/2^+$ ground state, and the levels $7/2^+$ 112.4keV, $9/2^+$ 133.0keV and $5/2^+$ 628.4keV are assigned to depopulate this level, and exclude $J^\pi = 3/2^+$. The (n,γ)-level population is consistent with the spin $J^\pi = 5/2$.

E_X in keV		J^π	
Present	Others [a]	Present	Others [a]
0.		$5/2^+$	
112.388(1)	112.27(7)	$7/2^+$	$7/2^+$
133.040(2)	132.95(15)	$9/2^+$	$9/2^+$
286.571(2)	286.54(6)	$3/2^-$	$3/2^-$
293.105(2)	293.07(9)	$1/2^-$	$(1/2)^-$
427.885(1)	427.81(7)	$5/2^-$	$5/2^-$
585.949(2)	585.98(9)	$3/2^-$	$(3/2)^-$
610.716(2)	610.87(20)	$1/2^+$	$1/2^+$
628.431(2)	628.28(10)	$5/2^+$	$5/2^+$
663.957(2)	663.91(9)	$5/2^-$	$5/2^-$
747.651(3)	747.47(11)	$7/2^-$ $(5/2^-)$	
777.321(2)	777.29(8)	$5/2^-$	
789.990(5)	789.74(10)	$7/2^{(+)}$ (5/2,9/2)	
839.893(3)	840.15(10)	$3/2^+$	
859.538(2)	859.47(8)	$3/2^-$	$3/2^-$
895.272(2)	895.41(13)	$1/2^-$ $(3/2^-)$	$1/2^-$,$3/2^-$
953.296(2)	953.6(3)	$(7/2,9/2)^{(+)}$	
962.644(2)	962.83(15)	$3/2^-$	$3/2^-$
1003.846(2)	1003.79(8)	$5/2^+$	$5/2^+$

a) Data compiled in Nucl.Data Sheets/Ek81/

Table 5.1 Precise energies of levels in ^{75}Se up to 1 MeV

5.2.2 Levels above 1 MeV

For the higher-lying levels it is harder to give complete descriptions. Therefore we list the level energies and the so far proposed possible spins and parities in Table 5.2 (next page). A few comments will be given about a few levels.

A direct β-feeding is reported to the level at 1144.5 keV /Co72, Ho75, Ek81/ with log ft = 7.0. However, we have shown in the present work that the log ft - value for a positive parity state is quite probably very large. So the depopulating γ-line observed in the β-decay study may possibly follow a cascade γ-line from higher-lying levels, which were not found in that work due to poor statistics.

The (d,p)-study /Sh78/ has shown a well separated proton peak and a typical angular distribution of $l_n = 0$ for the level at 1432.4 keV.

The γ-decay mode of the 1561.0 keV level in the present work provides possible spins and parities of $J = 5/2^{\pm}$. A direct β-feeding from ^{75}Br /Co72, Ho75, Ek81/ would prefer a negative parity for this level.

The 1643.2 keV level is a new level found by the Ritz combination principle. The (n,γ)-level population is consistent with J = 5/2.

An improved β-decay study would provide interesting informations on these higher-lying levels.

Level energy in keV	J^{π}	Comments	Level energy in keV	J^{π}	Comments
1020.5	$1/2^{-}(3/2^{-})$	$l_n=1$[a], No GST	1673.3	$3/2^{-}$	NGP, GDM, $(l_n=1)$[c]
1047.2	$7/2^{-}(5/2^{-})$	$l_n=3$[b),c], NGLP	1802.0	(1/2,3/2)	NGP, GDM
1073.8	$5/2^{-}$	$l_n=3$[b], GDM	1810.7	$(3/2^{-})$	GDM
1144.5	$3/2^{+}(5/2^{+})$	$l_n=2$[b], NGP, GDM	1894.9	(1/2,3/2)	GDM
1184.2	(1/2,3/2)	NGP, GDM, NGLP	1943.3	(1/2,3/2)	GDM
1198.5	(1/2,3/2)	NGP, GDM, NGLP	1958.3	$(3/2^{+})$	GDM, NGP
1245.2	$3/2^{-}$	$l_n=1$[a),c], GST	1985.9	(1/2,3/2)	NGP, GDM
1374.5	$(5/2^{-})$	GDM, NGLP	2030.6	$(3/2^{+})$	$l_n=2$[a], NGP
1432.4	$1/2^{+}$	$l_n=0$[a]	2166.7	(1/2,3/2)	NGP, GDM
1454.7	$(5/2^{-})$	GDM	2242.1	$(3/2^{+})$	NGP, GDM, $l_n=0+2$[a]
1561.0	$5/2^{-}$	GDM, β	2271.2	(1/2,3/2)	NGP, GDM
1589.5	$3/2^{+}(5/2^{+})$	$l_n=2$[a], NGP, GDM, NGLP	2298.6	(1/2,3/2)	NGP, GDM
1643.2	$((3/2^{+}),5/2)$	GDM, NGLP	2307.2	(1/2,3/2)	NGP, GDM
1652.9	$(3/2^{+})$	GDM	2355.9	(1/2,3/2)	NGP, GDM

GST : Groundstate transition is found.
β : Direct β-feeding is observed.
GDM : Based on the γ-decay mode.
NGLP : Based on the (n,γ)-level population.
NGP : Primary transition to this level is observed.
No : Not seen.

a) Ref./Sh78/ b) Ref./Sa73/ c) Ref./Ba79/ d) Ref./Co72/

Table 5.2 Prominent levels from 1 MeV to 2.5 MeV in ^{75}Se

5.3 The level scheme and level properties of ^{76}Se

The sudden increase of level density at ∿ 2.8 MeV excitation energy, which is somewhat lower than expected from the calculated gap energies(Table 5.3, below), is obvious in Fig. 2.26 and 2.27.

Nucleus	Gap energy
$^{74}_{32}Ge_{42}$	$2\Delta_n$ = 3.7 MeV
$^{75}_{33}As_{42}$	$2\Delta_n$ = 2.6 MeV
$^{76}_{34}Se_{42}$	$2\Delta_n$ = 3.4 MeV $2\Delta_p$ = 3.4 MeV
$^{77}_{35}Br_{42}$	$2\Delta_n$ = 2.3 MeV
$^{78}_{36}Kr_{42}$	$2\Delta_n$ = 3.2 MeV

Table 5.3

Calculated gap energies with eq. 2.92 in /Bo69/, using the data of Wapstra and Bos /Wa77/.

Therefore, a theoretical interpretation of the levels above this energy is quite difficult. We discuss here briefly the levels with energies up to the 2.429 MeV level, which is the well-known 3^- octupole state, and only several comments will be given about the levels above 2.4 MeV.

5.3.1 Levels up to 2.4 MeV excitation energy in ^{76}Se

On the next page the level scheme of ^{76}Se is shown. Only the γ-lines observed with the GAMS spectrometers are shown in Fig. 5.4. Groundstate transitions with energies above 1.8 MeV can be found in the references/Na73,Na74,Ka80/.
Precise level energies are given at the end of this chapter.

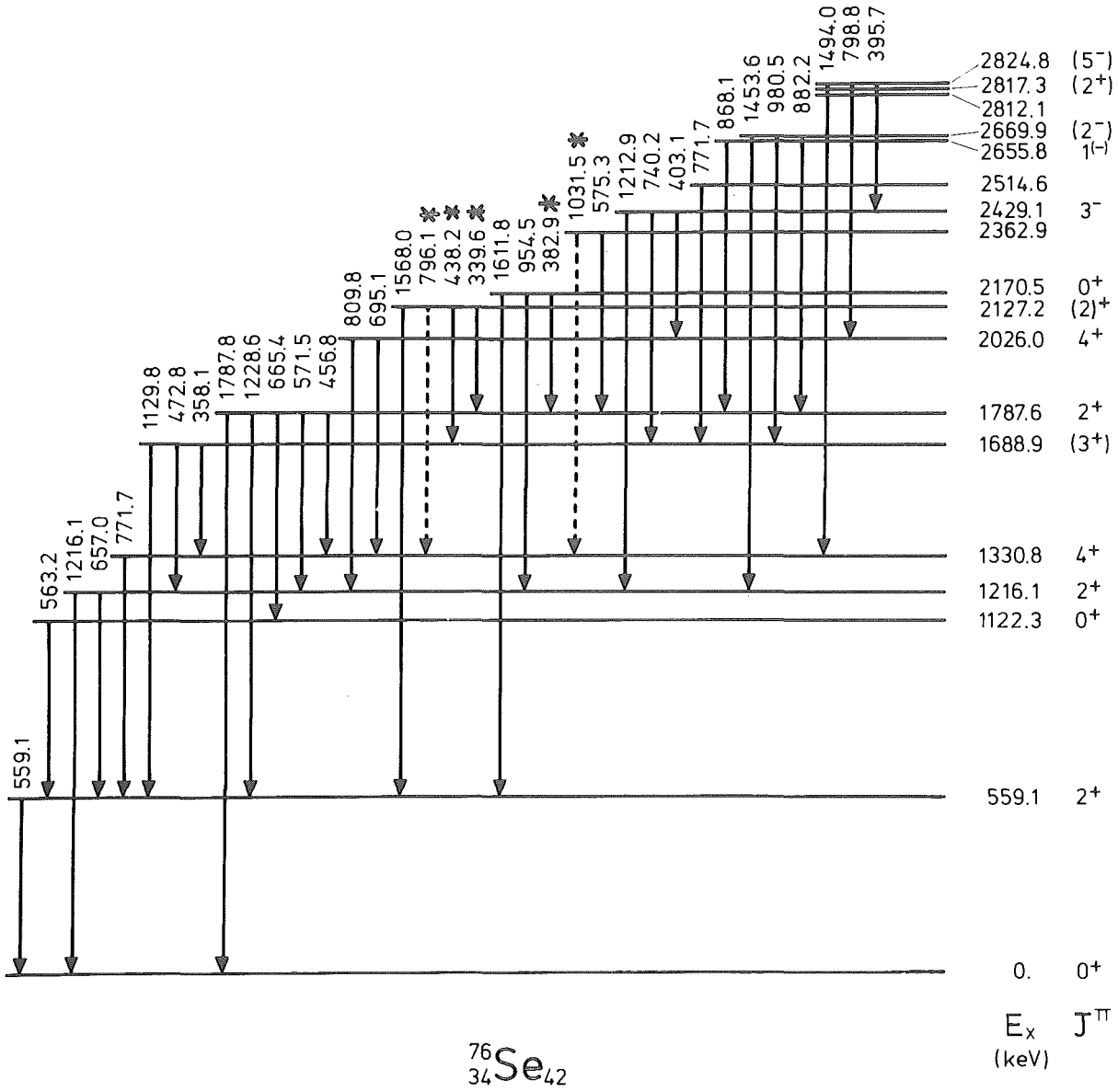

Fig. 5.4 Low-lying levels and low energy γ-transitions observed through double neutron capture using a ^{74}Se target (* shows a tentative assignment)

The 0_1^+-groundstate

Spin and parity $J^\pi = 0^+$ for the ground state of the even-even ^{76}Se establishes the E2 character of the primary transition from the neutron capture state ($5/2^+$(^{75}Se) + s-wave = 2^+ or 3^+), as well as in the case of the primary transition to the 0_2^+ 1122.3 keV level (see Fig. 2.27, Table 4.4 and Table 5.4). However, this does not mean directly that the neutron capture state is only an isolated $J^\pi = 2^+$ state. As shown in Table 5.4, several primary transitions to the levels with probable spin and parity of $J^\pi = 4^+$ are seen. This fact may suggest admixture of the 3^+-state in the 2^+-capture state, because the E2 primary transitions are quite rarely found (see § 6.1.3)

Because of the vibrational appearance of the level structure of ^{76}Se, a nearly spherical nuclear shape would be expected. On the other hand the in-beam studies /Li70,We80/ have revealed a nice rotational-like band based on the ground state. Actually it is an open question, whether the nuclear shape in this region is spherical or deformed. Theoretical calculations give also different results, i.e. oblate deformation /Di72,Re79/ and prolate deformation accompanied with more or less γ-instability /Ta73/.

The 2_1^+ 559.1 keV level

The spin and parity $J^\pi = 2^+$ is well established by various experiments : Coulomb excitations /Mc62,St62,By64,Ba74,Le77/, conversion electron measurements in the decay of ^{76}Br /De70,Wy73/, $\gamma(\theta)$- or $\gamma\gamma(\theta)$-measurements /By64,Na73,Li70,Ba76,We80, Ka80/, angular distribution of inelastically scattered particles /Da62,Li65b, Ma78,Sa81/ and particle transfer reactions /Ar75,Bo77/.

The E2 ground state transition is enhanced (B(E2) = 44 W.u./Ba74,Le77/). The static quadrupole moment is measured to be -0.34 ± 0.07 eb, which suggests a small prolate deformation for this state /Le77/.

In the present study a relatively strong primary transition was found to populate this level (see Table 4.4).

The 0_2^+ 1122.3 keV level

The first evidence for the possible existence of this 0_2^+ level was reported by Darcey et al./Da62/ and Bygrave et al./By64/. The $\gamma\gamma(\theta)$ measurements following the ^{76}As decay /Na73,Ba76/ have unambiguously determined the spin to be J = 0. The parity has been determined very clearly by the (^3He,d)-measurement /Ar75/. It is interesting to note that rather poor DWBA-fits were reported both in the (p,t) /Bo77/ and in the (p,p') reactions /Sa81/.

The high resolving power of the GAMS-spectrometers has clearly separated the

563.2 keV γ-transition, which populates the 2_1^+ level (559.1keV level), from the strong 559.1 keV γ-line. This was a long-standing problem for establishing this level /Na73/. Because the 563.2 keV γ-line is very close to the strong 559.1 keV γ-line in the spectrum taken with a Ge(Li)-detector , and because both these γ-lines have energies very near to the two γ-lines in ^{76}Ge (546keV and 563keV), which are in coincidence (see for ex. /Le78/ p.257), Morcos et al./Mo71/ have misassigned these γ-lines. The present results support the arguments of Nagahara /Na73/ and Barcley et al./Ba76/.
In the present study a primary transition was found to populate this level. This is the second primary E2 transition in this nucleus.

The 2_2^+ 1216.1 keV level

$J^\pi=2^+$ is well established through Coulomb excitation /Mc62,St62,By64,Ba74/, the (n,n'γ) reaction /Ni61/, angular distributions of inelastically scattered particles /Da62,Li65b,Se81/, conversion electron measurements /Dz70,Wy73/, $\gamma(\theta)$ and $\gamma\gamma(\theta)$ measurements /Li70,Na73,Ba76,We80,Ka80/, and particle transfer reactions /Ar75, Bo77/. Dzhelepov et al. /Dz70/ has reported a fairly large conversion coefficient for the 657keV transition,which populates the 2_1^+-state, indicating E0 admixture. However, the data of Wyckoff et al. /Wy73/ do not show a strong enhancement of this conversion coefficient.
The B(E2)-values of the depopulating transitions of 657keV ($2_2^+ \rightarrow 2_1^+$) and 1216 keV ($2_2^+ \rightarrow 0_1^+$) are reported to be 42.9 W.u. and 1.26 W.u. respectively /Ba74/. The B(E2, $2_2^+ \rightarrow 2_1^+$)/B(E2, $2_1^+ \rightarrow 0_1^+$)) is evaluated to be 0.98 /Ba74/, which should be compared with values of the vibrational (B(E2) ratio = 2) and rotational model (B(E2) ratio =1.33; Alaga's rule).

The 4_1^+ 1330.8 keV level

The spin and parity of the last member of the two phonon triplet $J^\pi= 4^+$ is well established by Coulomb excitation /By64,Ba74/, angular distributions of inelastically scattered particles /Da62,Li65b,Sa81/, the conversion electron measurement of the 772 keV transition ($4_1^+ \rightarrow 2_1^+$) /Wy73/, $\gamma(\theta)$ or $\gamma\gamma(\theta)$ measurements /By64,Li70,We80/, and particle transfer reaction /Ar75,Bo77/.
The B(E2)-value of the 772 keV transition is found to be 70.6 W.u., and the B(E2) ratio is determined to be B(E2, $4_1^+ \rightarrow 2_1^+$)/ B(E2, $2_1^+ \rightarrow 0_1^+$) = 1.61 /Ba74/. This ratio lies between the vibrational (B(E2) ratio =2) and the rotational (B(E2) ratio = 1.33) values.
It is very interesting that the (p,p')-reaction provides a farily poor DWBA-fit for this level /Sa81/, while in the (p,t)-reaction a reasonable fit was obtained.

The (3_1^+) 1688.9 keV level

This level was proposed by Dzhelepov et al. /Dz69/ in the study of the ^{77}Br-decay, and further confirmed by many γ-γ coincidence measurements /Dz70,La71,Mo71,Mc71,Ii71,Ar72,Na73,Na74,We80,Ka80/.

Several authors report a ground state transition from this level /La71,Mo71/. However,other authors, including the present work (upper limit for the ground state transition < 0.2/100n), show only two depopulating γ-lines, with 472.8 keV ($\rightarrow 2_2^+$) and 1129.8 keV ($\rightarrow 2_1^+$). (one more γ-line is found in the present work. See below)

The spin and parity assignment is still ambiguous. The high log ft - value (> 10.0) in the ^{76}As-decay (ground state is 2^-)/Ii71,At72,Na73,Ka80/ and the absence of a transition to 0^+-levels indicate $J^\pi = (3,4)^+$. However a direct β-feeding with log ft = 8.3 in the ^{76}Br-decay (ground state is 1^-) has been reported /Na74/, which suggests a spin of J=1,2,3. Nagahara /Na73/ has concluded that the possible spin and parity are $J^\pi = 3^+$ based on the γ-$\gamma(\theta)$ measurement, which provides J = 1,2,3, and on the high log ft - value in the ^{76}As-decay mentioned above. Another γ-$\gamma(\theta)$ measurement in the ^{76}As decay /Ka80/ has indicated J = 2,3. The spin and parity assignment $J^\pi = 3^+$ is supported by the fact that this level was not excited in the (p,t) /Bo77/ and (p,p') /Sa81/ reactions. The $\gamma(\theta)$ measurement in the decay study of polarized ^{76}As has also favored J = 3. However, $\gamma\gamma$-coincidence measurement from the oriented nuclei /We80/ has provided an evidence of J =2,4.

In the previous $(\alpha,2n\gamma)$-experiment /Li70/ a 1131 keV transition was placed between the 10^+ and 8^+ states and it was corrected in /We80/ based on the coincidence measurement (see also Table 1 in /Ze75/). The $\gamma(\theta)$-measurements of both investigators are in good agreement for this γ-line, showing a large positive A_2 and negative A_4. This is compatible with the spin and parity assignment of $J^\pi = 2^+,4^+$ for this level /Ya68/. The conversion coefficient of this γ-line is consistent with M1 or E2 /Wy73/.

In the present work a 358.1 keV line has been clearly identified to be from the ^{75}Se(n,γ) reaction, and this energy is in excellent agreement with the energy difference between this level and the 4_1^+ 1330.8 keV level. In the spectrum of /Na74/ this energy was probably mistyped as 385 keV and did not appear in the table and the γ-decay scheme.

A weak 438.2 keV γ-line whose intensity could not be well defined due to the time-growing nature of the double capture γ-line, is tentatively assigned to populate this level (Fig. 5.4). This might compensate the small log ft - value observed in the ^{76}Br-decay /Na74/. In the report of /Na74/ this γ-line should have been masked by a strong γ-line of ^{77}Se from the ^{77}Br-decay.

Theoretically one should expect a 3^+-level of the three phonon multiplet around this energy. The γ-decay mode in /Be76a/ as well as in the present work is consistent only with J = 2,3,4.

The 2_3^+ 1787.6 keV level

The earlier data of γ-$\gamma(\theta)$ and β-decay measurements were compiled in Nucl. Data /Ik66b/ and $2^{(+)}$ was suggested. The spin assignment has been confirmed by the γ-$\gamma(\theta)$ measurements /Na73,Ka80/ and the $\gamma(\theta)$-measurement in the oriented ^{76}As-decay /Ba76/. The parity has been unambiguously determined to be π=+ by the (^{3}He,d) reaction /Ar75/.
The previously reported five depopulating γ-lines were all identified due to the high sensitivity of GAMS-spectrometer (Fig. 5.4).
This level is very weakly populated in the (p,p') reaction /Sa81/ and not reported in the (p,t) reaction /Bo77/.

The 4_2^+ 2026.0 keV level

Darcey et al. /Da62/ proposed this level in the (p,p') reaction. Lieder et al. /Li70/ have proposed $J^\pi = 4^+$ based on the $\gamma(\theta)$-measurement in the (α,2nγ) reaction. This spin and parity assignment is supported by the high log ft - value (>10.7 /Be76/) in the ^{76}As-decay /Ii71,Na73,Ka80/, the absence of excitation in the ^{76}Br decay /Na74/, l_p = 3 in the (^{3}He,d) reaction, and the measurements of the excitation functions and the γ-angular distributions in the (^{7}Li,2nγ)-reaction /We80/.
In the present study a fairly strong primary transition has been observed, while for the 4_1^+-state no primary γ-transition has been seen. The recent (p,p') reaction /Sa81/ shows almost no excitation of this level. In the (p,t) reaction $J^\pi = (3^-,4^+)$ was given to this level /Bo77/.

The $(2_4)^+$ 2127.2 keV level

Darcey et al. /Da62/ have observed this level in the (p,p') reaction with 12 MeV protons, while the recent (p,p')-experiment with 65 MeV protons shows only a very weak excitation /Sa81/.
The parity of this level is unambiguously determined to be π=+ by the (^{3}He,d) reaction.
Two depopulating γ-lines at 2127 keV and 1568 keV,which populate the 0_1^+ and 2_1^+ levels, are observed commonly in the decay studies of ^{76}Br /Dz69,La70,Na74/ and ^{76}As /Na73,Ar72,Ka80/. Further several authors report the 796 keV transition populating the 4_1^+-level /Dz69,Mo71,Ar72,Ka80/. The intensities given for this 796 keV γ-line in these articles are rather different. However, if

this transition really depopulates this level, then the only possible spin and parity assignment is $J^\pi = 2^+$. In the present study a γ-line with 796.06 keV was found , and tentatively assigned to depopulate this level.
In the present work two additional γ-lines at 438.2 keV and 339.6 keV are tentatively assigned to depopulate this level. The latter γ-line was also identified in the $(n,n'\gamma)$ reaction /Be76/. The present results are consistent with a spin and parity assignment of $J^\pi = 2^+$.

The 0_3^+ 2170.5 keV level

This level was introduced by Dzhelepov et al. in the study of the ^{76}Br-decay /Dz69/, and the existence was confirmed by γ-γ coincidence measurements /Ii71, Me71,Na73,Ka80/.
A typical angular distribution for l=0 in the (p,t) reaction has established unambiguous spin and parity $J^\pi=0^+$ /Bo77/. Ardouin et al. /Ar75/ have reported a possible spin and parity of $J^\pi=1^+,2^+,3^+$ in the (^{3}He,d)-experiment, which contradicts the result of the (p,t) reaction. However, the deuteron angular distribution in /Ar75/ seems to provide no clear evidence of mixing of (l_n= 3) in l_n= 1 or showing rather pure l_n= 1 distribution. The ground state spin of the target nucleus ^{75}As in the (^{3}He,d) reaction is $J^\pi = 3/2^-$. So the pure $l_n = 1$ - distribution does not disagree with a $J^\pi = 0^+$ assignment for this level in /Bo77/.
Two γ-transitions at 955 keV ($\rightarrow 2_2^+$) and at 1612 keV ($\rightarrow 2_3^+$) are known to depopulate this level /Ii71,Na73,Ka80/. These two γ-lines possibly exist in the present γ-spectrum (Table 4.5). An apparent double neutron capture γ-line at 382.9 keV has been tentatively assigned to depopulate this level ($\rightarrow 2_3^+$). The 1612 keV γ-line is rather strong in the pair spectrum. The results of the analysis of the low-energy part of the spectrum coded as PG4 (see Table 4.1) will appear later. Consequently, three γ-transitions to the $2_1^+,2_2^+,2_3^+$ states were found and these are in accordance with $J^\pi = 0^+$ of this level.
This 0_3^+ level may possibly be understood as a member of the three phonon multiplet ($0^+,2^+,3^+,4^+,6^+$) together with other neighboring positive parity states.

The 2362.9 keV level

Nagahara /Na73/ has reported this level based on the fact that the 575.3 keV transition is coincident with 1228.6 keV transition in the ^{76}As-decay. This was confirmed in the similar measurements by Kaur et al. /Ka80/. The level found at 2365 keV by Iizawa et al. /Ii71/ is quite probably the same level. Additionally, the γ-transitions at 1071 keV /Na73,Ka80/ and 1808 keV /Ii71,

Na73/ were assigned to depopulate this level. Iizawa et al. have shown evidence of coincidence of the 1080 keV transition with the 559 keV transition.
The 575.3 keV γ-line was clearly identified in the present work and the 1031 keV γ-line possibly exists (Table 4.5). At higher energy the sensitivity of the GAMS-spectrometer decreases. Thus the presence of the 1808 keV γ-line could not be confirmed.
The assignment of $J^\pi = 2^+,3^+,4^+$ was proposed by Nagahara /Na73/ based on the γ-decay scheme and the log ft - value (=8.4). A higher spin may be favorable because no transition to 0^+ state was observed and because this level is not seen in the decay of ^{76}Br (ground state is 1^-, and the ground state of ^{76}As is 2^-). If this level had a spin of J = 3,4, one would be able to find this level in an in-beam study using heavy ions, because the level energy is not too high. However this is not clear in the study of the (^{7}Li,2n) reaction /We80/.

The 3_1^- 2429.1 keV level

$J^\pi = 3^-$ is well established by the following measurements: angular distribution of inelastically scattered particles /Da63,Li65NP,Ma79,Sa81/, the (^{3}He,d) reaction /Ar75/, and a $\gamma(\theta)$-measurement with oriented nuclei /Ba76/. The (p,t) reaction /Bo77/ showed rather poor DWBA fits. The results of the (^{7}Li,2n) reaction favour spin and parity of $J^\pi = 3^-$.
A strong primary transition to this level has been observed in the present work (see Fig. 2.27 and Table 4.4). Kane /Ka73/ has once pointed out,from systematics, that an exceptionally strong E1 primary transition to the octupole state would occur in the neighborhood of the closed neutron shells. In the case of ^{76}Se the neutron number is 42, and this is far away from the next magic number 50. Thus the strong E1 primary transition to the 3_1^- state in Se might be due to the subshell closure at N=40.
The E3 transition to the ground state is observed /Na69,Dz69,La70,Ii71,Mo71, Mc71,Ar72,Na74,Ba74,Ka80/. The B(E3) has been measured by Coulomb excitation /Ba74/ and is known to be 16.6 W.u..

In the present work no evidence has been found for the existence of the following levels at 1780 keV /Mo71/, 1881 keV /La70,Na73,Ka80/, 2048 keV /La70/, 2080 keV /Ka80/, 2088 keV /Ii71/, 2124 keV /Ka80/, 2128 keV /Ka80/, 2183 keV /Ka80/, 2347 keV /Ii71,Na73,Bo77,Ka80/,2374 keV /Na74/, and 2389 keV /La70/.

5.3.2 Levels above 2.4 MeV in ^{76}Se

As shown in Table 5.4 and Fig. 2.25,2.26,2.27 many new levels have been identified in the present work. As mentioned before the levels above $\sim$ 2.8 MeV may be thought of as two (quasi-)particle states. From the strong primary transitions the parities of these levels would be imagined to be mostly π = -. Ardouin et al. /Ar75/ have also reported many negative parity states above this energy. However, the level energies are not precisely measured by /Ar75/, and thus one can not compare them with the present results. In the (p,t) reaction study /Bo77/ few levels were reported.

Three levels at 2515 keV,2655 keV and 2670 keV which were seen in the decay studies of both ^{76}As /Ii71,Mc71,Ar71,Na73,Ka80/ and ^{76}Br /Dz70,Na74/ have been also identified in the present work.

Possible doublet levels at 2655 keV were reported in the (n,n'γ) reaction /Be76/. These levels may correspond to the levels at 2655 keV and 2669 keV in the present work. However, the levels at 2606 keV and 2620 keV reported there were not seen.

The 2825 keV level was observed in the (^{7}Li,2n) reaction by Wells et al. /We80/. They have reported three depopulating γ-lines at 396 keV, 799 keV and 1494 keV, and proposed J = 5 based on the $\gamma(\theta)$ measurements and mainly on the excitation functions. Further they suggested π = - from the systematic studies of neighboring nuclei. In the present study these three γ-lines, which populate the 4^{+}_{1},4^{+}_{2}, and 3^{-} levels, have all been identified.

The levels at 2805 keV, 3009 keV and 3101 keV which were found in the (n,n'γ) reaction /Be76a/ have not been identified in this work. The (p,t) reaction reported evidence of the 3106 keV level, but gave no spin and parity to this level.

Level energies in keV			Level energies in keV		
Present	Others [a]	J^{π} [b]	Present	Others [a]	J^{π} [b]
0.†	0.	0^+	(2968.7(7)†§)		
559.094(3)†	559.10(3)	2^+	2985.2(14)†§	3001	2^+
1122.263(4)†	1122.36(5)	0^+	3008.7(12)†§	3010.0 ?	
1216.127(7)†	1216.13(3)	2^+	3069.80(5)†	3069.8(5)	
1330.831(8)	1330.85(9)	4^+	3105.7(4)†§	3106.5 ?	3^- d)
1688.931(5)†	1689.00(6)	(3^+)	3161.8(4)†§	3160.1(5)	3^- d)
1787.618(7)†	1787.70(5)	2^+	3191.9(4)†§	3198(10)	π=+
2025.950(7)†	2025.9(2)	4^+	3219.5(4)†§	3216 d)	$3^-,4^+$ d)
2127.177(6)†	2127.5(2)	$(2)^+$	3269.1(4)†§	3268(10)	π=-
2170.5(2)	2170.8(4)	0^+ c)	3295.5(4)†§	3289 d)	4^+ d)
2362.915(12)	2362.7(3)	π=+	3350.8(4)†§	3351.8(5)	π=+
2429.079(21)†	2428.8(2)	3^-	3477.8(16)†§	3475	4^+ d)
2514.618(9)†	2514.9(4)	π=+	3509.0(5)†§	3530(10)	π=+
2651.8(5)†§			3558.2(5)†§	3558(10)	(π=+)
2655.83(7)	2655.5(3) 2658d)	$1^{(-)}$ $(0^+,3^-)$d)	3563.6(7)†§	3565 d)	$2^+,5^-$ d)
2669.9(5)†	2669.8(3)	(2^-)	3604.4(3)†§	3604.1(5)	π=+
2812.1(5)†§	2807 d)	4^+ d)	3651.3(4)†§	3655 d)	(4^+) d)
2817.3(5)†§	2817.0 ?	(2^+)	3731.0(10)†§	3732 d)	3^- d)
2824.8(1)	2823.9	(5^-)	3861.3(4)†§	3861 d)	4^+ d)
2860.7(5)†§	2853 d)	4^+ d)	3906.6(4)†§	3908(10) 3917d)	π=+ 4^+ d)
2869.5(5)†§	2862	π=-			
2910.7(18)†§	2915 d)	4^+ d)	3927.2(16)†§	3929.1(7)	
2920.7(10)†§	2923(10)	π=+	3932.9(4)†§	3948 d)	4^+
2950.5(4)†	2950.5(5)		3966.5(6)†§	3955(10)	π=+
(2968.7(7)†§)			4002.0(3)†§	3997 3999d)	π=+ 3^-

† Primary γ-transition to this level is found.

§ Level energy is determined only by the primary γ-energy.

a) Ref./Be76a,Na74,Ar75,We80/

b) Ref./Be76a,Ar75,Le78,We80/

c) Ref./Bo77/

d) Ref./Sa81/

Table 5.4 Level energies up to 4 MeV in ^{76}Se

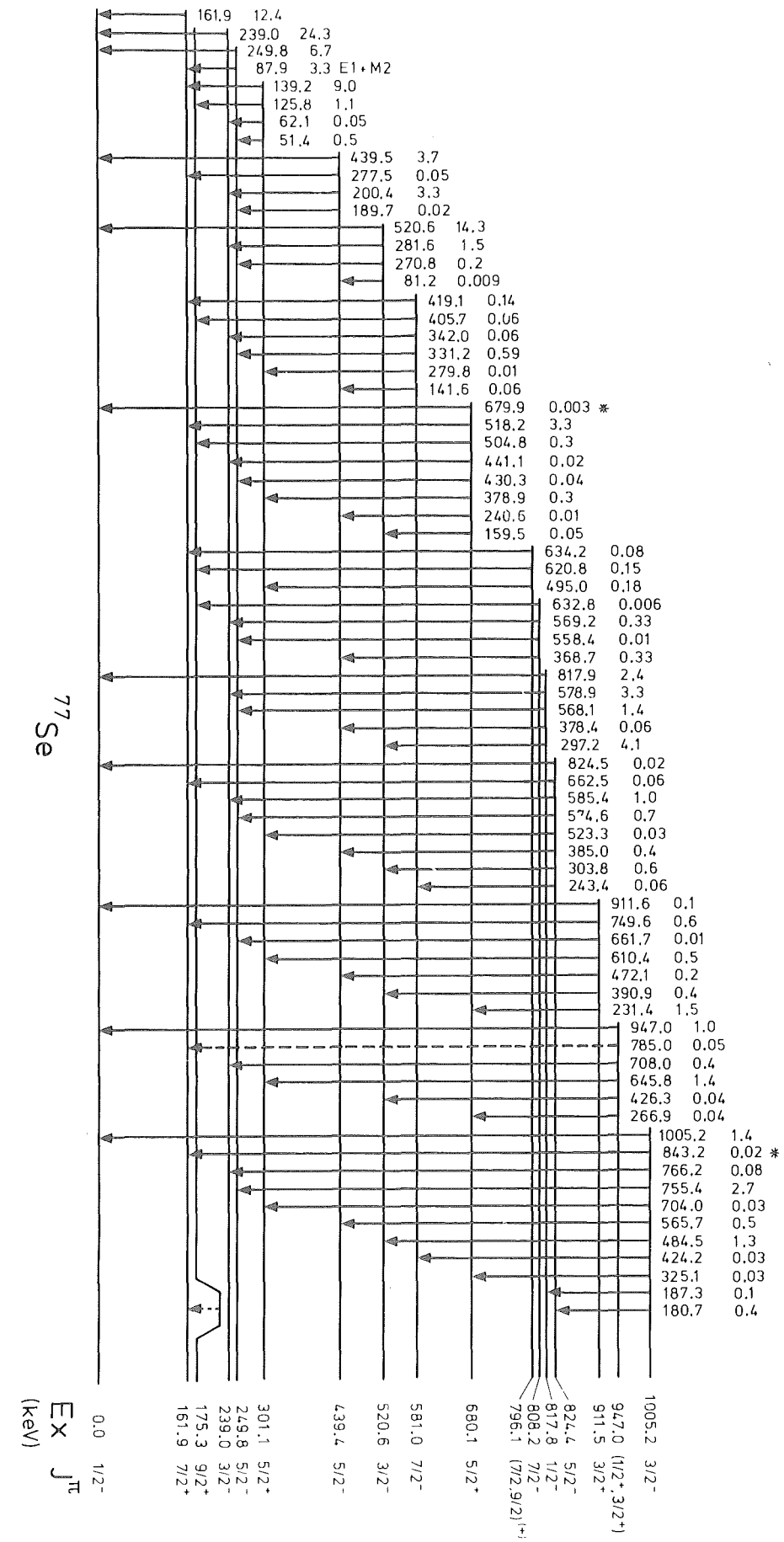

Fig. 5.5 Low-lying levels and low energy γ-transitions in ^{77}Se

(* shows a tentative assignment)

5.4 The level scheme and level properties of ^{77}Se

Fig. 5.5 shows the γ-decay scheme of levels up to 1 MeV in ^{77}Se. Assignments of spins and parities of each levels were done in a manner similar to the procedure in the case of ^{75}Se (see §5.2).

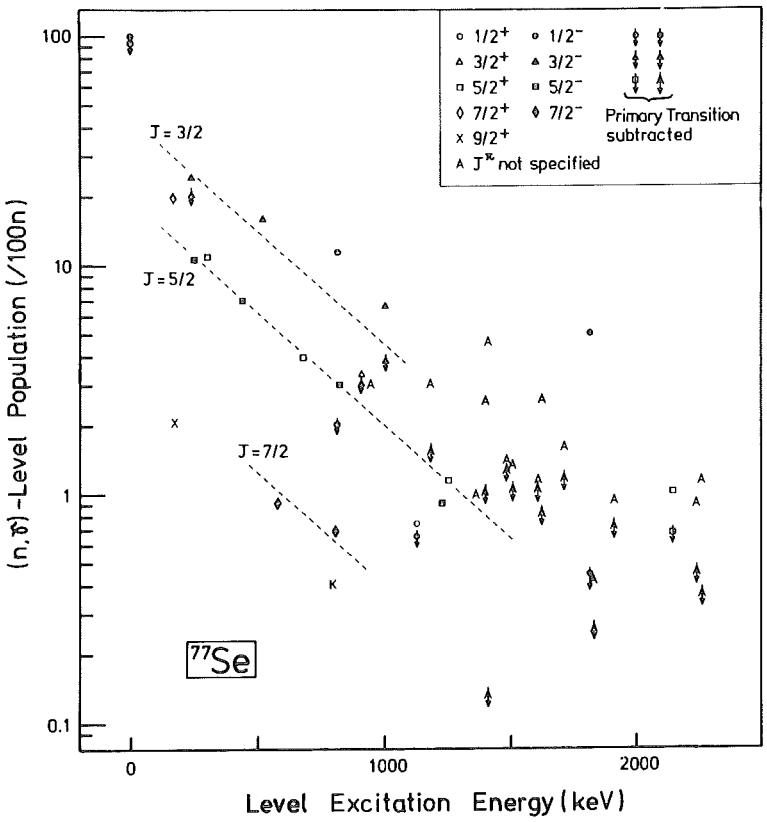

Fig.5.6

(n,γ)-level population in ^{77}Se. A level marked with K is the one which was proposed by Zell et al. /Ze76a/ (see text).

5.4.1 Levels up to 1 MeV excitation energy

The most precise level energies are given in Table 5.5 at the end of this section and compared with other data.

The $1/2^-$ ground state

The quadrapole moment Q is measured by microwave spectroscopy /Ge50/ to be practically zero, implying that the spin of this level is J = 1/2. The magnetic moment measured by NMR /We53,Wa54/ ($\mu \sim 0.534 \mu_N$) is quite close to the Schmidt value of a $p_{1/2}$ neutron /Ar66/†, which is one of the available

---

† $\mu_{p_{1/2}} = -\frac{1}{2} g_N \frac{\frac{1}{2}}{\frac{1}{2}+1} \mu_N = 0.638 \mu_N$ $\quad g_N = -3.826$ $\quad \mu_{p_{3/2}} = -1.913 \mu_N$

neutrons according to the shell model in this region of nuclei. The spin and parity assignment has been confirmed by the ^{76}Se(d,p) reaction (l_n = 1) /Li65a/, measurements of circular polarisation of γ-rays following the capture of polarized neutron in ^{76}Se /Kn71/, and by the ^{76}Se($\vec{d}$,p) reaction (J^{π}= 1/2$^-$) /Mo78/.
The strong primary transition in the (n,γ) reaction /Ra71, present/ strongly suggests that the multipolarity of this transition is E1, in accordance with the spin and parity of the ground state.
It should be noted that from systematics this ground state corresponds to the 293 KeV 1/2$^-$ level in ^{75}Se. There, the 1/2$^-$ level is lying higher than the 133.6 KeV 9/2$^+$ level. The $p_{1/2}$ neutron is lower than the Fermi level, which is lying on the $g_{9/2}$ orbit. If one has taken into account the effect of stronger pairing for $g_{9/2}$ than $p_{1/2}$, then one can explain the 1/2$^-$ ground state of ^{77}Se, but the problems in ^{75}Se still cannot be solved.

The 161.9 KeV 7/2$^+$ level

This level has a half life of $\tau_{1/2}$ = 17.45 s /Si80/. The multipolarity of the ground state transition is known to be E3 from the measurements of its conversion electron /We62, Sa69/. This multipolarity determines spin and parity J^{π}= 7/2$^+$ of the level. The calculated transition probability of the ground state E3 transition is, from the above mentioned half life, 3.5 x 10^{-2} (W.u.) (B(E3)).
In the present study, the conversion coefficient of the 163 KeV E3 transition is used for the intensity calibration of the electron-lines together with the pure E2 transitions with the result of full consistence.
In the (d,p) and (p,d) reactions /Ma63, Li65a , Mo78, Ba79/ the corresponding proton or deuteron peak is not well separated from the strong 175 keV line. The 162 KeV 7/2$^+$ level cannot be a single particle state; therefore, this level should be only weakly excited by the particle transfer reactions as seen in the neighbouring nuclei.
Lin /Li65b/ has once reported a level at 0.16 MeV, which is excited by the inelastic deuteron scattering. However, this is highly unlikely because of the large spin difference between this level and the ground state 1/2$^-$.
Braga et al. /Br74/ have reported a direct feeding of this level in the study of the electron capture decay of the ^{77}Br ground state 3/2$^-$. They showed that this direct feeding is 0.08% of all the ^{77}Br decay, and has a log ft -value of 8.7 (these values are revised to 0.12% and log ft = 8.19, respectively /Si80/) However it is unlikely that a direct β-feeding, accompanied by a spin difference ΔJ = 2 and parity change, has such a low log ft -value. In the

present study this point was reexamined from this decay scheme (see Fig. 5.5) and no evidence for a direct feeding was found. The main reasons for the difference between the present and former investigations is that Braga et al. did not place the 662.5 keV transition in the decay scheme because of absence of coincidence with the 180.7 keV γ-ray, which is a transition between 1005 keV level and this level. However,in the present precision γ-ray energy measurement, there is no other possibility for the 662.5 γ-ray than the present placement in the decay scheme. It may be possible that in the coincidence measurement the 662 keV line was too weak to be found (see the figures of /Sa69/).

The 175.3 keV $9/2^+$ level

The (d,p) and (p,d) reactions /Ma63, Li65a, Mo78, Ba69/ have provided clear evidence for the existence of this level, and shown that this level has a highly single particle-like nature. However in γ-spectroscopy, no depopulating γ-ray has been observed. From the decay scheme (see Fig. 5.5) a 13.4 keV transition should exist to the 162 keV $7/2^+$ level. However, this transition energy is too low for observation in the GAMS- and BILL-detection systems.
The above mentioned particle transfer reactions have shown that the value of angular momentum transfer to this level is $l_n = 4$, restricting the possible spin and and parity assignment to $(7/2,9/2)^+$. Most of the authors prefer $9/2^+$ because of the large spectroscopic factor.
In the present investigation, the conversion electron line of the 125.8 keV transition from the 301.1 keV $5/2^+$ state has been determined to have a multipolarity of pure E2, which also supports the $9/2^+$ assignment. Further no transition from the $5/2^-$ states to this level was observed, which is in accordance with $J = 9/2^+$ for this level. The (n,γ)-level population is consistent with $J^\pi = 9/2^+$, considering that the population for the 161.9 keV $7/2^+$ level is ten times higher than for this level (see Fig. 5.6).
The experiment of the $^{74}Ge(\alpha,n\gamma)^{77}Se$ reaction /Ze76/ showed that this level is the head of a positive parity band.

The 239.0 keV $3/2^-$ level

This level is quite well established /Ar67, Ur73, Si80/. In the (n,γ) reaction the 239 keV ground state transition is the strongest line, and the strong primary transition to this level clearly establishes this state /Ki53,Ra71,Kn71, Br79a, present/.
A direct β-feeding to this level from the $3/2^-$ ground states of ^{77}As /Ar71/ and ^{77}Br /Ar66, Sa69, Br74/, and the strong Coulomb excitation of this level /Ro62, An68/ have shown that its spin and parity are $(3/2,5/2)^-$. The $\gamma(\theta)$-measurement

/Ro62/ indicated that the spin of this level should be 3/2. This spin and parity assignment was further confirmed by the following experimental results:

- Existence of a strong primary transition in the (n,γ) reaction.
- The M1(+E2) character for the 239 keV transition determined by the conversion electron measurement /Sa68, present/.
- The γ-ray circular polarization measurement of the primary transition /Kn71/ in the $(\vec{n},\gamma)$ reaction has shown that the spin of this level is 3/2.
- The $\gamma\gamma(\theta)$-measurement /Br74/ agrees very well with the assumption of the spin of J = 3/2 for this level.
- Though the corresponding peak to this level in the particle transfer reactions /Ma63, Li65a, Mo78, Ba79/ is not well separated from the close-lying 249.8 keV $5/2^-$ level, the results of the particle angular distribution analysis is consistent with the assumption of two states (l_n= 1 and l_n= 3).

The data of the E2/M1-mixing ratio are compiled in /Si80/, showing δ=-0.184±0.030. The present measurement of conversion electrons has yielded the value of $|\delta|$ = 0.25±0.05. Using this mixing ratio and B(E2)↑-value of 0.181±0.013 e^2fm^2 /Si80,p.128/ the half life of this level is calculated to be 50±16ps. Due to the different value of δ^2, 27±7ps is shown as an average value in the Nucl. Data Sheets /Si80/. The present half life is in good agreement with that of Lynch et al.($\tau_{1/2}$= 48±25ps, pulsed beam method)

The 249.8 keV $5/2^-$ level

The close-lying levels at 239.0 and 249.8 keV were firstly identified by the Nuclear Data group and Robinson et al./Ro62/. From the presence of Coulomb excitation of this level /An68, Ag70/ and the existence of a 87.9 keV γ-transition to the 161.9 keV $7/2^+$ level, they also proposed $J^\pi = 5/2^-$ as a possible spin and parity for this level. Monaro /Mo63/ reported two depopulating γ-rays 249.8 keV and 87.9 keV to the ground state $1/2^-$ and 161.9 keV level, respectively, supporting this spin and parity assignment. The more refined measurements with a Ge(Li) detector /An68, Sa69, Ag70, Ar71, Ra71, Br74, Ze76a/ have confirmed these arguments.

From the above arguments the multipolarity of the 87.9 keV transition should be E1. The present value of the K-conversion coefficient is slightly larger than expected for a pure E1 transition. This implies that the 87.9 keV transition has an M2 admixture. This unusual admixture of E1+M2 has already been reported in the $\gamma\gamma(\theta)$-measurement /Br74/ with δ(M2/E1)=-0.09±0.05. The present study yields $|\delta(M2/E1)|$= 0.18±0.03. The conversion coefficient of the 249.8 keV ground state transition agrees quite well with the theoretical value for a pure E2 transition, which is consistent with the spin and parity $5/2^-$ of this level.

The half life of this level is reported to be 9.3±0.4ns /En64/. This yields for the partial transition rates for E1 and M2 of 87.9 keV: $1.8\pm0.8\times10^{-5}$(W.u.) and $3.4\pm1.1\times10^{2}$(W.u.).
The magnetic moment of this level is measured to be $\mu = 1.3\mu_N$ by the spin rotation method /Fu76/. This value is consistent with the Schmidt value ($\mu = 1.366\mu_N$) for pure $f_{5/2}$ configuration. Further the B(E2)-value of the 250 keV transition, which was measured by Coulomb excitation /An68,Ag70/, is not so different from the Weisskopf estimates. These facts suggests a rather pure single particle configuration for this level.

The 301.1 keV $5/2^+$ level

This level is only weakly excited by both the particle transfer reactions and the decay of ^{77}Br or ^{77}As. Sarantites et al./Sa74/ have proposed a spin and parity of $5/2^+$ for this level. However, their arguments were based on the (d,p)-measurements by Lin /Li65a/, which did not provide unambiguous data for this level. With $J^\pi = 9/2^+$ for the 175.3 keV level and the four γ-rays of 139.2 keV, 125.8 keV and 51.4 keV, which were found to depopulate this 301.1 keV level in the (n,γ)-experiment /Ra71, present/, the possible spin and parity for this level are restricted to $5/2^+$ or $7/2^-$ (see Fig. 5.5). Montesturque et al./Mo78/ have shown in their study of the ^{76}Se($\vec{d}$,p) reaction, that the spin-parity of this level is unambiguously $J^\pi = 5/2^+$, though this level is rather weakly populated. In the present study the multipolarities of the 139 keV and 125.8 keV transitions have been determined to be M1+E2 and pure E2, respectively, which strongly supports the spin and parity assignments $5/2^+$ for this level.

The 439.4 KeV $5/2^-$ level

Through Coulomb excitation /Ro62, An68, Ag70/, it has been shown that the B(E2↑)-value for this level is large, indicating strong collectivity of this level and a possible spin-parity of ($3/2^-$, $5/2^-$). The γ-angular distribution measurements in the Coulomb excitation experiments /Ro62, Al62/ have strongly supported the spin-parity of $5/2^-$. The particle transfer reactions /Li65a, Mo78, Ba79/ have shown that the spin-parity of this level is $J^\pi = 5/2^-$, $7/2^-$ ($l_n = 3$). This leads to an unambiguous $J^\pi = 5/2^-$ assignment for this level. The γ-$\gamma(\theta)$ measurements in the decay study of ^{77}Br /Br74/ are in good agreement with this assignment.

In the (n,γ) studies no primary transition to this level has been found /Ra71, present/ , which is consistent with the $5/2^-$ assignment. Four depopulating γ-rays (See Fig. 5.5) and the pure E2 (439 KeV) transition (See Table 4.7) also provide $J^\pi = 5/2^-$ as the only possible spin-parity for this level. It should be noted that the log ft-values in the decay studies of ^{77}As and ^{77}Br /Si80/ are quite different only for this level. The log ft - value in the decay of ^{77}As is 9.3, whereas in the decay of ^{77}Br it is 6.86. If the origin of the difference is not the experimental error, some physical reasons should be given to explain the difference. The ground states of ^{77}As and ^{77}Br are both $J^\pi = 3/2^-$. However, it is still not clear, whether both $3/2^-$ states have similar structures or not.

The 520.6 KeV $3/2^-$ level

The (d,p)-studies /Mo63, Li65a/ have indicated that the l_n-value for this state is 1, suggesting spin-parity ($1/2^-$, $3/2^-$). The γ-$\gamma(\theta)$ angular correlation measurement /Br74/ and the (d,p)-reaction have removed the ambiguity and shown that this level has $J^\pi = 3/2^-$.

This level is only weakly excited by the inelastic scattering of charged particles /Ro62, Au68, Ag70/ . It has been shown that the B(E2)-value of the 520.6 KeV transition is in the order of Weisskopf single particle estimates /An68, Bo69, Si80/. The sum of spectroscopic factors of the (d,p) /Mo78/ and (p,d)-reaction /Ba79/ is 1.65, which is fairly large and indicates single particle nature of this state (cf./En67/).

From the above arguments one would expect that a rotational band may be built on this level. However, this has not yet been found. The spin of this state allows an E1 primary transition to occur in the (n,γ) reaction /Ra71, present/. However, its intensity is very small compared with other E1 primary transitions, offering an example of anticorrelation with (d,p)-spectroscopic factor /Mu73/.

The 581.0 keV $7/2^-$ level

Sarantites et al./Sa69/ have reported evidence for the existence of this level in the decay study of ^{77}Br. This level has been further confirmed by the (n,γ)-study /Ra71/, the decay study of ^{77}Br /Br74/ and a ^{74}Ge$(\alpha,n\gamma)$-study /Ze76a/. Zell et al. /Ze76a/ have proposed an assignment of $J^\pi = 7/2^-$ for this level, based on the γ-decay mode of this level and on the γ-angular distribution of the 331.2 keV transition. The present investigation supports the arguments of Zell et al., and provides the only possible spin-parity assignment of $7/2^-$ for this level as following: the γ-decay mode of this level allows possible spin-parity of $J^\pi = 5/2^+$ and $7/2^-$ /Br74, Ze76a, Present/. The multipolarity of the 331.2 keV transition has been determined to be M1 + E2 by the present measurement of the internal conversion, which eliminates the possibility of $J^\pi = 5/2^+$. Further the systematics of the population of levels in the present (n,γ)-study (see Fig. 5.6) shows that the population of this level is too little for J = 5/2.
Zell et al. have shown that this level should be a member of the $5/2^-$ [303] band /En67/.
Braga et al. /Br74/ have reported a direct feeding to this level with a log ft-value of 8.6 in the study of electron capture decay of ^{77}Br. However, a re-investigation by the present decay scheme shows no evidence for direct feeding of this level. The main reason for this is that the branching ratio for the 243 keV transition, which populates this level, is nearly three times larger in the present work than in /Br74/.
A very weak 279.8 keV transition, which should have a E1-character, has been assigned to depopulate this level in the present work (see the observation in /Si80/).

The 680.1 keV $5/2^+$ level

The (d,p) reaction experiments /Ma63, Li65a/ have shown that the possible spin-parity for this level is $3/2^+$ or $5/2^+$ ($l_n = 2$). The (d,p) reaction /Mo78/ clearly determined the spin-parity to be $J^\pi = 5/2^+$. The results in the present study are in good agreement with $J^\pi = 5/2^+$. The systematics of population of the present ^{77}Se(n,γ) reaction shows that the population of this level is just on the line for J = 5/2, and that this level is too little populated to be assigned as J = 3/2. A very weak γ-line at 679.9 keV is tentatively assigned to be the ground state transition. From the spin sequence this transition should be M2. Considering the transition speed of single particle estimate and the branching ratios of this level (see Fig. 5.5), the existence of this M2 transition is not so very strange.

Excluding this γ-line the γ-decay mode of this level provides only two possible spin-parities, i.e. $J^{\pi} = 5/2^{+}$, $7/2^{-}$. The multipolarity of the 518.2 keV transition has been measured to be in agreement with the assumption of M1. Consequently the present data almost alone provide an only possible spin-parity assignment of $J^{\pi} = 5/2^{+}$ for this level.
A 99.5 keV γ-ray was reported to depopulate this level in the previous (n,γ)-study /Ra71/. However, in the present investigation this line has not been found in the spectrum.
This level is four times more strongly excited than the 301.1keV $5/2^{+}$ level by the (d,p) reaction /Li65a,Mo78/, which may indicate more mixing of the above lying $d_{5/2}$ orbital into this 680.1 keV level.

The 796.1 keV ($7/2^{+}$, $9/2^{+}$) level

This level was reported firstly by Zell et al. /Ze76a/ in the $^{74}Ge(\alpha,n\gamma)$ reaction study. They have proposed the spin parity of $J^{\pi} = 7/2^{+}$ based on the γ-decay mode and the angular distribution of the 495.0 keV γ-ray. Three γ-rays, 634.2 keV, 620.8 keV and 495.0 keV, which were reported in /Ze76a/, have also been found in the present (n,γ) study. They were already found in the work of Rabenstein /Ra71/. The population of this level is very weak. The systematics of the population would agree with J = 7/2,9/2.

The 808.2 keV $7/2^{-}$ level

Rabenstein et al. /Ra71/ have firstly proposed this level and they have tentatively assigned this level as a band member of the ground state /En67/. The presence of this band structure has been confirmed by the $^{74}Ge(\alpha,n\gamma)$ reaction /Ze76a/.
The γ-decay mode of this level in the present study is in perfect agreement with that of Rabenstein et al. /Ra71/. However, the intensities of the 632.8 keV and 558.4 keV transitions are much less than those of /Ra71/. The population of this level is consistent with spin of J = 7/2 in the present systematics of population.

The 817.8 keV $1/2^{-}$ level

The four levels around this energy, 796 keV, 808 keV, 818 keV and 824 keV cannot be resolved in the particle transfer reactions. However, the good agreement with the theoretical angular distribution for $l_n = 1$ /Ma63, Li65a, Mo78, Ba79/ may indicate that only the 817.8 keV level has been excited in these reactions. This l_n-value and the allowed electron capture decay of

^{77}Br to this level (log ft = 5.6 /Br74, Si 80/) have provided the spin-parity assignment of ($1/2^-$, $3/2^-$). By the experiments of γ-ray circular polarization /Kn71/ and the (d,p) reaction with polarized deuteron /Mo78/ the spin and parity have been unambiguously determined to be $J^\pi = 1/2^-$.
The γ-decay mode in the present study is in good agreement with that in /Ra71, Br74/. The strongest primary γ-transition to this level in the (n,γ) studies /Ki53, Ra71, present/ is also consistent with the assumed E1-multipolarity.

The 824.4 keV $5/2^-$ level

This level has firstly appeared in the article by Sarantites et al. /Sa69/, who have studied the decay of ^{77}Br. The log ft-value of 5.9 from the decay of ^{77}Br /Sa69, Br74, Si80/ indicates an allowed transition, providing possible spin-parities of $(1/2, 3/2, 5/2)^-$ for this level.
The high sensitivity of GAMS 1, 2/3 has enabled the identification of eight γ-rays depopulating this level to the levels ground state $1/2^-$, 161.9 keV $7/2^+$, 239.0 keV $3/2^-$, 249.8 keV $5/2^-$, 301.1 keV $5/2^+$, 439.4 keV $5/2^-$, 520.6 keV $3/2^-$ and 581.0 keV $7/2^-$, which are showing that the only possible spin-parity for this level is $J^\pi = 5/2^-$. The 662.5 keV transition, which decays to the 161.9 keV $7/2^+$ level and excludes the possibility of $J^\pi = 3/2^-$, is not placed in the decay scheme in /Ra71, Br74/, based on the coincidence measurement. However, if the spin-parity for this level were $J^\pi = 3/2^-$, there could be a strong primary γ-transition to this level in the (n,γ)-reaction, which has never been reported /Ra71, Kn71, Br79a, present/. It might be possible that in the coincidence measurements the 662.5 keV γ-ray was too weak to be found. The systematic study of population is consistent with the $J^\pi = 5/2^-$ assignment, while for $J^\pi = 3/2^-$ one might expect three times more population of this level.
The multipolarity of the 303.8 keV transition has been measured to be M1, in agreement with the negative parity assignment for this level.

The 911.5 keV $3/2^+$ level

This level was firstly observed in the decay of ^{77}Br /Sa69/, and has been well established /Ra71, Br74/. The presence of a strong primary transition in the (n,γ) reaction restricts the spin of this level to (1/2, 3/2). The γ-decay mode of this level clearly establishes the spin-parity of this level as $J^\pi = 3/2^+$ /Ra71, Br74, present/ (see Fig. 5.5). The 661.7 keV transition, which is placed in the present decay scheme to depopulate this level, was tentatively doubly assigned in the work of Rabenstein /Ra71/. Present work

has shown that this γ-line is a multiplet (661.7, 662.5,663.8,...), confirming the argument of /Ra71/. This level is the first positive parity state for J = 3/2, however the population of this level is too low, which would indicate the need of additional depopulating transition not found until now.

The 947.0 keV ($1/2^+$, $3/2^+$) level

A typical proton angular distribution of $l_n = 0$ is obvious in the (d,p)-study by Macefield et al. /Ma67/, providing a unique spin-parity assignment of $J^\pi = 1/2^+$ for this level. Because of the higher energy of the incident deuteron beam this typical ($l_n = 0$)-pattern is less distinctive in the later (d,p)-studies /Mo78, Ba79/.
This level was also found as a isobaric analog state in the ^{76}Br(p,p) reaction /Ba68/, reporting again $l_p = 0$ from the R-matrix analysis of proton angular distribution. The observed spectroscopic factor (S = 0.16) in this reaction is in reasonable agreement with that in the (d,p)-study by Lin /Li65a/ (S = 0.25), but not in good agreement with the value of Montesturque et al. /Mo78/ (S = 0.36). However, the (n,γ)-studies /Ra71, present/ indicate that $J^\pi = 3/2^+$ is much more favourable. The γ-decay mode in the present study agrees with that of /Ra71/ excluding the 947.0 keV ground state transition, which was not definitely placed in the decay scheme due to the complexity of the γ-ray spectrum.
The placement of the 771.7 keV γ-ray as a transition to the 175.3 keV $9/2^+$ level is questionable because of the spin-sequence, and is less accurate because of weak intensity. However, the presence of the 785.0 keV transition to the 161.9 keV $7/2^+$ level may strongly support the spin-parity assignment of $J^\pi = 3/2^+$ instead of $1/2^+$. The conversion coefficient of the 645.8 keV transition to the 301.1 keV $5/2^+$ level, though ICC-data are less reliable above 500 keV in this work, prefers the multipolarity of M1, again favouring $J^\pi = 3/2^+$ for this level.

The 1005.2 keV $3/2^-$ level

Sarantites et al. /Sa68/ have proposed the spin and parity of $J^\pi = 3/2^-$, based on the allowed electron capture transition from ^{77}Br (log ft = 5.5, /Si80/) and the γ-decay mode of this level. This spin-parity has been further confirmed by the (d,p) reaction /Mo78/.
The γ-decay mode in the present work is in agreement with that of Rabenstein et al. /Ra71/ and Braga et al. /Br74/. The presence of a strong primary transition to this level in the (n,γ)-reaction /Ra71, present/ is consistent with $J^\pi = 3/2^-$.

The B(E2)↑ value has been once measured by Gal'perin et al. (B(E2)↑ = 0.007 ± 0.003 e^2 b^2) /Ga70/. They have further deduced the $\tau_{1/2}$(E2)-value of this level to be 23 ps, which is just in the order of the single particle estimate (28 ps).

E_x in keV		J^π	
Present	Others [a]	Present	Others [a]
0.		$1/2^-$	
161.9195(11)	161.97(6)	$7/2^+$	$7/2^+$
175.3033(15)	175.47(9)	$9/2^+$	$9/2^+$
238.9950(13)	238.95(5)	$3/2^-$	$3/2^-$
249.7845(11)	249.70(6)	$5/2^-$	$5/2^-$
301.1449(13)	301.07(7)	$5/2^+$	$5/2^+$
439.445(2)	439.46(7)	$5/2^-$	$5/2^-$
520.630(2)	520.60(5)	$3/2^-$	$3/2^-$
581.001(2)	580.92(8)	$7/2^-$	$7/2^-$
680.093(2)	680.0(1)	$5/2^+$	$5/2^+$
796.138(4)	795.9(4)	$(7/2,9/2)^{(+)}$	$(7/2^+)$
808.174(2)	808.42(17)	$7/2^-$	$(7/2^-)$
817.845(3)	817.81(5)	$1/2^-$	$1/2^-$
824.417(2)	824.40(6)	$5/2^-$	$(3/2^-,5/2^-)$
911.517(2)	911.50(8)	$3/2^+$	$(3/2^+)$
946.967(2)	946.98(13)	$(1/2^+,3/2^+)$	$1/2^+$
1005.168(2)	1005.12(6)	$3/2^-$	$3/2^-$

a) Data compiled in Nucl. Data Sheets/Si80/.

Table 5.5 Precise energies of levels in ^{77}Se up to 1 MeV

5.4.2 Levels above 1 MeV

As in the case of ^{75}Se these levels are only briefly discussed together. Table 5.6 contains the prominent levels up to $\sim$ 3 MeV. The spin of the 1411.6 keV level is determined to be J = 3/2 by the measurement of circular polarization of the 5007.2 keV primary transition to this level /Kn71/. In the present decay scheme a fairly strong γ-line of 830.6 keV is placed between this level and the 581.0 keV $7/2^-$ level, which provides only $J^\pi = 3/2^-$ for this level.

The 1817.6 keV level is again unambiguously determined to have $J^\pi = 1/2^-$ because of the γ-ray polarization measurement /Kn71/ and the γ-ray decay mode. A level at 1.83 MeV with $l_n = 1$ is reported in a (d,p)-measurement /Li65a/. We cannot decide if this level corresponds to the 1817.6 keV level or to the newly found 1830.8 keV state.

A primary γ-line of 5588.04 keV has been already reported previously /Br79a, En81/. The present study has established clearly this 1830.8 keV level.

The level at 2142.4 keV has been reported to have spin and parity of $J^\pi=5/2^+$ /Mo78/. If this assignment is correct a fairly strong ($I\gamma$= 0.34/100n) primary transition (5276.4 keV) to this level should have multipolarity E2. The present decay scheme shows that this level is somewhat too much populated for J = 5/2. Thus $J^\pi= 3/2^+$ is preferable.

Level energies					
Present	Ref./Ra71/	Ref./Br79a/	Ref./Si80/	J^{π}	Comments
1128.1	1128.2	1128.1	1128.4	$1/2^+$	$l_n=0$ a),b),c)
1187.0	1186.7	1186.7	1186.8	(3/2)	NGP,GDM
1230.6	1230.5	1230.6	1230.6	$5/2^-$	$l_n=3$ d),GDM,NGLP
1252.9	1252.8	1252.8	1252.6	$5/2^+$	$l_n=2$ a),b),c),GDM
1367.0	1367.1	1365.8	1367.2		GDM,NGLP,($l_n=1$)d)
1402.5	1402.6	1402.5	1402.7	$3/2(1/2^-)$	PGP,GDM
1411.6	1411.7	1411.6	1411.7	$3/2^-$	PGP,GDM
1488.2	1488.4	1488.3	1488.3	$3/2^-$	$l_n=1$ c),GDM
1511.0	1511.4	1511.2	1511.4	(3/2)	NGP,GDM
1607.7	1607.3	1607.9	1607.5	(3/2)	NGP,GDM
1623.1	1623.2	1623.4	1623.3	$3/2^-$	PGP,GDM
1714.7	1715.6	1715.1	1714.9	$1/2^-,3/2^-$	$l_n=1$ b)?,d)
1817.6	1818.5	1818.2	1818.4	$1/2^-$	PGP,GDM
1830.8				(1/2,3/2)	$l_n=1$ at 1.83MeV b) NGP,GDM
1916.0	1915.6	1916.5	1915.9	(1/2,3/2)	NGP,GDM
2142.4	2142.3	2142.9	2142.4	$5/2^+(3/2^+)$	$l_n=2$ b),d),NGP,GDM
2213.0	2212.3	2213.1	2212.1	(1/2,3/2)	NGP,GDM
2248.3	2249.2	2248.7	2249.2	(1/2,3/2)	NGP,GDM
2264.3	2263.9	2264.1	2264.0	(1/2,3/2)	NGP,GDM
2320.1	2319.3	2319.9	2319.7	(1/2,3/2)	$l_n=2$ at 2.29MeV b) NGP,GDM
2340.0	2339.1	2339.8	2338.9	(1/2,3/2)	NGP,GDM
2392.9	2392.7	2392.6	2392.8	$3/2^-$	PGP,GDM
2456.0	2456.6	2456.0	2456.5	(1/2,3/2)	NGP
2492.1	2490.6	2491.7	2490.5	(1/2,3/2)	NGP,GDM
2853.2	2853.6	2853.3	2853.6	$1/2^-(3/2^-)$	PGP,GDM
2891.9	2892.1	2891.9	2892.1	(1/2,3/2)	NGP,GDM
3040.5			3040.5	(1/2,3/2)	NGP,GDM

NGP : Primary transition to this level is found.

GDM : Based on the γ-decay scheme. NGLP : Based on the (n,γ)-level population

PGP : Based on the polarization measurement of primary γ-rays./Kn71/

a) Ref./Ma63/ b) Ref./Li65/ c) Ref./Ba69/ d) Ref./Mo78/

Table 5.6 Prominent levels above 1 MeV in ^{77}Se. Level energies are given in keV.

6. Discussion

In chapters 1 to 5 we have shown two interesting aspects to be investigated by various instruments, i.e. ① neutron capture and primary transitions, and ② excitation and structure of low-lying states. In the present work we are mainly interested in the low-lying level structures of the Se-isotopes. Only a few special facts will be discussed with respect to the first subject.

6.1 The neutron capture state and the mechanism of the decay process by primary transitions

6.1.1 The neutron capture state

The cross sections of light Se-isotopes are considerably larger than the value calculated with the use of the formalism of Lane and Lynn /La60,Ly68/, which describes the direct potential capture:

$$\sigma_\gamma(\text{one primary transition}) \lesssim \frac{0.062}{R \cdot \sqrt{E_n}} \cdot \left(\frac{Z}{A}\right)^2 \cdot \left(\frac{y+3}{y+1}\right)^2 \quad \text{..... eq. 6.1}$$

$$= 0.22 \text{ b}$$

where $R = 1.35 \times A^{1/3}$ fm : Nuclear radius

$E_n = 0.025$ eV : Incident neutron energy (average)

$Z = 34$ $A = 76$

$y = k_\mu R$

k_μ : Neutron wave number corresponding to the 7 MeV transition energy (in units of fm^{-1})

Therefore , another mechanism is required for the explanation of the neutron capture by these nuclei, for ex. resonance (compound) capture. In the case of the ^{74}Se-target the contribution of the higher lying resonances is estimated to be nearly 4/5 of the reported capture cross section σ_γ = 51.8 barns /Mu73/ (see §2.4). However, in the case of the ^{76}Se-target all the observed resonances are far away from thermal energy. In such a case the contribution from a bound state must be considered, which can be checked by a measurement of the neutron scattering length.

Koester et al./Ko80a/ have provided evidence of a strong bound level for the ^{76}Se + n system, but no evidence for the ^{74}Se + n system. This large difference between ^{75}Se and ^{77}Se would provide a significantly different capture mechanism for both nuclei. This will be discussed in the following section.
In the present study we have observed a fairly large cross section (∿300b) for the ^{75}Se(n,γ) reaction. Though there exist no neutron resonance data for the ^{75}Se-target, it is highly probable that a resonance lies near the thermal energy. From a calculation of the energies of single particle states (see for ex. /Ly68/ p.103 and /Al78/), the $3S_{1/2}$ orbital would be the only available state for S-wave neutron capture in this region of nuclei. However, this single particle $3S_{1/2}$ state lies somewhat lower (2 ∿ 3 MeV) than the zero energy (neutron capture state). Therefore, a capture mechanism which is dependent purely on the $3S_{1/2}$ orbital, is not possible.

6.1.2 Correlation between the (n,γ) and (d,p) strengths

The (d,p) reaction strongly excites single particle states (see for ex. /Ki68/). Especially in the case of direct neutron capture (see for ex. /Ly68/ p.335), the E1 primary transition strengths are expected to have positive correlation with the (d,p) spectroscopic factors of $l_n = 1$. Therefore a positive correlation between the (n,γ) primary transition strengths and the (d,p) spectroscopic factors is an indication that the neutron capture state prefers to decay to single particle states, hence providing a key to understand the structure of the capture state.
In figures 6.1 and 6.2 are shown the primary transition strengths in the (n,γ) reaction and the corresponding (d,p)-spectroscopic strengths. The primary γ-intensities were divided by the traditional E_γ^3, which is valid also for the capture mechanisms through the "valency neutron" /Ly68, p.326/ and the "doorway state" /Al78/. Other reduction factors of E_γ^1 and E_γ^5 (for the potential capture /Ly68, p.333/ and the giant dipole resonance model /Ax67/ respectively) may be considered. However, in the present figures the available (d,p)-data up to 1 MeV excitation energy are used, and therefore different energy reduction factors do not influence significantly the transition strengths.

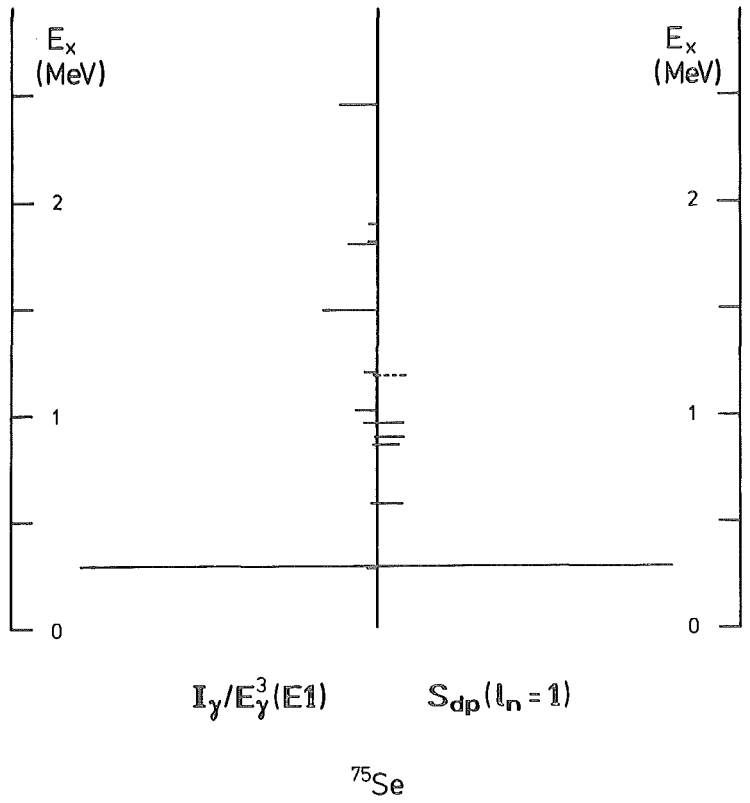

Fig. 6.1

Comparison of the primary transition strength in the $^{74}Se(n,\gamma)$ reaction and the (d,p) reaction /Su78/. The correlation coefficient is $\rho = 0.99$.

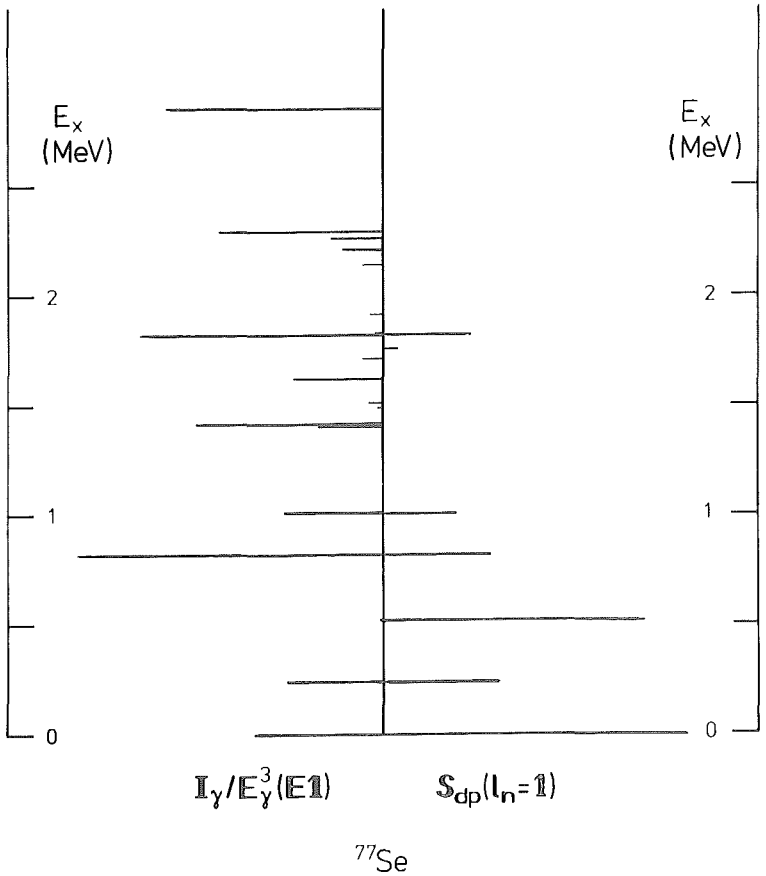

Fig. 6.2

Comparison of the primary transition strength in the $^{76}Se(n,\gamma)$ reaction and the (d,p) reaction /Mo78/. The correlation coefficient is $\rho = -0.30$.

The correlation coefficient is calculated by the following formula

$$\rho = \frac{\sum_i (x_i - \bar{x})(y_i - \bar{y})}{\sqrt{\sum_i (x_i - \bar{x})^2 \cdot \sum_i (y_i - \bar{y})^2}} \qquad \ldots\ldots \text{ eq. 6.2}$$

x_i : reduced γ-ray transition strength
$\bar{x}$: average of x_i
y_i : (d,p)-spectroscopic strength
$\bar{y}$: average of y_i

A strikingly different feature between Fig.6.1 and Fig.6.2 is apparent. The strong positive correlation in Fig.6.1 is mainly due to the very strong primary transition to the 293.1 keV level and correspondingly large (d,p) spectroscopic factor. However, the non-statistical nature in Fig.6.1 is rather obvious. On the contrary in Fig.6.2 no strong correlation is observed, eventually there exists slightly negative correlation. This anticorrelation between the primary transition strengths in the $^{76}Se(n,\gamma)$ reaction and the corresponding (d,p)-spectroscopic factors has been pointed out previously by Murzin and Kolomiets /Mu73/. They have suggested a possible capture mechanism through a doorway state composed of several quasiparticles coupled to phonons. A coupling of phonons may reduce the correlation.
However, such mechanism cannot be applied to the case of the $^{75}Se(n,\gamma)$ reaction as mentioned above. On the other hand the direct capture process is not applicable either, as is shown in the previous section.
The strong primary E1 transition to the 293.1 level is also seen in resonance capture at 27.1 keV and 293.1 keV /En81/. Therefore, the valency nucleon model seems to be also applicable. However, the Se isotopes are rather far away from the 3S size resonance as stated before, and this model explains only a few percent of the observed cross section /Ly68, p.346 and En81/.
Recently the mechanism of slow neutron capture has been further developed by Ho et al. /Ho81/. They have proposed a process, where the elastically scattered neutron wave from the compound channel is reabsorbed in the region outside the nuclear surface, which causes strong transitions to the single particle states. Ho et al. have estimated that the contribution of this process may reach 20 to 30% at the observed capture cross section in the region of the 3S size resonance ($A \simeq 50$ to 60). The validity of their theory should be proven by applying it to various nuclei.
In the present work no effort was made to check the statistical theory of

Porter and Thomas /Po56/, because of the low number of primary γ-lines of well established multipolarity obtained in both the $^{74}Se(n,\gamma)$ and $^{76}Se(n,\gamma)$ reactions.

6.1.3 Primary E2-transitions in the $^{74}Se(n,\gamma)$ and $^{75}Se(n,\gamma)$ reactions

The observation of E2 primary transitions in (n,γ) reactions is rather difficult /Ra78/. The previous data were tabulated by Raman /Ra78/ and by Kopecky /Ko81/. The latter has reported 24 primary E2 transitions.
In Table 6.1 are listed the E2 primary transitions observed in the present work.

E_γ(trans.) in keV	Reaction	Assignment	Intensity /100n
8027.6	$^{74}Se(n,\gamma)$	$1/2^+ \rightarrow 5/2^+$	0.07
7399.0	$^{74}Se(n,\gamma)$	$1/2^+ \rightarrow 5/2^+$	0.23
11154.	$^{75}Se(n,\gamma)$	$2^+ \rightarrow 0^+$	$\sim$ 0.1
10032.	$^{75}Se(n,\gamma)$	$2^+ \rightarrow 0^+$	$\sim$ 0.1

Table 6.1 E2 primary transitions observed in the present work

The rareness of E2 primary transitions is also reflected in the empirical hindrance factors of γ-transitions which were adopted by von Egidy /Eg68/ for the statistical calculation of a γ-ray spectrum. He has used 100 times larger hindrance for the E2 transitions in the energy region of capture states than in the ground state region.
Because of the insufficient data about E2 primary transitions, and further because it is rather difficult to estimate the quantity Γ_γ in the case of thermal neutron capture, it is less meaningful to try to perform a theoretical analysis for these transitions at this stage. Based on the argument about empirical hindrance factors mentioned above, it is of interest to consider the ratio between reduced transition strengths or between intensities of transitions of about the same energies, and to study their mass dependence.
Our data yield

$$\sum_{i}^{E_X<650keV} I_{\gamma i}(E2) \Big/ \sum_{i}^{E_X<650keV} I_{\gamma i}(E1) \sim 10^{-2} \quad \text{for } ^{74}Se(n,\gamma)$$

6.2 Strange phenomena in Se-nuclei and neighboring nuclei

Several interesting problems have been already pointed out in the introduction. Here we discuss these problems in greater detail, mainly from the experimental viewpoint. Possible theoretical interpretations will be given in later sections.

6.2.1 Spins and parities of ground states in ^{75}Se and ^{77}Se

As pointed out already in chapter 5.4, it is not understood why the ground state of ^{75}Se is $5/2^+$ and that of ^{77}Se is $1/2^-$. Further in ^{75}Se the first $1/2^-$ state is lying above the $9/2^+$ level.
In most theoretical calculations the positive parity level energies are obtained relative to for ex. the $9/2^+$ state and the negative parity level energies are determined relative to for ex. the $1/2^-$ state. The level energies of $9/2^+$ and $1/2^-$ are adjusted to explain the experimental spectra. However, with this method it is rather hard to understand the reversed position of $9/2^+$ and $1/2^-$ in ^{75}Se and ^{77}Se.
The $5/2^+$ state can be explained as lowest positive parity state either from the Nilsson model /Ni55/ or from other more complicated rotor models /Sa73, He74,He75,La78/. However, these models always predict other low-lying positive parity states such as $1/2^+$ and $3/2^+$ which are not observed experimentally and which do no exist at low excitation energies, because they would have been populated strongly in the non-selective (n,γ) cascade process and they would thus have been observed in the present work. In heavier odd mass Se-isotopes ($A \geq 77$) the $5/2^+$ state is lying always higher than the $9/2^+$ state. From these facts it is rather clear that the simple Nilsson model has difficulty in explaining the ground state spin and that a rapid change of parameters is required in theoretical calculations.

6.2.2 Anomalous positive parity states and N = 41 anomaly

The anomalous positive parity states $5/2^+$,$7/2^+$ /Ik66a/ in this region of nuclei are arising from $g_{9/2}$-neutrons. The lowering of the $7/2^+$ state, which is often seen lower than the $9/2^+$ state in this region, is easily obtained from the $(g_{9/2})^{n\geq 3}$ - configuration or from the particle-phonon coupling /Bo75, p.540/, mainly due to the fact that the 6j symbol has a different sign for J = 7/2 /Ki66/ (see §6.3.2). However, it is rather difficult to lower the J = 5/2 state sufficiently with these models.

The ground states of ^{75}Se and ^{77}Kr /No75,Ca79/ are $J^{\pi} = 5/2^{+}$, and in ^{73}Ge the $5/2^{+}$ state is lying only 13 keV higher than the $9/2^{+}$ ground state /Le78/. The lowering of the $5/2^{+}$ state occurs not only for neutron states as shown below.

6.2.3 Anomalous positive parity states in the nuclei with odd protons and even neutrons around A = 75

Similar to the cases of odd mass Se and Ge isotopes strange phenomena may be occuring also in the odd mass As and Br isotopes.
The odd mass As isotopes (Z = 33, see Fig.2.1) have always low-lying $9/2^{+}$ and $5/2^{+}$ states together (see for ex. Fig.7 in /Ro80/). These positive parity states have lowest excitation energies ($\sim$ 0.38 MeV) at N = 42, and the energy difference between the $9/2^{+}$ and the $5/2^{+}$ becomes smallest ($\sim$ 65 keV) at N = 40. The situation of Br isotopes (Z = 35) is more complex. The in-beam studies on ^{75}Br /Be76b,Wi79,Kr81,Wi81/ and ^{77}Br /De74,Mo75/ (+decay study of ^{77}Kr /No75/) have revealed the low-lying positive parity states $5/2^{+}$, $7/2^{+}$, $9/2^{+}$ and $3/2^{+}$. In ^{75}Br (N = 40) the $5/2^{+}$ state is the lowest positive parity state (Ex = 132.4 keV). Kreiner et al. /Kr81/ have performed a theoretical calculation,where a quasi proton ($\tilde{\pi}g_{9/2}$) is coupled to a deformed core. They could predict the experimental level sequence of positive parity states in ^{75}Br fairly well. However, their calculation assumes a very large deformation ($\beta = 0.40$) in order to reproduce the observed level sequence, and with more reasonable deformation ($\beta \lesssim 0.30$) the obtained level spectrum is far from satisfaction. Other similar theoretical calculations on ^{77}Br /De74,Sa79/ do not explain the level sequence satisfactorily.

6.2.4 Anomalous ground state of $^{76}_{35}Br_{41}$

The ground state of ^{76}Br has spin and parity of $J^{\pi} = 1^{-}$ /Fu69,Pa73a/. As shown in Fig.1.1, $J^{\pi} = 1/2^{-}$, $3/2^{-}$ and $5/2^{-}$ states are available for negative parity states in this region of nuclei, and the ground state of ^{75}Br is $3/2^{-}$ /Ek80,Ek81/. If we adopted only the $9/2^{+}$ state ($\nu g_{9/2}$) as positive parity state, we can therefore not explain the spin and parity of the ^{76}Br ground state. The possible configurations for the 1^{-} state are $5/2^{+}(^{75}\text{Se}) \otimes 3/2^{-}(^{75}\text{Br})$ or $7/2^{+}(^{75}\text{Se}) \otimes 5/2^{-}(^{75}\text{Br})$, adopting the low-lying positive parity states $5/2^{+}$ and $7/2^{+}$ in ^{75}Se. However, the former configuration is more natural, because the ground state of ^{75}Se is $5/2^{+}$ and that of ^{75}Br, ^{77}Br, ^{79}Br is $3/2^{-}$ /Fu76,Le78/, and further,

because the ground state spin and parity of 1^+ in ^{78}Br and ^{80}Br is reasonably well understood by assuming the configuration $1/2^-(^{77}Se, ^{79}Se) \otimes 3/2^-(^{77}Br, ^{79}Br)$ (see also /Pa73a,Ek80/).
In conclusion, the anomalous spin and parity $5/2^+$ of ^{75}Se does not seem to be affected by adding one proton (^{76}Br). A similar relation is found between the nuclei ^{77}Kr and ^{78}Rb /Ek78/.

6.2.5 Very low-lying 0_2^+ state in the nuclei of N = 40

In the nuclei with neutron number 40 ($^{70}_{30}Zn$, $^{72}_{32}Ge$, $^{74}_{34}Se$, $^{76}_{36}Kr$ /Le78, Ha81/) the 0_2^+ states appear with excitation energies lower than in their isotopes. The extreme case is ^{72}Ge, where the 0_2^+ state is lower than the 2_1^+ state. A considerable lowering is also seen in the ^{70}Ge and ^{72}Se (N = 38).
It is interesting to note that the special lowering of the 0_2^+ states occurs also in the $_{40}$Zr and $_{42}$Mo nuclei around A ≈ 90 - 100 (see /Le78/). Further in $^{99}_{43}Tc$ and ^{101}Tc there exist very low-lying $5/2^+$ and $7/2^+$ states. The lowering of $5/2^+$ and $7/2^+$ states is not so distinct in $_{41}$Nb. However, these states have lowest excitation energy in $^{99}_{41}$Nb.
Hamilton et al. /Ha74a,Ha78,Pi81/ have proposed that the 0_1^+ and 0_2^+ states have different nuclear deformations /St70/, i.e. spherical 0_1^+ and deformed 0_2^+ states or vice versa are encountered.
Another interpretation for the lowering of the 0_2^+ is pairing vibration /Ha74b/, which is also accounted for by the low-lying 0_2^+ in the nuclei around Z = 40. Kumar /Ku78/ has suggested that the shape coexistence may be induced by pairing vibration, and further he has pointed out the possibility of a shape transition. If the low-lying 0_2^+ state has a deformed nuclear shape, it can not be expected that the (p,t) or (t,p) cross sections for this state are largely enhanced around N = 40 /Bo77,Ve78b,Ar78,Re80/, while excluding the 0_2^+ state most of the other levels seem to follow the vibrational model. As the large enhancement of the two neutron transfer cross section and the low-lying 0_2^+ state can be nicely explained by including pairing vibration /Sa78,Sa79,We81/, it would be of interest to carry out a systematic study with (p,t) and (t,p) reactions for Se-isotopes.

6.3 Theoretical interpretation of the low-lying level structure in Se-isotopes and neighbouring nuclei

In many nuclear models it may be thought to be fundamental to understand the structure of e-e nuclei, because the low-lying level structures in these nuclei are relatively simple and the structure of odd mass nuclei can be understood in a first step by coupling a proton or a neutron to this core-state (e-e nuclei). Therefore, here in this section we first deal with these theories which are suitable for the description of e-e nuclei, and secondly we discuss odd-mass nuclei.

6.3.1 Theory for e-e Se isotopes

So far considerable success was obtained for the description of e-e nuclei in this region by the following theoretical calculations,

- Boson expansion with a phenomenological Hamiltonian /Li75/ (for ^{76}Se)
- Dynamic deformation theory /Ku78,Re79/
- Pairing vibration coupled to the basis of dressed n-quasiparticle state /Sa78,Sa79/
- Pairing vibration coupled to the basis of Boson expansion theory (BET) /We81/ (for Ge-isotopes)

The first calculation by Lie et.al. does not include the term of pairing vibration and it was not applied to the ^{72}Ge and ^{74}Se nuclei. The second calculation by Kumar has explained the experimental B(E2)'s and observed level scheme fairly well as reviewed by Vergnes /Ve79/. Because in this calculation the 0_2^+ states in Ge-isotopes are essentialy the β-vibrational states, the results of (p,t) and (t,p) reactions are hard to explain in this theory. Further in the frame work of the dynamic deformation theory the nuclear shape of the ground state in ^{74}Se and ^{76}Se is expected to be oblate. If we assume that the shape of the 2_1^+ state is not so different from the ground state 0_1^+, the negative quadrapole moment of the 2_1^+ state in the even mass Se-isotopes /Le77/ does not favour oblate shape.

Thus considering the result of (p,t) and (t,p) experiments, the theories which include pairing vibrations (third and fourth calculation), would be the best suited for the nuclei in this region. The calculations of Sakata et al. /Sa79/ and Weeks /We81/ have been able to reproduce the electromagnetic properties of Se and Ge nuclei, respectively.

The pairing vibration can occur when there is an orbital with high spin lying above the valence orbital with low spin. In a spherical potential the pairing force is proportional to 2j+1, where j is the spin of relevant particle orbital,

$$\langle j^2 ; JM \mid H_{pair} \mid j^2 ; JM \rangle = - \frac{G}{2} (2j + 1) \delta(J,0) \quad \text{..... eq. 6.3}$$

where G containes the value of the radial integral (see for ex. /Bo75/,p.642). Thus in the case of ^{72}Ge and ^{74}Se the $g_{9/2}$ neutron pair has more pairing energy than the $p_{1/2}$ neutron pair or other neutron pairs (see Fig.1.1).
In the real calculation, the 0^+ state of pairing vibration is strongly coupled to the 0^+ two phonon state /Sa78,Sa79/, thus the 0_2^+ state is lowered in energy. This picture leads to the conclusion that the enhancement of the (p,t) and (t,p) reactions for the low-lying 0_2^+ state is well described by the large admixture of the $(g_{9/2})^2_{J=0}$ configuration in this state. Rester et al. /Re80/ have reported such evidence in the studies of ^{74,76}Se(p,t) reactions.
Recently the theoretical frame work, which takes into account the pairing reaction, has been outlined by Suzuki et al. /Su81/. Though the results of numerical calculations will appear later, their theory should be quite effective for the Ge and Se nuclei.
Besides these theoretical calculations, a considerable success in describing the level sequence of ^{76}Se has been shown using IBA1 (Interacting Boson approximation) /Ve82/, and further its associated IBFA (Interacting Boson Fermion approximation) has reproduced the negative parity state of ^{77}Se fairly well. It is interesting to see whether these calculation can explain the experimental electromagnetic properties of each level. However, because the IBA dose not include the term of pairing vibration, it would be difficult to reproduce the results of (p,t) and (t,p) reactions. Another code based on IBA2, which makes a distinction between the proton bosons and neutron bosons, has failed to produce the lower-lying 0_2^+ state in ^{76}Se /Ma80/, or it may be just a difference in the values of parameters.

6.3.2 Theory for odd mass Se-isotopes

As has been pointed out through this work, the most difficult thing to handle in odd mass Ge, Se and Kr nuclei are the low-lying positive parity states $5/2^+$ and $7/2^+$ arising from the $(\nu g_{9/2})^n$ configuration. Compared to the positive parity states the negative parity states are explained fairly well by various theoretical calculations, which will be referred to in the following. Even the simplest core-particle coupling model seems to work satisfactorily well for negative parity states /De61/ (see also /Ve82/). Thus we concentrate our atten-

tion on the low-lying positive parity states $5/2^+$ and $7/2^+$.
The two positive parity states $5/2^+$ and $7/2^+$ show different characters, which is clear in the systematics of level energies (Fig. 6.3).

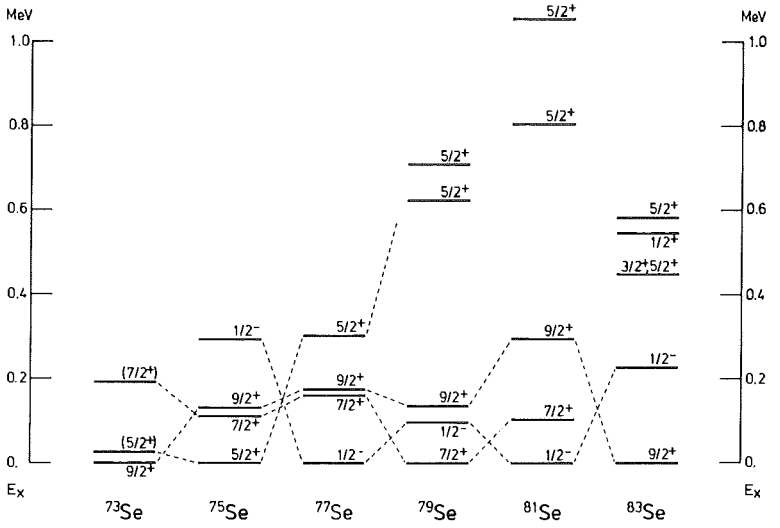

Fig. 6.3

Systematics of some low-lying levels ($5/2^+_1$, $7/2^+_1$, $9/2^+_1$ and $1/2^-_1$) in Se-isotopes.

As mentioned in 6.2.2, the low-lying $7/2^+$ state can be obtained by coupling a $g_{9/2}$-quasiparticle to one phonon state $J^\pi=2$, n=1 (or this phonon state is obtained from two quasiparticles, thus implying $(\tilde{g}_{9/2})^3$).
The energy-splitting ΔE after coupling a $g_{9/2}$-quasiparticle to the one phonon state is given by (see /Bo75/ p.541)

$$\Delta E(j,I) = h^2(j,j2)\left(\delta(j,I)\left(\frac{(u^2(j)-v^2(j))^2}{\hbar\omega} + \frac{4u^2(j)v^2(j)}{2E(j)+\hbar\omega}\right) + (2j+1)\begin{Bmatrix} 2 & j & j \\ 2 & j & I \end{Bmatrix}\left(\frac{(u^2(j)-v^2(j))^2}{\hbar\omega} - \frac{4u^2(j)v^2(j)}{2E(j)-\hbar\omega}\right)\right)$$

..... eq. 6.4

h(j,j2) : matrix element including the radial integral
u(j),v(j) : occupation and non-occupation amplitude
$\hbar\omega$: phonon energy
E(j) : quasi-particle energy
j : $g_{9/2}$ neutron in this case

Adopting j=9/2 in this case, the values of the 6j-symbols for various final spins I from $9/2^+ \otimes 2^+(5/2^+,7/2^+,9/2^+,11/2^+,13/2^+)$ are shown below.

$$\begin{Bmatrix} 2 & 9/2 & 9/2 \\ 2 & 9/2 & 13/2 \end{Bmatrix} = -0.009091 \qquad \begin{Bmatrix} 2 & 9/2 & 9/2 \\ 2 & 9/2 & 11/2 \end{Bmatrix} = -0.048485$$

$$\begin{Bmatrix} 2 & 9/2 & 9/2 \\ 2 & 9/2 & 9/2 \end{Bmatrix} = -0.065152 \qquad \begin{Bmatrix} 2 & 9/2 & 9/2 \\ 2 & 9/2 & 7/2 \end{Bmatrix} = 0.057576$$

$$\begin{Bmatrix} 2 & 9/2 & 9/2 \\ 2 & 9/2 & 5/2 \end{Bmatrix} = -0.016667$$

Table 6.2 6j-symbols for $g_{9/2} \otimes 2^+$ multiplets. Values are from /Sc68/.

Because the 6j symbols have different sign for the $7/2^+$ state, the special lowering of the $7/2^+$ state is understood by the second term multiplied by the 6j symbol in eq.6.4 (when $u(j) \sim v(j)$). The lowering of the $7/2^+$ state provided by the Alaga model (three-particle (hole) cluster + core vibration model, see for example /Pa73b/) is essentially caused by this different sign of the 6j symbol for the j-1 state.

The electromagnetic properties are quite sensitive to a small admixture of various wave functions. Further the B(E2) or B(M1) values of the $9/2^+ \rightarrow 7/2^+$ transition are not well measured, and the magnetic dipole and electric quadrupole moments of the $9/2^+$ and $7/2^+$ states are still not well known. Therefore, it is rather hard to determine which teoretical calculation can reproduce the level properties most reasonably.

The $5/2^+$ state is not fully lowered to the ground state within a picture of particle phonon coupling or of microscopic treatment using three quasi-particles /Ku75/. A recent calculation including up to five quasiparticle states could only predict that the $5/2^+$ state of the one quasiparticle two phonon multiplets becomes the lowest among these multiplets /Na80/.

On the other hand, the theories which assume a stable deformed core including the Coriolis interaction (with attenuation) was performed by Heller et al. /He74,He75/, and could bring down the $5/2^+$ state to the ground state in the case of ^{75}Se. An apparent serious difficulty in their calculation is that the deformation parameter β is positive (0.2-0.3) for ^{75}Se, ^{79}Se, ^{84}Se and most of the other nuclei in this region, but negative (-0.28) for ^{77}Se. Further they could not lower the $7/2^+$ state sufficiently in the case of ^{75}Se.

A similar calculation was also done by Sanderson /Sa73/, who could explain the

(d,t) spectroscopic strength fairly well, though he could not lower the $5/2^+$ state sufficiently. The $5/2^+$ state has a main component of the [422↑] orbital in the calculation of Sanderson, and the [440↑] orbital in the case of Heller et al.. Both of these calculations were not able to reproduce the large quadrupole moment (1.0 barn /Fu76/) of the $5/2^+$ ground state in ^{75}Se, and the magnetic moment for this level given by Heller et al.($-1.447\mu_N$) is not in good agreement with the experimental value ($\mu = 0.67\pm0.04\mu_N$ /Ca74/).
A calculation based on the tri-axial rotor model was performed by Larsson et al. /La78/. They could predict the $5/2^+$ ground state and also the low-lying $7/2^+$ state, by adopting an attenuation of the Coriolis term. The electromagnetic properties of the low-lying positive parity state are again not satisfactorily reproduced.
It is another question, whether it is appropriate to assume a stably deformed core, when the core states are well described within a picture of a nearly spherical nulear shape as described in the previous section. When we adopt a picture of a deformed core, the 0_2^+ state of the e-e core can be thought to be caused by the β-vibration, which leads again to the problem of the large (p,t) and (t,p) cross sections for the 0_2^+ states around N=40.
Consequently, by now there is no theory which works satisfactorily well for the nuclei around the neutron number 40. However, we should recall that the lowering of the 0_2^+ states in the e-e nuclei and the lowering of the $5/2^+$ states in the odd mass nuclei are coincident (§ 6.2.5 and the next section), which implies a close relation between the 0_2^+ and $5/2^+$ states.

6.4 A possible correlation between the 0_2^+ state in the e-e Se nuclei and the $5/2^+$ state in the odd mass Se-nuclei

The coincidence of occurrence of the low-lying 0_2^+ and $5/2^+$ states has been pointed out by Kuriyama et al./Ku75/. However, since that time the quantity of the experimental data has largely increased. In this section we would therefore like to show clear evidence of correlation between the 0_2^+ states in the e-e Se nuclei and the $5/2^+$ states in the odd mass Se nuclei.
In Fig.6.4 are drawn the energies of the 0_2^+ states in the e-e Se nuclei, and the energy differences between the lowest (possible) $5/2^+$ states and the $9/2^+$ states, i.e. $E_x(5/2_1^+)-E_x(9/2_1^+)$.

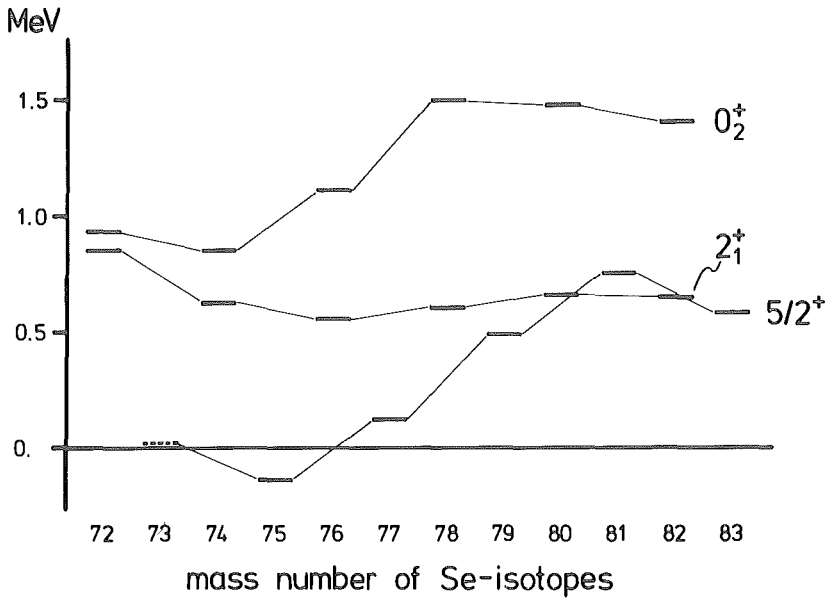

Fig. 6.4

Systematics of the low-lying 0_2^+ state in even Se nuclei and $5/2^+$ state in odd-A Se isotopes (see text).

The occurrence of the 0_2^+ ($5/2^+$) state is most prominent for n=40 (41). It is obvious that the level energy of the $5/2^+$ in the odd mass nuclei is clearly correlated with the 0_2^+ level of the core states, but not so distinctly with the 2_1^+ state. Further, the level energies of the 2_1^+ states are nearly constant. This fact can be understood since the occurrence of the low-lying $5/2^+$ state is not so closely related with the nuclear deformation, because the location of the 2_1^+ states can be assumed to be a good measure for the nuclear deformation as pointed out by Sakai /Sa67/.

A similar correlation between the low-lying 0_2^+ and $5/2^+$ states can be seen also in the Ge-isotopes (N = 40), Kr-isotopes (N = 40) and the nuclei around A=100 (Z = 40). Since the lowering of the 0_2^+ state in the Ge and Se isotope is nicely explained by the pairing vibration /We81,Se78/, the lowering of the $5/2^+$ state may be somehow related to the pairing vibration.

There are several ways to obtain the $5/2^+$ state, i.e.

- 1 phonon $\otimes$ $g_{9/2}$
- 2 phonon $\otimes$ $g_{9/2}$
- 1 phonon $\otimes$ $g_{9/2}$ $\otimes$ pairing vibration
- higher lying $d_{5/2}$
- $d_{5/2}$ $\otimes$ pairing vibration

  etc.

It is interesting to know, how these states are correlated and whether these states can lower the $5/2^+$ states. It is desirable to extend the theoretical frame work of e-e nuclei proposed by Weeks et al. /We81/ or by Suzuki et al. /Su81/ to the odd mass nuclei.

7. Conclusion

In the present work the low spin states have been studied of $^{75,76,77}Se$ in order to obtain the information complementary to the high spin states studied by other research groups. Use was made of the (n,γ) reaction because of its non-selectivity.
The high-energy (n,γ) spectra were measured for $^{75,77}Se$ both at Jülich and at Grenoble, where in addition the $^{75}Se(n,\gamma)$ reaction was observed due to consecutive neutron capture in the high neutron flux.
With the curved crystal spectrometers at Grenoble the low-energy γ-ray spectra were measured with very high resolution, energy accuracy and a large dynamic range, so that also very weak lines were seen. For the stronger transitions also conversion-electron data were obtained with the high resolution β-spectrometer.

The information resulting from the analysis of the measured spectra is the following:

- Complete low spin level schemes in the low-energy regions of ^{75}Se, ^{76}Se, ^{77}Se, ^{78}Se and ^{75}As with very accurate level energies.
- Very accurate neutron separation energies for ^{75}Se, ^{76}Se, ^{77}Se and ^{78}Se. The neutron binding energy for ^{76}Se has been measured for the first time due to consecutive neutron capture. The value of 11154.2 ± 0.2 keV is clearly less than the adopted /Wa77/ energy of 11161.7 ± 2.2 keV, casting doubts on $Q_{EC}(^{75}Se)$ or $Q_{\beta}(^{76}As)$.
- The cross section for thermal neutron capture by the β-unstable ^{75}Se ($\tau_{1/2}$ = 120 days) was found to be ∼ 300 b . This number is of interest for astrophysics especially in connection with the question of the "origin of the elements".
- Because of the use of PbSe targets intense Pb X-rays were observed and the natural widths were measured for all practically accessible K X-ray lines. The observed widths were compared with semiempilical and purely theoretical values. Apparent slight discrepancies require further study.

The spectra of high-energy γ-transitions show significant differences regarding the reaction mechanisms. A strong positive correlation is observed of the primary $^{74}Se(n,\gamma)$ intensities and $^{76}Se(d,p)$ spectroscopic strengths, but the correlation for $^{76}Se(n,\gamma)$ and $^{76}Se(d,p)$ is

absent or slightly negative. This result is not yet understood. Furthermore, two E2 primary transitions were found both in the $^{74}Se(n,\gamma)$ reaction and in the $^{75}Se(n,\gamma)$ process. The observation of such E2 transitions is rare. In fact only 24 primary E2 transitions were seen before in the whole nuclear chart, two of them in $^{73}Ge(n,\gamma)$. The strength of the E2 transitions in $^{75,76}Se$ are somewhat more than but not inconsistent with the expected average.

The emphasis of the present work was the structure of the low-lying levels in $^{75,76,77}Se$. Through the very detailed and accurate (n,γ) data several ambiguities could be removed in the previously known level schemes, and for several levels new spin and parity assignments could be made. The systematics of low-lying levels in the Se isotopes revealed clear evidence for a correlation of the lowering of the 0_1^+ -levels in the even Se isotopes and the $5/2^+$ states in the odd-A seleniums. Such a correlation is also seen in the Ge and Kr isotopes and it may even exist in nuclei with $A \simeq 100$. Therfore, the understanding of the lowering of the 0_2^+ states appears to be the key to understand the $5/2^+$ states which so far have escaped theoretical explanation. Comparison of the level schemes with various models show that at present there is no theory that can explain well the low-lying level structures of the Se isotopes. It seems that these isotopes are mainly vibrational in character as far as low spin states are concerned. The most promising interpretation of the lowering of the 0_2^+ states may be pairing vibration. Probably a more detailed interpretation of the low-lying level structures of the Se isotopes has to await microscopic calculations in this nuclear region.

Acknowledgement

I express my sincere thanks to Professor O. Schult, who has given me the opportunity to do this work. His continuous encouragement and advice are deeply appreciated.

Thanks are also given to Dr. H. Börner at ILL/Grenoble. Without his support I could not have finished this work.

The kind assistance of Drs. G. Barreau, R. Brissot, H. Faust, C. Hofmeyr, K. Schreckenbach, D. D. Warner at ILL/Grenoble, and H. Seyfarth, R. Weinreich at IKP/KFA Jülich is greatfully acknowledged. For their technical assistance thanks are also due to Messrs. G. Blanc at ILL/Grenoble and W. Ermer, J. Pfeiffer at IKP/KFA Jülich.

The discussion with Dr. T. Suzuki at IKP/KFA Jülich was quite enlightening and useful.

The kindness of two senior scientists T. von Egidy and F. Gönnenwein at ILL/Grenoble is very much appreciated.

I am very much thankfull to all staff and friends at ILL/Grenoble and at IKP/KFA Jülich for their hospitality extended to me during the stay in Grenoble and in Jülich. I am indebted to Mrs. H. Sieling and Mrs. M. Heese at IKP/KFA Jülich for help in typing.

I have enjoyed carrying out a significant part of the measurements at an international laboratory supported by the countries, die Bundesrepublik Deutschland, la République Française and the United Kingdom. This and the support by the KFA and the ILL have helped me to increase my linguistic knowledge.

References

/Aa55/ L.C. Aamodt and P.C. Fletcher, Phys. Rev. vol. 98, pp 1224 (1955)

/Al62/ D.J. Alkhazov, V.D. Vasil'ev, G.M. Gusinski, I.Kh. Lemberg and V.A. Nabichvrishvili, Izv. Akad. Nauk SSSR, Ser. Fiz. Vol. 26, p. 1014 (1962)

/Ax62/ P. Axell, Phys. Rev. Vol. 126, p. 671 (1962)

/Ar66/ A. Artna, Nuclear Data Sheets section B, Vol. 1, No. 4 (1966)

/An68/ D.S. Andrev, L.N. Gal'perin, A.Z. Il'yasov, I. Kh. Lemberg and I.N. Chugunov, Izv. Akad. Nauk. SSSR, Ser. Fiz. Vol. 32, p. 276 (1968)

/Ag70/ A.P. Agnihotry, K.P. Gopinathan, M.C. Joshi and K.G. Prasad, Proc. 15th Nucl. Phys. and Solid State Phys. Symp., Vol. 2, Nucl. Phys. Madurai, India, p. 161 (1970)

/Ar71/ G. Ardisson and C. Marsol, Can. J. Phys. Vol. 49, p. 1731 (1971)

/Ar72/ G. Ardisson, C. Marsol, O. Rahmouni and P. Aguer, Nucl. Phys. A179, p. 545 (1972)

/Ag73/ Y.K. Agarwal, S.M. Bharathi, S.K. Bhattacherjee, B. Lal and Baldev Sahai, Proc. Int. Conf. Nucl. Phys. (München) p. 288 (1973)

/Ak73a/ M.R. Akhmed, A.M. Demidov, M.A. Khalil and F.A. Khussein, Izv. Akad. Nauk SSSR, Ser. Fiz. 37 (1973) p. 993

/Ak73b/ M.R. Akhmed, A.M. Demidov, M.A. Khalil, S. Al-Nazar, Izv. Akad. Nauk. SSSR, ser. Fiz. vol. 37, p. 1004 (1973)

/Ag74/ Y.K. Agarwal, C.V.K. Baba, S.M. Bharathi, S.K. Bhattacherjee, B. Lal and Baldev Sahai, Pramana, Vol. 3, No. 4, p. 243 (1974)

/Ar75/ D. Ardouin, R. Tamisier, M. Vergnes, G. Rotbard, T. Kalifa and G. Berrier Phys. Rev. C., Vol. 12, p. 1745 (1975)

/Aj76/ F. Ajzenberg-Selove, Nucl. Phys. A 268, p. 138 (1976)

/Al78/ B.J. Allen and A.R. de Musgrove, "Advances in Nuclear Physics", Vol. 10, p. 129, Plenum Press, New York (1978)

/Ar78/ D. Ardouin , C. Lebrun, F. Guilbault, B. Remaud, E.R. Flynn, D.L. Hanson, S.D. Orbesen, M.N. Vergnes, G. Rotbard, and K. Kumar, Phys. Rev. C18, 1701 (1978)

/Ah81/ A. Ahmed, A.V. Ramayya, D.L. Sastry, J.H. Hamilton, R.B. Piercy, H. Kawakami, A.P. de Lima and C.F. Maguire, Phys. Rev. C., Vol. 24, p. 1486 (1981)

/Ba61/ K.A. Baskova, S.S. Vasilev, No. Seng Ch'ang and L. Ya. Shavtvalor, Soviet Physics JETP, Vol. 41, p. 1484 (1961)

/By64/ W. Bygrave, D. Eccleshall and M.J.L. Yates, Nucl. Phys. Vol. 53, p. 385 (1964)

/Ba67/ G.A. Bartholomew, L.V. Groshev, et al., Nuclear data tables A3, p. 367 (1967) and ibid. vol. 5, p. 1 (1968)

/Ba68/ D.P. Balamuth, G.P. Couchell and G.E. Mitchell, Phys. Rev. Vol. 170, p. 995 (1968)

/Bo69a/ A. Bohr and B.R. Mottelson, "Nuclear structure", Vol. 1, W.A. Benjamin, Inc. New York, Amsterdam (1969)

/Bo69b/ M. Boivin, Y. Cauchois, and Y. Heno, Nucl. Phys. A137, p. 520 (1968)

/Ba71/ G. Bauer and H. Seyfarth, Atomkernenergie, Vol. 18, p. 236 (1971)

/Be71/ D. Bellmann, Atomkernenergie, Kerntechnik, Vol. 17, p. 145 (1971)

/Bu72/ E.H.S Burhop and W.N. Asaad, Advances in Atomic and Molecular Physics (Academic Press New York 1972), Vol. 8, p. 163 (1977)

/Ba74/ J. Barrette, M. Barrette, G. Lamoureux, S. Monaro, and S. Markiza, Nucl. Phys. A235, p. 154 (1974)

/Br74/ R.A. Braga and D.G. Sarantites, Phys. Rev. C3, p. 1493 (1974)

/Bo75/ A. Bohr and B.R. Mottelson, "Nuclear Structure", Vol. 2, W.A. Benjamin, Inc.

/Ba76/ J.A. Barclay, S.S. Rosenblum and W.A. Steyert, Phys. Rev. C13, p. 1991 (1976)

/Be76a/ F.E. Bertrand and R.L. Auble, Nucl. Data Sheets, Vol. 19, p. 507 (1976)

/Be76b/ M. Behar, A. Filevich, G. Garcia-Bermudez, A.M. Hernandez and M.A.J. Mariscotti, Nucl. Phys. A261, p. 317 (1976)

/Bö76/ H.G. Börner, Thesis (Technical University Munich, 1976)

/Bo77/ M. Borsaru, D.W. Gebbie, J. Nurzynski, C.L. Hollas, L.O. Barbopoulos and A.R. Quinton, Nucl. Phys. A284, p. 379 (1977)

/Ba79/ L.O. Barbopoulos, D.W. Gebbie, J. Nurzynski, M. Borsaru and C.L. Hollas, Nucl. Phys. A331, p. 502 (1979)

/Bö79/ H.G. Börner, private communication

/Br79a/ P. Brewster, Ph. D. thesis, McMaster Univ. (Canada)

/Br79b/ F. Braumandl, Thesis 1979, Technical University Munich

/Ba81/ G. Barreau, private communication

/Bo81/ G.L. Borchert, P.G. Hansen, B. Jonson, H.L. Ravn and O.W.B. Schult, Hyperfine interactions 10, p.1115 (1981)

/Bl81/ S. Blakeway, Ph. D. Thesis, Manchester University, 1981

/Ca63/ A.B.W. Cameron, N.H. Lazar, and H.W. Schmitt, in "Fast neutron physics" part 2, ed. by J.B. Marion and J.L. Fowler, Interscience Publishers New York - London (1963)

/Co72/ A. Coban, J.C. Willmott, J.C. Lisle and G. Murray, Nucl. Phys. A182, p. 385 (1972)

/Ca74/ P.T. Callaghan, N.J. Stone, and B.G. Turrell, Phys. Rev. B 10, p. 1075 (1974)

/Ca78/ R.R. Cadmus, Jr., T.B. Clegg, E.J. Ludwig and S.A. Wender, Nucl. Phys. A319, p. 165 (1979)

/Du47/ J.W.M. DuMond, Rev. Sci. Instr. Vol. 18, p. 626 (1947)

/Da54/ Handel Davies, H.A. Bethe, and L.C. Maximon, Phys. Rev. Vol. 93, p. 788 (1954)

/Da62/ W. Darcey, D.J. Pullen, and N.W. Tauner, Proc. Int. Symp. on Direct Interactions and Nuclear Reaction Mechanisms, ed. E. Clementel and C. Villi, Gordon and Breach, New York, 1963, p. 795

/Dz70/ B.S. Dzhelepov, A.G. Dmitriev, Zh. Zhelev, N.N. Zhoukovskii, L.N. Moskvin and V.I. Fominykh, Izv. Akad. Nauk. SSSR, Ser. Fiz., Vol. 34, p. 2062 (1970)

/Di72/ F. Dickmann, V. Metag and R. Repnow, Phys. Lett. Vol. 38B, p. 287 (1972)

/De74/ M.A. Deleplanque, C. Gerschel, N. Perrin, B. Ader and M. Ishihara, J. Phys. Lett. (Paris), Vol. 35, p.L-237 (1974)

/El58/ A.J. Elwyn, H.H. Landon, Sophie Oleska, and G.N. Glasoe, Phys. Rev. Vol. 112, p. 1200 (1958)

/En64/ W. Engels, W. Delang, U. Wehmann, and E. Bodenstedt, Phys. Lett., Vol. 11, p. 57 (1964)

/En67/ W. Engels, Z. Naturforschg. Vol. 22a, p. 2004 (1967)

/Eg68/ T. von Egidy, Habilitationsschrift, Technical University Munich,(1968)

/Eg69/ T. von Egidy, Contribution to the Int. Symp. on Neutron Capture Gamma-Ray Spectroscopy, 11.-15. August 1969, Studsvik, Sweden

/Ek78/ C. Ekström, S. Ingelman, G. Wannberg and M. Skarestad, Nucl. Phys. A311, p. 269 (1978)

/Ek80a/ C. Ekström and L. Robertson, Phys. Scr., Vol. 22, p. 347 (1980)

/Ek80b/ L.P. Ekström and F. Kearns, Nucl. Data Sheets, Vol. 29, p. 1 (1980)

/En80/ H. En'yo, T. Numao and T. Yamazaki, Phys. Rev. A, Vol. 21, p. 1439 (1980)

/Ek81/ L.P. Ekström, Nucl. Data Sheets, Vol. 32, p. 211 (1981)

/En81/ G. Engler, R.E. Chrien and H.I. Liou, Nucl. Phys. A372, p. 125 (1981)

/Fu69/ G.H. Fuller and V.W. Cohen, Nucl. Data Tables, A5, p. 433 (1969)

/Fi70/ E. Finckh, W. Jahnke, B. Schreiber and A. Weidinger, Nucl. Phys. A144, p. 67 (1970) and the quoted data of (p,nγ) reaction investigated by N.A. Tubbs (Thesis, Oxford University 1966)

/Fu76/ G.H. Fuller, J. Phys. Chem. Ref., vol. 5, p. 835 (1976)

/Ge50/ S. Geschwind, H. Minden, C.H. Townes, Phys. Rev. Vol. 79, p. 212 (1950)

/Gu64/ G.M. Gusinskii, I.Kh. Lemberg, and Z. Treibal, Izv. Akad. Nauk SSSR, Ser. Fiz. vol. 28, p. 1683 (1964)

/Ga70/ L.N. Gal'perin, A.Z. Il'yasov, I. Kh. Lemberg and G.A. Firsanov, Izv. Akad. Nauk SSSR, Ser. Fiz. Vol. 34, p. 1650 (1970)

/Gr69/ P. Gryska, P. Richs and K. Rampold, Nucl. Phys. A132, p. 123 (1969)

/Gr78/ R.C. Greenwood and R.E. Chrien, Proceeding of the 3rd International Symposium on Neutron Capture and Related Topics, ed. R.E. Chrien and W. Kane, p. 618 (1978)

/Gr80/ R.C. Greenwood and R.E. Chrien, Nucl. Instr. Meth. Vol. 175, p. 515 (1980)

/He57/ W. Heitler, "Quantum Theory of Radiation", 3rd edition, Clarendon Press, p. 268 (1957)

/Ha58/ Max Hansen and Kurt Anderko, "Constitution of Binary Alloys", McGraw-Hill Book Company, Inc., p. 1104 (1958)

/Ho61/ R.E. Holland and F.J. Lynch, Phys. Rev. Vol. 121, p. 1464 (1961)

/Ha68/ R.S. Hager and E.C. Seltzer, Nucl. Data Tables A4, p. 1 (1968)

/He74/ S.L. Heller and J.N. Friedman, Phys. Rev. C10, p. 1509 (1974)

/Ha74/ J.H. Hamilton, A.V. Ramayya, W.T. Pinkston, R.M. Ronningen, G. Garcia-Bermudez, H.K. Carter, R.L. Robinson, H.J. Kim, and O. Sayer, Phys. Rev. Lett. Vol. 32, p. 239 (1974)

/Ha74b/ J. Hadermann and J.C. Rester, Nucl. Phys. A231, p. 120 (1974)

/He75/ S.L. Heller and J.N. Friedmann, Phys. Rev. C12, p. 1006 (1975)

/Ho75/ D.J. Horen and M.B. Lewis, Nucl. Data Sheets, Vol. 16, p. 25 (1975)

/Ha78/ J.H. Hamilton, R.L. Robinson and A.V. Ramayya, Lecture notes in Physics (Series 92) "Nuclear Interactions", ed. B.A. Robson, conference held in Canberra, 28th August - 1st September 1978

/He78/ T. Heck, L. Cleemann, J. Eberth, W. Neumann, N. Wiehl and V. Zobel, Proc. 6th european phys. soc. nucl. divs. conf. on the structure of medium-heavy nuclei, Rhodos, Greece, 1 - 4 May 1979, (Inst. phys. conf. ser. No. 48, p. 231)

/Ha81/ J.H. Hamilton, R.B. Piercy, R. Soundranayagam, A.V. Ramayya, C.F. Maguire, X.J. Sun, Z.Z. Zhao, J. Roth, L. Cleeman, J. Eberth, T. Heck, W. Neumann, M. Nolte, R.L. Robinson, H.J. Kim, S. Frauendorf, J. Döring, L. Funke, G. Winter, J.C. Weller, J. Lin, A.C. Rester, and H.K. Carter, preprint

/Ho81/ Y.-K. Ho, T.-S. Qi, and Z.-Y. Pan, preprint (Physics Dept. Zhengchou Univ.).

/Ik66a/ H. Ikegami and M. Sano, Phys. Lett. Vol. 21, p. 323 (1966)

/Ik66b/ H. Ikegami, W.B. Ewbank, and K. Way, Nucl. Data B1-6-103

/Ii71/ K. Iizawa, I. Kitamura, K. Kawade, H. Yamamoto, K. Yoshikawa, S. Amemiya, and T. Katoh, J. Phys. Soc. Jap. Vol. 30, p. 901 (1971)

/Ik72/ H. Ikegami and M. Sano, Proc. Int. Conf. Nucl. Moments and Nucl. Structure, Tokyo, 1977, J. Phys. Soc. Jap. vol. 34, Supplement, p. 451 (1973)

/Jo64/ C.H. Johnson, C.C. Trail, and A. Galonsky, Phys. Rev. vol. 136B, p. 1719 (1964)

/Jo68/ L.V. Johnson and T.J. Kenett, Nucl. Phys. A. vol. 113, p. 104 (1968)

/Je76/ P. Jeuch , Thesis 1976, Technical University Munich

/Ki53/ B.B. Kinsey and G.A. Bartholomew, Can. J. Phys. Vol. 31, p. 1051 (1953)

/Ki63/ L.S. Kisslinger and R.A. Sorenson, Rev. Mod. Phys. vol. 35, p. 853 (1963)

/Ka67/ W.R. Kane and M.A. Mariscotti, Nucl. Instr. Meth., vol. 56, p. 189 (1967)

/Ki68/ K. Kikuchi and M. Kawai, "Nuclear Matter and Nuclear Reactions", North-Holland Publ. Comp. Amsterdam (1968)

/Kn71/ R. Knerr and H. Vonach, Z. Phys. vol. 24b, p. 151 (1971)

/Ke74/ O. Keski-Rahkonen and M.O. Krause, Atom. Data and Nucl. Data Tables, vol. 14, pp. 139 (1974)

/Ku75/ A. Kuriyama , T. Marumori, and K. Matsuyanagi, Prog. Theo. Phys. suppl. vol. 58, p. 53 (1975)

/Kr77/ K.S. Krane , Atomic Data and Nuclear Data Tables, vol. 19, p. 375 (1977)

/Km78/ K. Kumar, J. Phys. 6, vol. 4, p. 849 (1978)

/Ko78/ H.R. Koch, Report Jülich-Spez-10 (1978)

/Kn79/ J.W. Knowles, Nucl. Instr. Meth. vol. 162, p. 677 (1979)

/Kr79/ M.O. Krause and J.H. Oliver, J. Phys. Chem. Ref. Data, vol.8, p.329 (1979)

/Ka80/ R. Kaur, A.K. Sharma, S.S. Sooch, H.R. Verma and P.N. Trehan, J. Phys. Soc. vol. 49, p. 1214 (1980)

/Ko80a/ L. Koester, K. Knopf and W. Waschkowski, Z. Phys. A296, p. 43 (1980)

/Ko80b/ H.R. Koch, H.G. Börner, J.A. Pinston, W.F. Davidson, J. Faudou, R. Roussille and O.W.B. Schult, Nucl. Instr. Meth. vol. 175, p. 401 (1980)

/Ke81/ T.J. Kennett, M.A. Islam and W.V. Prestwich, Can. J. Phys. vol. 59, pp. 93 (1981)

/Ko81/ J. Kopecky, contribution to the 4th Int. Symp. on neutron capture gamma-ray spectroscopy and related topics, 7. - 11. Sept. 1981, ISN Grenoble and ECN report, ECN-99, Petten

/Kr81/ A.J. Kreiner and M.A.J. Mariscotti, Phys. Rev. C24, p. 148 (1981)

/La57/ A.M. Lane and J.E. Lynn, Proc. Phys. Soc. (London) vol. 70A, p. 557 (1957)

/La60/ A.M. Lane and J.E. Lynn, Nucl. Phys. vol. 17, p. 553 (1960)

/Lo61/ B. Lobkowicz and P. Marmier, Helv. Phys. Acta, vol. 34, p. 85 (1961)

/Ly63/ F.J. Lynch and E.N. Shipley, Report ANL-6679, p. 5 (1963)

/Li65a/ E.K. Lin, Phys. Rev. vol. 139B, p. 340 (1965)

/Li65b/ E.K. Lin, Nucl. Phys., vol. 73, p. 613 (1965)

/Li68/ V.F. Litvin, Yu. A. Nemilov, K.I. Zherebtsova, K.A. Gridnev, L.V. Krasnov, V.A. Komatov, Yu.A. Lakomkin and T.V. Orlova, Izv. Fiz. vol. 32, p. 276 (1968)

/Ly68/ J.E. Lynn "The theory of neutron resonance reactions", Clarendon Press, Oxford (1968)

/La69/ I.-M. Ladenbauer-Bellis and H. Bakhru, Phys. Rev., vol. 178, p. 2019 (1969)

/Li70/ R.M. Lieder and J.E. Draper, Phys. Rev. C2, p. 531 (1970)

/La71/ I.M. Ladenbauer-Bellis, H. Bakhru and R. Bakhru, Can. J. Phys., vol. 48, p. 54 (1971)

/La74/ B. Lal and Baldev Sahai, Proc. Nucl. Phys. and Solid State Phys. Symp. section B, Nucl. Phys. 14B, p. 27 (1974)

/Li75/ S.G. Lie and G. Holzwarth, Phys. Rev. C12, p. 1035 (1975)

/La77/ F.P. Larkins, Nucl. Data and Nucl. Data Tables, vol. 20, p. 311 (1977)

/Le77/ R. Lecomte, P. Paradis, J. Barrette, M. Barrette, G. Lamoureux and S. Monaro, Nucl. Phys. A284, p. 123 (1977)

/La78/ S.E. Larsson, G. Leander, and I. Ragnarsson, Nucl. Phys. A307, p. 189 (1978)

/Le78/ "Table of Isotopes" 7th Edition, John Wiley and Sons, ed. M. Lederer and V.S. Shirley

/Mc62/ F.K. McGowan and P.H. Stelson, Phys. Rev., vol. 126, p. 257 (1962)

/Ma63/ B.E.F. Macefield, R. Middleton, and D.J. Pullen, Nucl. Phys., vol. 44, p. 309 (1963)

/Mo63/ S. Monaro, Nuovo Cimento, vol. 30, p. 1379 (1963)

/Mc71/ D.K. McMillan and B.D. Pate, Nucl. Phys. A174, p. 604 (1971)

/Mo71/ N.A. Morcos, T.E. Ward and P.K. Kuroda, Nucl. Phys. A171, p. 647 (1971)

/Ma72/ M.A.J. Mariscotti, W. Gelletly and W.R. Kane, Phys. Rev. C5, p. 178 (1972)

/Mu73/ "Neutron Cross Sections", vol. 1, "Resonance Parameters", BNL 325, ed. S.F. Mughabghab and D.I. Garber (1973)

/Mo75/ H. Morinaga and T. Yamazaki, § 6 in "in-beam gamma-ray spectroscopy" North-Holland publ. Co. (1975)

/Mo75/ B.W. Motal, D.H. Lueders, J.M. Daley, F.E. Durham, S.G. Buccino, C.E. Hollandsworth, W.P. Bucher and H.D. Jones, Phys. Rev. C12, p. 63 (1975)

/Ma78/ W. Mampe, K. Schreckenbach, P. Jeuch, B.P.K. Maier, F. Braumandl, J. Larysz and T. v. Egidy, Nucl. Instr. Meth., vol. 154, p. 127 (1978)

/Mo78/ L.A. Montestruque, M.C. Cobian-Rozale, G. Szaloky, J.D. Zumbro, and S.E. Darden, Nucl. Phys. A305, p. 29 (1978)

/Ma79/ M. Matoba, M. Hyakutake, N. Koori and Y. Irie, Nucl. Phys. A325, p. 389 (1979)

/Mc79/ J.M. McKenzie, Nucl. Instr. Meth., vol. 162, p. 49 (1979)

/Ma80/ T. Matsuzaki, M. Adachi, T. Kohno, N. Morishima, N. Endo, A. Nakashima and H. Taketani, INS annual report 1980 (Tokyo Univ.), p. 31, 1980

/Mi80/ T. Mitsunari, internal report at the University of London Reactor Center (ULRC), and private communication. A good explanation is given in the instruction of the program LEVELS written by him.

/Ma81/ "Neutron Beam Facilities Available for Users" ed. B.P.K. Maier

/Ni55/ S.G. Nilsson, Mat. Fys. Medd. Dan. Vid. Selsk., Vol. 29, No. 16 (1955)

/Ni61/ K. Nishimura, J. Phys. Soc. Jap., vol. 16, p. 355 (1961)

/Na69/ T. Nagarajan, M. Ravindranath and K.V. Reddy, Nucl. Phys. A137, p. 467 (1969)

/Ne69/ G.C. Nelson, W. John and B.G. Saunders, Phys. Rev. 2nd Ser., vol. 187, p. 1 (1969)

/No75/ E. Nolte and P. Vogt, Z. Physik A275, p. 33 (1975)

/Na73/ T. Nagahara, J. Phys. Soc. Jap., vol. 34, p. 579 (1973)

/Na74/ T. Nagahara, J.-Z. Ruan, H. Nakayama, Y. Ishizuka and M. Okano, J. Phys. Soc. Jap., vol. 37, p. 1 (1974)

/Na75/ A.I. Namensson, ILL, 1975

/Na79/ M. Nakano, Progr. theo. Phys., vol. 63, p. 160 (1980)

/Ov68/ Ingjald Øverbø, Kjell J. Mork and Haakon A. Olsen, Phys. Rev., vol. 175, p. 1978 (1968)

/Po56/ C.E. Porter and R.G. Thomas, Phys. Rev., vol. 104, p. 483 (1956)

/Pa66/ S.C. Pancholi, H. Ikegami, Nuclear Data B1, p. 83 (1966)

/Pa73a/ T. Paradellis, A. Houdayer and S.K. Mark, Nucl. Phys. A201, p. 113 (1973)
/Pa73b/ V. Paar, Nucl. Phys. A211, p. 29 (1973)
/Pi79/ R.B. Piercy, A.V. Ramayya, R.M. Ronninger, J.H. Hamilton, V. Maruhn-Rezwani, R.L. Robinson and H.J. Kim, ibid /He79/
/Pi81/ R.B. Pierey, J.H. Hamilton, R. Soundranayagan, A.V. Ramayya, C.F. Maguire, R.L. Robinson, H.J. Kim, J. Döring, L. Funke, G. Winter, J. Roth, L. Cleeman, J. Eberth, W. Neumann, J.C. Wells, J. Lin, A.C. Rester and H.K. Carter, Phys. Rev. Lett., vol. 47, p. 1514 (1981)
/Ro62/ R.L. Robinson, F.K. McGowan and P.H. Stelson, Phys. Rev., vol. 125, p. 1373 (1962)
/Ri68/ F.W. Richter, J. Schütt and D. Wiegandt, Z. Phys., vol. 217, p. 1 (1968)
/Ra69/ S. Ray, J.N. Mo, S. Muszynski and S.K. Mark, Nucl. Phys. A138, p. 49 (1969)
/Ru70/ E.A. Rudak, E.I. Firsov, and A.M. Khil'manovich, Yad. Fiz. vol. 11, p. 627 (1970)
/Ra71/ D. Rabenstein and H. Vonach, Z. Naturforsch. 26a (1971) p. 458
/Ra78/ S. Raman, contribution to the 3rd Int. Symp. on Neutron Capture Gamma-ray Spectroscopy and Related Topics, 18. - 22. Sept. 1978, BNL, Upton, New York
/Ro80/ G. Rotbard, M. Vergnes, G. Berrier-Ronsin and J. Vernotte, Phys. Rev. C21, vol. 21, p. 2283 (1980)
/Rö78/ F. Rösel, H.M. Fries, K. Alder and H.C. Pauli, Atomic Data and Nuclear Data Tables, vol. 21, p. 81 (1978)
/Re79/ B. Remaud and K. Kumar, ibid /He78/, p. 232
/Re80/ A.C. Rester, J.B. Ball and R.L. Auble, Nucl. Phys. A346, p. 371 (1980)
/Su / O.I. Sumbaev, "Diffraction of γ-Radiation from a crystal", chapt. 1 in "Crystal Diffraction Gamma-Spectrometers" (translated from Russish to English at University of Colorado)
/Sh61/ A. de-Shalit, Phys. Rev., vol. 122, p. 1530 (1961)
/St62/ P.H. Stelson and I.K. McGowan, Nucl. Phys., vol. 32, p. 652 (1962)
/Sa67/ M. Sakai, Nucl. Phys. A104, p. 301 (1967)
/Sc68/ Landolt-Börnstein, new series, group 1, vol. 3, ed. H. Schopper
/Sa69/ D.G. Sarantites and B.R. Erdal, Phys. Rev., vol. 177, p. 1631 (1969)
/St70/ K.W.C. Stewart and B. Castel, Nuovo Cimento Lett., vol. 4, p. 589 (1970)
/Sa73/ N.E. Sanderson, Nucl. Phys. A216, p. 173 (1973)

/Sc74/ J.H. Scofield, Atom. Data and Nucl. Data Tables, vol. 14, p. 121 (1974)

/Su74/ T. Sugimitsu, Nucl. Phys. A224, p. 199 (1974)

/Sm75/ L.G. Smith and A.H. Wapstra, Phys. Rev. C11, p. 1392 (1975)

/Sc75/ Programm LEVEL written by K. Schreckenbach, ILL, 1975, unpublished

/Sa76a/ N.E. Sanderson and R.G. Summers-Gill, Nucl. Phys. A261, pp. 93 (1976)

/Sa76b/ S.I. Salem and P.L. Lee, Atom. Data and Nucl. Data Tables, vol. 18, pp. 233 (1976)

/Sa78/ I. Sakata, S. Iwasaki, T. Marumori and K. Takada, Z. Phys. A286, p. 195 (1978)

/Sh78/ A.Shibuya, M. Dojo, T. Sugimitsu and N. Kato, Nucl. Phys. A301, p. 15 (1978)

/St78/ M.L. Stelts and R.E. Chrien, Nucl. Instr. Meth., vol. 155, p. 253 (1978)

/Sa79/ F. Sakata and G. Holzwarth, Prog. Theo. Phys., vol. 61, p. 1649 (1979)

/Sc79a/ H. Schäfer, A. Dewald, A. Gelberg, W. Kaup, K.O. Zell, and P. von Brentano, Z. Phys. A293, p. 85 (1979)

/Sc79b/ K. Schreckenbach, private communication

/Sc80a/ H.H. Schmidt, P. Hungerford, H. Daniel, T. von Egidy, R. Brissot, G. Barreau, H.G. Börner, S. Kerr, C. Hofmeyr, K.P. Lieb, ILL internal report 80 SC 35S (1980), Grenoble

/Sc80b/ U. Schötig, K. Debertin and K.F. Walz, Nucl. Instr. Methods, vol. 169, p. 43 (1980)

/Si80/ B. Singh and D.A. Viggars, Nuclear Data Sheets, vol. 29, p. 75 (1980)

/Sa81/ N. Sakamoto, K. Ogino, Y. Kadota, K. Obori, T. Taniguchi, Y. Okuma, T. Higo, Y. Iwashita, S. Matsuki and T. Yanabu, RCNP Annual Report 1980, RCNP, Osaka Univ., Osaka, Japan (1981) and private communication

/Su81/ T. Suzuki, M. Fuyuki and K. Matsuyanagi, Prog. Ther. Phys., vol. 65, p. 1667 (1981)

/Si81/ B. Singh and D.A. Viggars, Nucl. Data Sheets, vol. 33, p. 189 (1981)

/Th67/ G.E. Thomas, D.E. Blatchley and L.M. Bollinger, Nucl. Instr. Meth., vol. 56, p. 325 (1967)

/Ta73/ Y. Tanaka and T. Tomoda, Prog. Theo. Phys., vol. 50, p. 123

/To78/ Y. Tokunaga, master thesis, unpublished, Tokyo Institute of Technology, Tokyo (1978)

/To82/ Y. Tokunaga and H.G. Börner, report, Jülich-Spez-145

/Ur73/ P.P. Urone, L.L. Lee, Jr., and S. Raman, Nuclear Data Sheets, vol. 9, P. 229 (1973)

/Ve73/ W.J. Veigele, E. Briggs, L. Bates, E.M. Henry and B. Brauwell, Atomic Data, vol. 5, p. 51 (1973)

/Vy77/ T. Vylov, contribution to the 27. meeting on nuclear spectroscopic and Nuclear Structure, Tashkent, March 1977, JINR-P6-10417

/Ve78a/ H. Verheul and R.L. Auble, Nucl. Data Sheets, vol. 23, p. 487 (1978)

/Ve78b/ M.N. Vergnes, G. Rotbard, F. Guilbault, D. Ardouin, C. Lebrun, E.R. Flynn, D.L. Hanson and S.D. Orbesen, Phys. Lett. 72B, p. 447 (1978)

/Ve79/ M. Vergnes, ibid /He79/p. 25

/Ve82/ J. Vervier, private communication and J. Vervier and R.V.F. Janssens, Phys. Lett., vol. 108B, p. 1 (1982)

/We53/ H.E. Weaver, Jr., Phys. Rev., vol. 89, p. 923 (1953)

/Wa54/ H.E. Walchli, Report ORNL-1775 (1954)

/We62/ H. Weigmann, Z. Phys., vol. 167, p. 547 (1962)

/Wy73/ W.G. Wyckoff and J.E. Draper, Phys. Rev. C8, p. 796 (1973)

/Wa77/ A.H. Wapstra and K. Bos, Atomic Data and Nuclear Data Tables, Vol. 19, p. 231 (1977)

/Wi79/ G. Winter, J. Döring, F. Dubbers, L. Funke, P. Kemnitz and E. Will, Gemeinsamer Jahresbericht, p. 44, Zentralinstitut für Kernforschung, Rossendorf, German Democratic Republic (1979)

/Wa80/ E.K. Warburton, D.E. Alburger and D.J. Millener, Phys. Rev. C22, p. 2330 (1980)

/We80/ J.C. Wells, Jr., R.L. Robinson, H.J. Kim, O. Sayer, R.B. Piercy, A.V. Ramayya, J.H. Hamilton and C.F. Maguire, Phys. Rev. C22, p. 1126 (1980)

/Wa81/ A.H. Wapstra, private communication

/We81/ K.J. Weeks, T. Tamura, and T. Udagawa, Phys. Rev., C24, p. 703 (1981)

/Wi81/ G. Winter, J. Döring, W.D. Fromm, L. Funke, P. Kemnitz, H. Prade and E. Will, Nucl. Phys. A367, p. 95 (1981)

/Ya68/ T. Yamazaki and G.T. Ewan, Nucl. Instr. Methods, vol. 62, p. 101 (1968)

/Ze75/ K.O. Zell, H.-G. Friedrichs, B. Heits, P. von Brentano, and C. Protop, Z. Physik A272, p. 27 (1975)

/Ze76a/ K.O. Zell, H.-G. Friedrichs, B. Heits, D. Hippe, H.W. Schuh and P. von Brentano, Z. Physik A276, pp. 371 (1976)

/Ze76b/ K.O. Zell, B. Heits, W. Gast, D. Hippe, W. Schuh and P. von Brentano, Z. Phys. A279, p. 373 (1976)